Pharmacological manipulation of skeletal stem/progenitor cell fate decisions

Medjie Piron

A thesis submitted to the University of Ottawa in partial fulfillment of the requirements for the master's degree in Cellular and Molecular Medicine

Department of Cellular and Molecular Medicine

Faculty of Medicine

University of Ottawa

Table of Contents

Acknowledgement ..... *vi*

Abstract ..... *ix*

Abbreviations ..... *xi*

List of figures ..... *xiii*

List of tables ..... *xiv*

Chapter 1: Introduction *1*

1.1 The Skeletal system **1**

1.2 Bone development **2**

1.2.1 Fetal bone development: endochondral and intramembranous ossification 2

1.2.2 Postnatal growth 5

1.3 Skeletal stem and progenitor cells (SSPCs) **7**

1.3.1 Skeletal stem and progenitor cells (SSPCs) in vivo 7

1.3.2 Mesenchymal Stem cells (MSCs) and bone marrow stromal cells (BMSCs) 12

1.4 Sexual dimorphism of skeletal growth and aging **13**

1.4.1 Role of Sex steroids in skeletal sexual dimorphism 14

1.4.2 Role of the growth hormone–insulin growth factor 1 (GH/IGF-1) axis in skeletal sexual dimorphism 15

1.4.3 Sexual dimorphism in skeletal cells 15

1.5 Skeletal system aging and senescence **15**

1.5.1 Cellular senescence and aging 16

1.5.2 Cellular senescence in bone cells 17

1.6 Rationale **18**

1.7 Hypothesis **18**

1.8 Specific aims **18**

Chapter 2: Materials and methods ***20***

2.1 Animals **20**

2.2 Genotyping **20**

2.3 Pharmacological compounds **22**

2.4 Bone tissue processing for in vivo experiments **24**

2.4.1 Bone harvest and processing 24

2.4.2 Senescence-associated beta-galactosidase (SA-β-gal) expression detection 25

2.4.3 Blocking and permeabilization 25

2.4.4 EdU proliferation assay 25

2.4.5 Immunohistochemistry 26

2.4.6 Histodenz clearing and slide mounting 26

2.4.7 Confocal microscopy 27

2.4.8 Image Analysis 28

2.5 Skeletal cell processing for in vitro experiments **28**

2.5.1 Skeletal cell isolation 29

2.5.2 Skeletal cell enrichment 29

2.5.3 Skeletal cell senescence detection: SA-β-gal detection and $p16^{INK4A}$ staining 30

2.5.4 Skeletal cell imaging 31

2.6 In vitro differentiation potential assessment **32**

2.7 Graphs and Statistics **33**

Chapter 3: Effect of sex and age on Sox9+ SSPCs proliferation and senescence 34

3.1 SSPCs proliferation and senescence rate with sex and age in vivo 34

3.2. SSPCs proliferation kinetics and senescence with sex and age in vitro 40

3.3 Multilineage differentiation potential of SSPCs with age 44

3.4 Summary 49

Chapter 4. Pharmacological manipulation of SSPCs fate decisions..... 50

4.1. Effect of PTH and Hh pathway regulators on SSPCs proliferation and senescence in vitro..... 51

4.2 Effect of prolonged stimulation with 20(S)-OHC on SSPCs proliferation and senescence in vitro53

4.3 Effect of PTH on the SSPCs population size in vivo 57

4.4. Sex-dependent effects of tamoxifen (TAM) on growth plate chondrocytes proliferation and senescence 59

Chapter 5: Discussion, limitations, future directions and conclusion 63

5.1 Discussion 63

5.1.1 SSPCs proliferation and senescence rate with sex and age in vivo 63

5.1.2 SSPCs proliferation kinetics and senescence with sex and age in vitro..... 65

5.1.3 Multilineage differentiation potential of SSCs with age..... 66

5.1.4 Effect of PTH and Hh pathway regulators on SSPCs proliferation and senescence in vitro. 67

5.1.5 Effect of PTH on the SSPC population size in vivo 70

5.1.6 Sex-dependent Tamoxifen (TAM) effect on growth plate (GP) chondrocytes proliferation and senescence in C57Bl/6 mice 71

5.2 Limitations and future directions 72

5.3 Conclusion 74

Chapter 6: References 76

Acknowledgement

I would like to convey my deepest thanks to my supervisor, Dan, for accepting me into his lab. It has been a wonderful opportunity for me to grow over the years. Thank you for this incredible chance and for guiding me throughout this project. Milles mercis!

I would also like to express my sincere gratitude to my thesis advisory committee: Dr Barbara Vanderhyden, Dr Michael Rudnicki, and Dr George Grammatopoulos. Their inestimable guidance and insights were essential to the completion of this work.

Thanks to my lab colleagues Baha and Spencer, who trained me when I first started in the lab, and to Vanessa, who joined later but whom I would have missed greatly if she hadn't come. You are all wonderful colleagues.

To you, Natasha, thank you for your amazing friendship! You weren't part of the lab, but you were always there for me. You're the best.

Thanks also to Billy, Devansh, Morgan, and so many others whose company at the hospital was precious to me.

Thanks to my husband, Wislet. Your love and support are invaluable to me. This work would have been impossible without you by my side.

Thanks to my son, Wendgy, for making me a mother and giving me an additional source of inspiration.

Thank you to my mother, Murtha, and my sister, Saradjie. This work would have been much more difficult without your support.

To my family in Haiti, especially my aunt Lucita, my cousins Jennie and Nyckson, and my little cousins, you inspire me to keep going.

Finally, I thank the Creator.

I dedicate this work to my grandmother, who left us too soon.

Abstract

The mature bone houses a population of multipotent stem/progenitor cells named the skeletal stem/progenitor cells (SSPCs). Studies carried out in our lab proved the existence, in the growth plate of postnatal mice, of self-renewing putative skeletal stem cells (SSCs) thought to be involved with progenitor cells in the growth, homeostatic maintenance and repair of skeletal tissue following trauma.

As the organism ages, bone mass is lost and the prevalence of age-related conditions of the skeletal system increases. Unlike in young individuals, SSPCs are less likely to ensure perfect bone maintenance in the elderly, despite their presence in the aged bone. In the setting of this work, I hypothesized that: the decrease in their proliferative capacity as they enter senescence is responsible for the phenotypic and pathological changes observed in the bones with age; and, the pharmacological targeting of signaling pathways activated during bone development and growth can change SSPCs fate decisions, alleviate age-related bone loss and modify the pathological outcome in the aging organisms. I pursued the following aims: 1) to study SSPCs proliferation and senescence in aged mice; 2) to pharmacologically manipulate SSPCs fate decisions.

With methods involving lineage tracing and imaging cytometry, the conducted experiments showed that the SSPC population shrinks in aged mice growth plate and their proliferation and senescence levels decrease. Of the compounds tested, 20(S)-hydroxycholesterol, a Hedgehog pathway agonist, keeps SSPCs quiescent/non-proliferative in vitro; and tamoxifen exerts a sex-dependent effect on growth plate chondrocytes (including SSPCs) in vivo. Tamoxifen stimulates chondrocytes proliferation and senescence entry in male mice, while protecting them from senescence in female mice.

This is the first report of its kind on the Sox9+ SSPC population. More in-depth investigations into the specific mechanisms of action of these compounds are necessary.

This work brings us closer to our goal of addressing acute and chronic age-related conditions of the skeletal system with novel stem-cell based therapies.

Abbreviations

20(S)-OHC	20(S)-hydroxycholesterol
ALP	Alkaline Phosphatase
ANOVA	Analysis of Variance
BM	Bone marrow
BMI1	B lymphoma Mo-MLV insertion region 1 homolog
BODIPY	4,4-Difluoro-1,3,5,7,8-Pentamethyl-4-Bora-3a,4a-Diaza-s-Indacene
Bp	Base pair
CD	Cluster of differentiation
Col2a1	Collagen type II alpha 1 chain
Ctrl	Control
DAPI	4′,6-diamidino-2-phenylindole
ddH2O	Distilled water
DMSO	Dimethyl Sulfoxide
DNA	Deoxyribonucleic acid
Dpt	Days post-tamoxifen
EdU	5-ethyl-2’-deoxyuridine
ETOH	Ethanol
Exp	Experimental
FBS	Fetal bovine serum
FGF	Fibroblast growth factor
FGFR	Fibroblast growth factor receptor
FMO	Fluorescence minus one
GFP	Green fluorescent protein
GH	Growth hormone
GP	Growth plate

Hh	Hedgehog
IGF-1	Insulin-like growth factor 1
Ihh	Indian Hedgehog
IP	Intraperitoneal
M	Molar
MSCs	Mesenchymal stem cells
P	Postnatal day
PBS	Phosphate-buffered saline
PFA	Paraformaldehyde
PTH	Parathyroid hormone
PTHrP	Parathyroid hormone-related protein
RT	Room temperature
RZ-Ch	Resting zone chondrocytes
SA-β-gal	Senescence-associated beta-galactosidase
scRNA-seq	Single cell RNA sequencing
Sox9	SRY-Box Transcription Factor 9
Sp7	Specificity protein 7
SSC	Skeletal stem cell
SSPC	Skeletal stem/progenitor cell
TAM	Tamoxifen
TB	Trabecular bone
tdT	tdTomato

List of figures

Figure 1.1. Representation of the growth plate 6

Figure 1.2. Schematic drawing and crystal structure of SOX9 10

Figure 1.3. CellChat analysis demonstrates molecular crosstalk between several cell types and resting zone chondrocytes 12

Figure 2.1. Procedural workflow for proliferation assay and senescence quantification. 24

Figure 2.3. Procedural workflow for skeletal cell processing. 29

Figure 3.1. Sox9+ SSPCs population size and proliferation rate in aged male and female mouse GP 35

Figure 3.2. Senescence rate of Sox9+ SSPCs in young and aged mice of both sexes 39

Figure 3.3. Isolation and in vitro culture of young and aged SSPCs 43

Figure 3.4. Osteogenic differentiation potential of SSPCs in aged mice 46

Figure 3.5. Adipogenic differentiation potential of SSPCs in aged mice 47

Figure 3.6. Chondrogenic differentiation potential of SSPCs in aged mice. 48

Figure 4.1. In vitro assays in basal medium with supplementation of PTH, cyclopamine, purmorphamine and 20(S)-OHC 52

Figure 4.2. In vitro colony assays in basal medium with supplementation with 20(S)-OHC and its combination with cyclopamine 55

Figure 4.3. Quantification of Sox9+ SSPCs in mouse femur sections exposed to PTH. 58

Figure 4.4. Tamoxifen effect on growth plate chondrocytes 62

List of tables

Table 2.1. Primer sequences used for Cre and Ai14 genotyping. 21

Table 2.2. Thermal cycler settings for genotyping. 22

Table 2.3: Pharmacological compounds 23

Table 2.4. Antibodies/reagents 27

Chapter 1: Introduction

1.1 The Skeletal system

The skeletal system is an important system in mammals. In humans, it is divided into the axial skeleton (vertebral column and much of the skull) and appendicular skeleton (pelvic, pectoral girdles and limbs). It is composed of bones, cartilages and ligaments.

Bones are the main components of the skeleton. They are specialized connective tissues that provide support to the body in general and a lever to muscles during movement[1]. They also protect vital organs, house the bone marrow (BM)—main site of postnatal hematopoiesis—and play a major role as reservoirs of calcium and phosphate ions[2]. Cartilages are flexible connective tissues found in joints—amongst other locations[3]. Joints are the point of contact between bones in the organism. They can be immovable (synarthroses), slightly movable (amphiarthroses) or highly movable (diarthroses). Diarthroses—or synovial joints—are the most common joint type. They feature a synovial space bordered by the articular capsule (a synovial membrane and fibrous capsule) and the hyaline cartilage covering the bone extremities. The synovial space is filled with synovial fluid produced by the synovial membrane. Cartilages highly contribute to movement by forming a cushion that can absorb shocks, reduce frictions of the joints and provide support to their function. Joints are further strengthened by ligaments and tendons. The former are fibrous connective tissues that connect bones to each other. They maintain the stability of the skeleton and prevent out-of-range movements of the joints. The skeletal system is connected to the muscular system by tendons—connective tissues that attach muscles to bones.

1.2 Bone development

Bones are dynamic organs. Their development begins in utero and proceeds well after birth, until the end of puberty. Even at maturity, bones are capable of adaptative changes, regeneration/repair, and are constantly being remodelled through a balance between bone deposition and resorption. The evolution through these phases depends on the dynamic changes happening in the cells (epigenetic changes, senescence), their local environment (mechanical loading) and paracrine/endocrine factors (hormones and growth factors).

1.2.1 Fetal bone development: endochondral and intramembranous ossification

Organs of the body derive from the three primary germ layers: endoderm, mesoderm and ectoderm. Bones derive from the neural crest—a derivative of the ectoderm—and the mesoderm [4,5]. Mesenchymal cells, destined to give rise to the facial bones, originate from the neural crest; the cranial base, the thoracic cage and the vertebral column derive from the paraxial mesoderm; and bones of the limbs and pelvis, arise from the lateral plate mesoderm. Bone formation or ossification begins between the sixth and seventh week of human embryonic life and takes place through two main processes: endochondral ossification and intramembranous ossification. In the latter processes, similar sets of markers, transcription factors and secreted proteins are involved and activated. They instruct cell differentiation as the bone is going through the different steps of its development.

1.2.1.1 Endochondral ossification

Most bones of the axial and appendicular skeleton develop through endochondral ossification[6,7]. It is a two-step process where the establishment of a hyaline cartilage template is

followed by its replacement with bone tissue. Mesenchymal cells condense at the ossification site and form a cluster of cells adhering to each other[8]. They differentiate into chondrocytes at the center and perichondrial cells on the outside. Chondrocytes at the center of the cartilage proliferate while producing a type II collagen-rich extracellular matrix as the cartilage thickens[9]. They later stop proliferating, undergo hypertrophic changes and synthesize type X collagen. These hypertrophic chondrocytes drive blood vessel invasion of the cartilage and osteoblast (osteoid-secreting cells) differentiation of perichondrial cells. This forms the primary ossification center. As per some reports, hypertrophic chondrocytes can also transdifferentiate into osteoblasts[10–13]. The latter express multiple markers such as alkaline phosphatase (ALP), osteopontin, osteocalcin and specificity protein 7 (Sp7)/osterix (Osx) amongst others [14–16]. Secondary ossification centers, characterized by the advent of the same set of events, will appear in the epiphysis. Between primary and secondary ossification centers, chondrocytes remain to form the growth plate (GP) cartilage—or physis—responsible for longitudinal bone growth that will be described in more detail below.

Several signaling pathways and transcription factors are activated during endochondral bone formation. The transcription factors: Paired related homeobox 1 (Prx1), SRY-box transcription factor 5 (Sox5), SRY-box transcription factor 6 (Sox6) and SRY-box transcription factor 9 (Sox9) play a crucial role in early mesenchymal cell differentiation into chondrocytes[17–19]. Prx1 and Sox9 are expressed as early as the mesenchymal condensation phase and drive the expression of cartilaginous genes: *Collagen type II alpha 1 chain* (*Col2a1)* and *Aggrecan (Acan)* [20–23]. Sox9 is also expressed in proliferating chondrocytes—but not in hypertrophic chondrocytes—whereas Prx1 remains expressed in perichondral and periosteal cells[24]. Sox5 and Sox6 mainly support Sox9 in its regulation of chondrogenesis[22,25,26]. Other pathways and factors

influence Sox9 in its chondrogenic role[27]. For example, the Wnt/β-catenin signaling pathway seems to be responsible for the restriction of Sox9 expression in proliferating chondrocytes[28].

The Indian hedgehog (Ihh)–parathyroid hormone-related protein (PTHrP) signaling pathway regulates the chondrocyte proliferation–hypertrophy balance within the GP. Ihh is secreted by prehypertrophic and early hypertrophic chondrocytes. It has been shown to stimulate chondrocyte proliferation, while inhibiting chondrocyte hypertrophy, through the secretion of PTHrP by perichondrial cells and early proliferating chondrocytes[29,30]. It also induces the osteoblast differentiation of perichondrial cells. PTHrP acts through the PTH/PTHrP receptor, the parathyroid hormone 1 receptor (PTH1R) expressed by proliferating cells. Cells located far away from the PTHrP signal escape its control and become prehypertrophic. They can then produce Ihh that will maintain the PTHrP secretion, in a tightly regulated feedback loop[31–34].

The fibroblast growth factor (FGF) signaling pathway also plays a role in embryonic bone development. FGFs act on Sox9 by inducing its expression, thus indirectly inhibiting chondrocytes proliferation[35–37]. FGF receptors (FGFRs) expression is highly variable throughout the different phases of endochondral bone formation. FGF18, signalling through FGFR3 in proliferating and early hypertrophic chondrocytes, inhibits chondrocyte proliferation while stimulating their hypertrophy[38,39].

The vascular invasion of the primary ossification center is driven by the vascular endothelial growth factor (VEGF) (the expression of which is stimulated by FGF18) secretion by hypertrophic chondrocytes[40–42]. Other signaling pathways involved are the bone morphogenetic protein (BMP) (stimulates Ihh production)[43], platelet-derived growth factor (PDGF) (stimulates angiogenesis)[44], transforming growth factor-beta (TGF-β) (inhibition of chondrocyte hypertrophy)[45] and Notch (decreases Sox9 expression) [46–48] signaling pathways. The growth

hormone (GH), through the insulin-like growth factor 1 (IGF1) pathway, stimulates chondrocyte proliferation and hypertrophy during bone formation [49]. There is a complex interplay of well-known signaling pathways, transcription factors and secreted proteins affecting endochondral ossification.

1.2.1.2 Intramembranous ossification

Most flat bones from the cranio-facial area arise from the neural crest (ectomesenchyme), through a process called intramembranous ossification. Although most of the transcription factors and signaling pathways involved in endochondral ossification are also at play, it is a less complex process of bone formation. Bones go through: 1) a mesenchymatous/precondensation phase; 2) a condensation phase, where mesenchymal cells become tightly packed and a membrane is formed; and 3) a calcification phase, preceded by the establishment of an ossification center on the outer layer of the previously formed membrane[50].

1.2.2 Postnatal growth

After birth, bone thickness and length keep increasing. Longitudinal bone growth only stops in adulthood. For flat and long bones, it happens through different mechanisms. Flat bones formed by intramembranous ossification grow by the apposition of new layers on the external surface, with concomitant osteoclastic activity on the endosteal surface.

In long bones, postnatal GPs are formed between the primary and secondary ossification centers. The GP is the main driver of longitudinal bone growth in the postnatal skeleton (figure 1.1). It is organized in different zones housing multiple layers of chondrocytes: 1) the resting chondrocyte zone, where quiescent skeletal stem cells (SSCs) are believed to be housed[51]; 2) the proliferation zone, where proliferating chondrocytes are tightly housed forming columns of

flattened cells; 3) the pre-hypertrophic chondrocyte zone, where chondrocytes stop proliferating, enlarge, and start expressing an osteoblastic gene program; and 4) the hypertrophic chondrocyte zone, where cells promote vascularization, start matrix mineralization, and either die from apoptosis or transdifferentiate into osteoblasts [52,53]. At this point, a reorganization of the surrounding tissue takes place. Blood vessels, osteoclasts, bone marrow cells and osteoblast precursors—arising from other osteochondroprogenitors—invade the area. The osteoblasts are responsible for the secretion of bone matrix, replacing the cartilage matrix resorbed by osteoclasts[54]. When maximal bone growth is reached in adult organisms, the restricted ossification taking place at the edge of the GP takes over and primary and secondary ossification centers meet while the GP cartilage disappears (GP fusion).

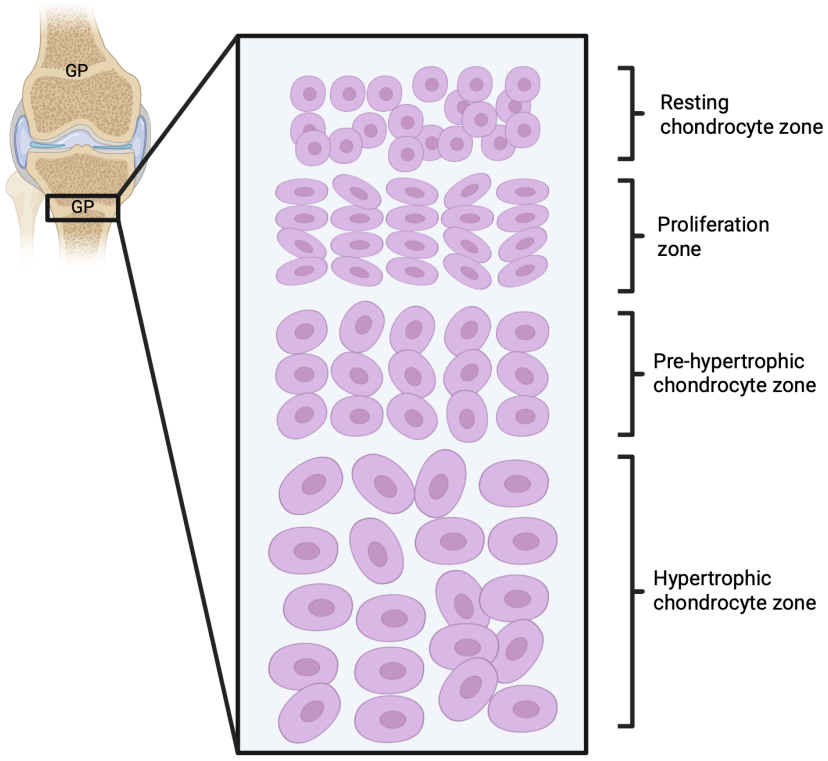

Figure 1.1. Representation of the growth plate. From the metaphysis edge to the diaphysis, resting chondrocyte zone, proliferation zone, pre-hypertrophic chondrocyte zone and hypertrophic chondrocyte zone are represented. GP: growth plate (Image created in Biorender)

1.3 Skeletal stem and progenitor cells (SSPCs)

Stem cells exist in almost all tissues and organs and are responsible for tissue growth, maintenance, and repair. In the skeletal system, SSCs participate in postnatal growth, homeostatic maintenance, and repair of bones after trauma[55]. As for all stem cells, they are defined mainly by two characteristics: their self-renewal capacity and multipotency[56]. Since SSCs remain poorly defined and few assays exist to discriminate them from their more committed progenitors, we will hereby use the term skeletal stem/progenitor cells (SSPCs) to define all skeletal cells involved in bone growth, maintenance and repair—independently of their self-renewing capacity.

1.3.1 Skeletal stem and progenitor cells (SSPCs) in vivo

Lineage tracing is the gold standard to identify putative stem cells in vivo, test their self-renewal and multipotency, and provide information about the population kinetics downstream of the stem cells[57]. Multiple labelling strategies have been developed. The first one is based on the incorporation of nucleotide analogues like 5-bromodeoxyuridine (BrdU) or 5-ethyl-2'-deoxyuridine (EdU) into cellular DNA during the S phase of the cell cycle[12,58–61]. Subsequent divisions result in dilution of the label as it partitions between the two daughter cells. After a while, the tissue becomes heterogenous in that certain cells have retained much more of the DNA label than others. This latter phenomenon can testify about the existence of long-lived post-mitotic cells, which has incorporated EdU before becoming post-mitotic; but also, it can put into evidence putative quiescent/slow-cycling stem cells in the tissue (long-term label-retaining cells). In such assays, cells retaining EdU are most likely stem cells as even when long-lived post-mitotic cells had incorporated EdU before entering the post-mitotic stage, they would eventually die due to cell turnover. Nucleotides analogues are a reliable tool in the identification of stem cells.

A second strategy uses a transgenic mouse model expressing a fluorescent protein—like the green fluorescent protein (GFP)—whose expression depends on the presence or absence of doxycycline/tetracycline (Tet-on and Tet-off gene expression systems) [62–65]. In such systems, the cells of interest express a fluorophore under the control of a tetracycline/doxycycline response element (TRE) promoter. In the Tet-Off system, gene expression is silenced by tetracycline/doxycycline administration. In the Tet-On system, tetracycline/doxycycline administration activates gene expression. In these systems, stem cells are labelled via the targeting of promoters of markers of interest. For instance, the H2B-GFP mouse line (JAX:005104) expresses the histone H2B-GFP (H2B-GFP) fusion protein under the control of a TRE. When bred with another line expressing the tetracycline-controlled transactivator (tTA) or the reverse tetracycline-controlled transactivator (rtTA) under a ubiquitous or tissue specific promoter, pulse-chase administration of doxycycline results in GFP nuclear labeling of slow-cycling cells. In a Tet-Off system, mice are continuously given doxycycline to prevent tTA from inducing gene expression. The pulse consists of a few days without doxycycline, before the drug is being reintroduced for the chase period (the H2B-GFP label is produced as long as no drug is administered). In a Tet-On system, the H2B-GFP transgene expression is induced by doxycycline administration to activate the rtTA (the pulse), and the drug is removed to start the chase. In both cases, after the chase is started, only slow-dividing cells will retain the label long-term since the H2B-GFP fusion is segregated equally between daughter cells during cell division, resulting in rapid dilution below detection levels in fast cycling cells[66]. This is a highly reliable system in the identification of stem cells in vivo.

The latest and more popular technique is based on the use of a drug-inducible Cre-recombinase (CreERT) expressed under a cell type-specific promoter or stem cell-specific

promoters in the case of stem cell-related research, and a fluorescent Cre-reporter[67–72]. This reporter is expressed in Cre+ cells after administration of the drug (tamoxifen/TAM or 4-hydroxytamoxifen/4-OHT). In the skeletal system, multiple investigations have been conducted using, amongst others, Actin-CreERT[73], Osterix (Osx/Sp7)-CreERT[74], Col2a1-CreERT[75,76] and Acan-CreERT[77], Grem1-CreERT[76], and PTHrP-CreERT[78]. In the previously mentioned reports, the presence of osteochondral cells in the GP and periosteum was noted; but none of these studies could prove the self-renewal of these cell types; and multipotency was never shown at the single cell level. Moreover, most of these investigations focused on embryonic or perinatal developmental stages. A few have been conducted in postnatal mice expressing Sox9-CreERT for example and reported labeling of osteochondral progenitor cells[75]. A key limitation of these studies is the lack of truly quantitative data, and the very limited number of lineage traces performed.

1.3.1.1 Putative Sox9+ SSCs identification in the postnatal skeleton

Sox9 is crucial in skeletal development and chondrogenesis-more specifically. It is one of the twenty SRY-related HMG box-containing (SOX) protein (figure 1.2)[79,80]. The identification of its crucial role in chondrogenesis was made when its heterozygous mutation was found responsible for campomelic chondrodysplasia[81,82]. The heterozygous deletion of the gene in mice produces a similar phenotype. Sox9 is present in diverse other tissues of the organism: hair follicle[83–87], breast[88,89] , liver[88,90], intestine[91] and pancreas[92–94]. Its role in skeletal development is not restricted to fetal life; and Sox9 is a known marker of chondrocytes in postnatal bone[95].

Research in our lab used the Sox9-CreERT mouse model and EdU retention and proliferation assays[58]. Cre-induced recombination results in the expression of tdTomato (tdT) in Sox9+ cells (see section 2.1). Results obtained on mice pulsed at 8 weeks and 6 months of age and

chased for six (6) additional months showed the existence of a population of Sox9+ and EdU-retaining cells [96]. They are localized in the GP and can be considered as slow-cycling (EdU-retaining), self-renewing (Sox9 expression remained over time) and multipotent cells, as evidenced by their differentiation into osteoblasts, chondrocytes and adipocytes during in vitro and in vivo assays. These results are in concordance with recent reports on the major role of Sox9 in putative SSCs population differentiation into chondrogenic, adipogenic and osteogenic cell lineages[97].

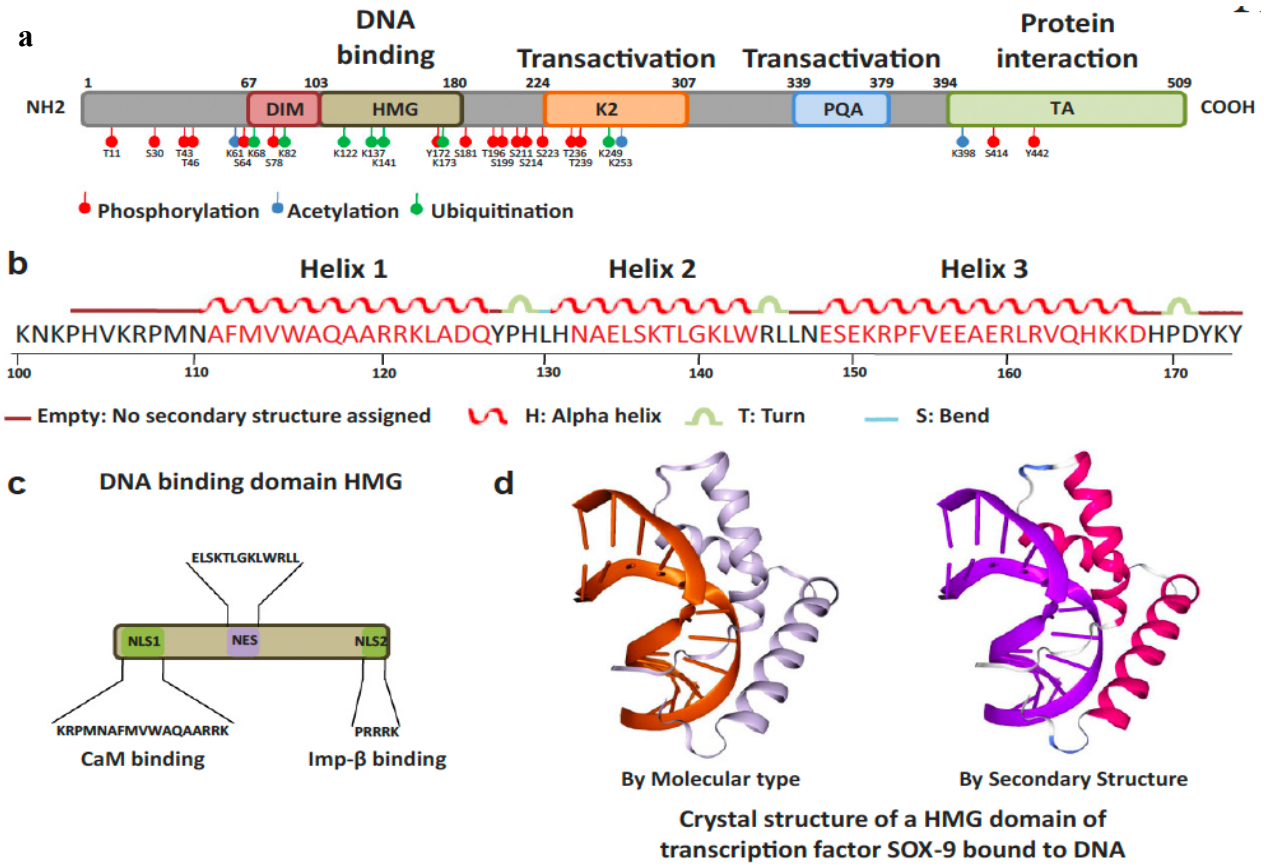

Figure 1.2. Schematic drawing and crystal structure of SOX9.The SOX9 protein has five different domains: the dimerization domain (DIM), followed by the DNA-binding high-mobility group (HMG) domain, two transactivation domains (K2 and PQA) located in a central position, and one at the C-terminal domain (TA). Post-translational modifications identified by phosphorylation sites (red), acetylation sites (blue), and ubiquitination/sumoylation sites (green) are highlighted (a). Schematic diagrams of the SOX9 DNA-binding HMG domain, showing the amino acid sequence involved in the production of its secondary helix structure (b), two independent nuclear localization signal (NLS) sequences that interact with calmodulin (CaM) and importin-β, and nuclear export signal (NES) sequences (c). Crystal structural illustrations of the SOX9 HMG domain (PDB ID: 4EUW) bound to DNA (d) [230].

1.3.1.2 Molecular pathways potentially affecting Sox9+ cells fate and dynamics

Single cell RNA sequencing (scRNA-seq) assessing differential gene expression in clusters of cells from mice bones showed that, in comparison to Sox9- cells of the GP, Sox9+ cells expressed chondrogenesis-related genes *Acan, chondroitin sulfate proteoglycan 4* (*Cspg4)/nerve/glial-antigen 2* (*NG2)*, and *Col2a1*, and early osteogenesis-related genes such as *runt-related transcription factor 2* (*Runx2)* and *Sp7*[98–104]. With respect to skeletal development, self-renewal and asymmetric cell division, genes such as *protein patched homolog 1* (*Ptch1)*, *smoothened* (*Smo)*, *Pth1r*, *Gli2/3*, *5''-nucleotidase ecto (Nt5e)/Cluster of differentiation 73 (CD73)* were also expressed as well as *B lymphoma Mo-MLV insertion region 1 homolog* (*Bmi1)*, linked to stem cell self-renewal[105]. New scRNA-seq analyses performed by members of our lab on young mice bones identified genes involved in the Wnt and Indian hedgehog (Ihh) signaling pathways—two key molecular pathways involved in endochondral ossification—in Sox9+ cells [106–110]. Putative Sox9+ SSCs also express *Pth1r*, another key player in bone development and homeostasis[31,33].

A CellChat analysis performed by our lab, to study the communication pattern between cellular types of the GP, demonstrated molecular crosstalk between several cell types and resting zone chondrocytes (RZ-Ch)—which comprise most SSCs [58]. The RZ-Ch receive canonical and non-canonical Wnt signaling from hypertrophic chondrocytes. Perichondral cells, osteoblasts, and fibroblasts send Hedgehog (Hh), FGF and PTH signals to the RZ-Ch, respectively (figure 1.3).

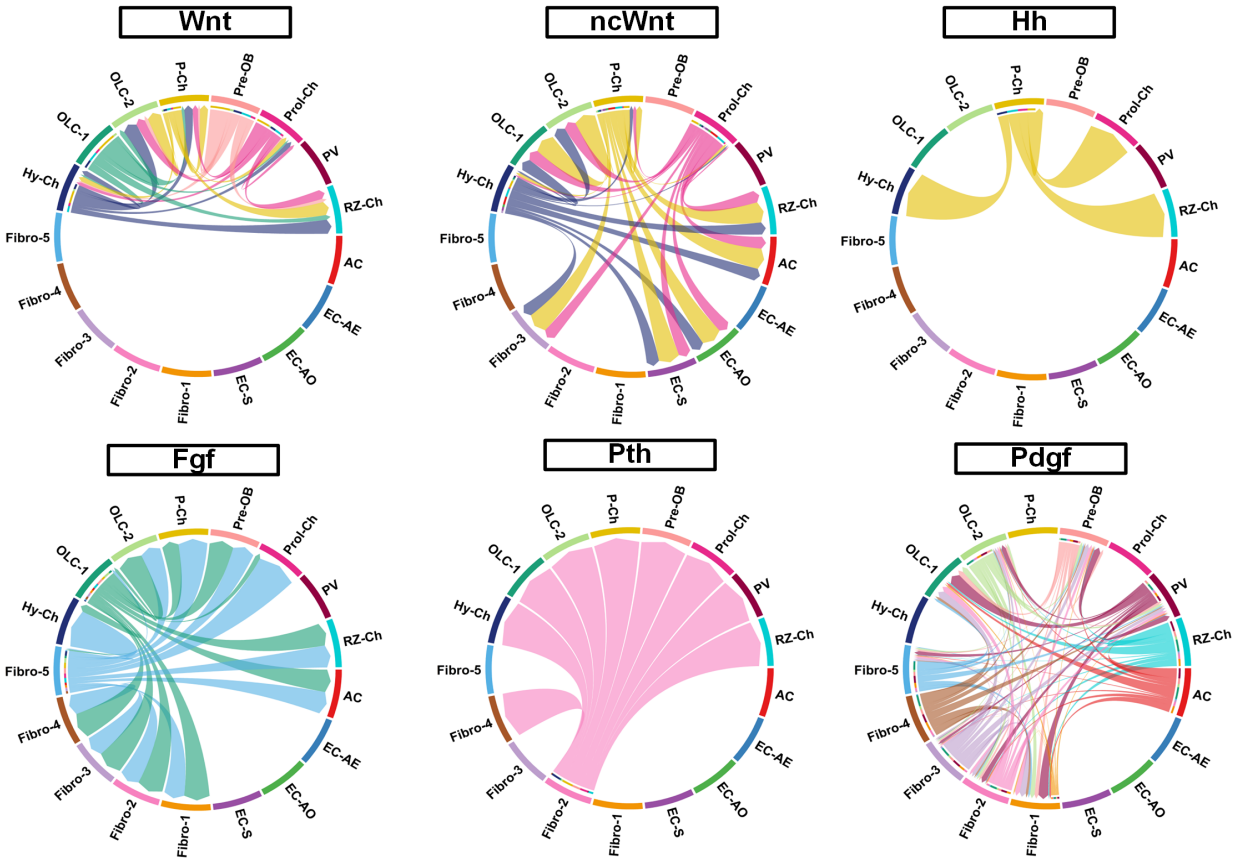

Figure 1.3. CellChat analysis demonstrates molecular crosstalk between several cell types and resting zone chondrocytes, involving mainly Wnt, non-canonical Wnt (ncWnt), Hh, FGF, PTH and PDGF signaling. RZ-Ch: resting zone chondrocytes; AC: articular chondrocytes; EC-AE : endothelial cells – arterial; EC-AO : endothelial cells – arteriolar; EC-S : endothelial cells – sinusoidal; Fibro 1-5: fibroblast-like cells; Hy-Ch: hypertrophic chondrocytes; OLC-1-2: Osteoblast-like cells; P-Ch: perichondral cells; pre-OB: pre-osteoblasts; Prol-Ch: proliferative chondrocytes; PV: perivascular cells. Analysis by B. Tilouche. (Farhat S. et al.)

1.3.2 Mesenchymal Stem cells (MSCs) and bone marrow stromal cells (BMSCs)

The identification of mesenchymal stem cells (MSCs) in bone marrow started in the 19th century. Transplantation of bone marrow or periosteum in highly vascularized region (muscle, skin) of animals, such as rabbits, formed bone tissue. The cell progenitors responsible for such effect will be described later. Friedenstein et al., 1968, identified a subpopulation of cells different from the hematopoietic cell population and responsible for the bone regeneration observed in transplantation assays. These cells are elongated and adhere to plastic dishes in culture. Also, Friedenstein demonstrated the capacity of these single cells to form colonies [111]. They were coined

colony-forming unit-fibroblasts (CFU-Fs) as their properties in vitro resembled the different colony-forming units (CFUs) identified in the hematopoietic system[112]. Further in vivo transplantation assays involving these CFU-Fs, showed the generation of multiple tissues (bone, cartilage and adipose tissue amongst others)[113–115]. They were called osteogenic stem cells or bone marrow stromal cells (BMSCs). These were later referred to as "mesenchymal stem cells" (MSCs)[116–118]. They constitute a fraction of the CFU-Fs. Their multilineage potential has been proven in vitro[119–122]. While remaining poorly defined, they are thoroughly studied and multiple cell markers are now used in their identification (in human and mice tissue): STRO-1[123–125], CD13[121,126], CD29[126], CD44[126–129], CD51[130], CD73[120–122,126–128,131,132], CD90[120–122,126–128,131], CD105(endoglin)[120,121,126–129,131], CD106[120], CD146[122,123,128,129,132], CD151[126], CD164, CD166[120,127,128], CD271[122,128], platelet-derived growth factor receptor alpha (PDGFRα)[114,130,133,134], stem cell antigen -1 (Sca1)[114,133,134], chemokine (C-X-C motif) ligand 12 (CXCL12)[135], nestin[130,135], α-smooth muscle actin (αSMA)[134,136], and connective tissue growth factor (CTGF)[137] -amongst other markers. For clarity, as MSCs are found in various tissues, the term "skeletal stem cells" (SSCs) is preferred to designate stem cells when studying the skeleton.

Throughout the years, multiple in vivo cell populations have been studied using lineage tracing methods—as presented in section 1.3.1. The multilineage potential of these cells, identified in vivo and expressing novel identified markers, is often studied in vitro.

1.4 Sexual dimorphism of skeletal growth and aging

At birth, girls are 1% shorter than boys, but the phenotypic difference between male and female skeleton arises mainly during puberty. This period is a crucial stage for bone mass acquisition in both sexes. It starts and stops earlier with the fusion of the GP in female adolescents[138]. Women reach a lower peak bone mass than men. Boys start puberty later and tend

to develop stronger and bigger bones[139–141]. In this sex, radial bone expansion is favored during growth whereas endocortical bone apposition is in girls. On the contrary, both sexes reach the same bone mineral density. With age, however, bone mineral density decreases; and male bones being stronger and larger, are less prone to fractures, making age-related bone mineral density loss less problematic in this sex[142].

1.4.1 Role of Sex steroids in skeletal sexual dimorphism

Estrogen and testosterone play key roles in the skeletal sexual dimorphism[141,143,144]. Sex steroids have different effects on bone mass. Both sex steroids have an anabolic effect on bones but sex-related variations of this effect at certain stages of the organism development have been reported[141,145–147]. During early puberty, estrogens stimulate bone growth in girls, which start growing earlier than boys. This rapid growth also leads to earlier GP closure (fusion), probably through stem cells exhaustion. Therefore, girls stop growing earlier than boys. In boys, some of the testosterone is converted to estrogen to stimulate bone growth-amongst other things. But the later onset of puberty in boys results in later and longer phases of bone growth. It has also been reported an inhibitory action of estrogen on female bone growth during the early stages of puberty[148]. This latter phenomenon would further accentuate the disparity between female and male bone mass acquisition at puberty. The advent of conditions implying sex steroids deficiencies in mature organisms provided a more thorough understanding of sex steroids-dependent bone acquisition and maintenance. Sex steroids deficiencies, like the estrogen deficiency happening in women during menopause and the secondary testosterone deficiency in men taking anti-testosterone therapy (for prostate cancer) induce bone loss[149]. In rodents, ovariectomy (estrogen deficiency) provokes bone loss and orchiectomy (testosterone deficiency) induces a decrease radial bone growth[150]. Sex steroids play a significant role in skeletal development and homeostasis.

1.4.2 Role of the growth hormone–insulin growth factor 1 (GH/IGF-1) axis in skeletal sexual dimorphism

The GH/IGF-1 axis plays an important role in skeletal sexual dimorphism[144,151]. During early puberty, IGF-1 levels are superior in boys versus girls. This contributes to a greater mass acquisition in boys. In mice, GH receptor deficiency or knockout, resulting in low IGF-1 levels, provokes a decrease in radial bone growth. IGF-1 treatment reestablishes the physiologic phenotype[152]. This hormonal axis also interacts with sex steroids in establishing the different skeletal phenotypes between the two sexes.

1.4.3 Sexual dimorphism in skeletal cells

The sexual dimorphism in osteoclast fate decision is well-known. Sex steroids decrease osteoclastic bone resorption[153,154]. Both estrogen and testosterone inhibit osteoclast differentiation while stimulating osteoclast apoptosis[155–157]. They limit bone resorption during puberty and bone formation takes over. Bone growth is maximal during that period. In mice, the female skeleton houses more trabecular osteoclasts[158,159]. This supposes a higher baseline bone resorption rate in females.

1.5 Skeletal system aging and senescence

Aging is the main risk factor for multiple conditions[160–162]. In the skeletal system, conditions such as osteoarthritis (OA) and osteoporosis which increases bone vulnerability to fracture are age-related[163]. Also, the regeneration potential of bones decreases as the organism ages. Recovery from bone injury is quicker and more complete in young individuals in comparison to aged ones. As the

population ages in Canada, understanding the pathways involved in skeletal aging can provide ways of addressing these situations and conditions more effectively.

1.5.1 Cellular senescence and aging

Diseases affecting the aged organisms have been linked to cellular senescence[164,165]. In this latter state, cells undergo phenotypic alterations, stop proliferating, become lineage-biased and express a pro-inflammatory phenotype [166] [167,168]. This is known as Hayflick's theory of aging[169,170]. He noticed that cells had a finite proliferation capacity-contrary to the belief that they possess immortality in vitro. It is explained by their senescence after multiple passages due to telomere shortening and somatic mutations accumulation. A corollary of this theory known as the stem cell theory of aging, stipulates that since stem cells are responsible for generating differentiated cells, stem cell depletion or senescence is likely the culprit in age-related conditions [167]. For instance, studies conducted into our lab showed the existence of a self-renewing stem cell population in the bone tissue[58]. This population of cells was present in aged mice bone. Even though we did not compare the numbers of stem cells between age group, since their presence was asserted in the aged skeleton, we favored the senescence hypothesis as an explanation for the age-related bone changes in this work.

Senescence leads to loss-of-function and the blunting of stem cells capacity to commit toward differentiated cells constituting the tissue. Due to this fact, conditions develop, and injury repair becomes less effective[171,172].

Cellular senescence has recently begun to be seen as an escape/defense mechanism used by cells to prevent further division after assessing the presence of damaged DNA, thus preventing cancer in living organisms[173]. Intrinsic factors, like genome instability after extended proliferation

period, induce the exit of the cell from the cell cycle and its entering into senescence. DNA damage also comes from extrinsic factors like ultraviolet (UV) radiation or oncogenic viruses. The pathways involved in senescence include several cell cycle inhibitory proteins such as $p15^{INK4b}$, $p16^{INK4a}$, $p19^{ARF}$ encoded at the INK4/ARF locus [105,167,174]. Their activation leads to cellular senescence, and their presence in tissues can be used as a marker of senescence.

1.5.2 Cellular senescence in bone cells

SSPCs senescence has not yet been fully studied, as SSPCs have not been fully described and characterized. Farr et al, 2019, put into evidence increased $p16^{INK4A}$ levels in vivo in osteoprogenitor cells, osteoblast and osteocytes of 24-month-old C57BL/6 mice in comparison to young 6-month-old ones. This observation was made in both males and females[175]. On the molecular level, BMI1, a polycomb group protein that represses the INK4/ARF locus, has been manipulated to understand the role of senescence in pathological phenotypes in bones. Consistent expression of INK4/ARF proteins in BMI1 knockout mice led to an osteopenic phenotype [176]. Also, transplantation assays with aged mice cells have been performed to uncover a possible role of the senescence-associated secretory phenotype (SASP) in age-related bone conditions. Young healthy mice injected with senescent articular cartilage cells developed osteoarthritis when re-evaluated three months after injection [177]. Both intracellular and extra-cellular factors are at play in the senescence of bone tissue and their associated pathological implications.

As postulated by the stem cell theory of aging, it would be interesting to go beyond mature cells and study the phenomenon in SSPCs, as we might find the answer to the etiology of certain conditions affecting bones and their inability to recover when confronted with injury.

Our lab assessed the presence of self-renewing Sox9+ SSCs in the young skeleton (section 1.3.1.1), but also in the mature one[58]. Chases were performed in six-month-old mice, and the

fraction of putative Sox9+ SSCs retaining EdU in long chases (over a six-month period) remained constant. This confirmed the existence of putative self-renewing and multipotent Sox9+ cells in the skeleton of mature mice. Neither their number nor their proliferation kinetic was assessed during this assay. Further investigations assessing senescence, loss of function or exhaustion of putative SSCs is needed.

1.6 Rationale

Based on the observations and previously mentioned studies, it is likely that cellular proliferation and senescence play a role in the blunted regenerative capacity of SSPCs during aging (see section 1.3.1.1). Identifying the molecular pathways orchestrating SSPCs proliferation and senescence could provide actionable targets that can be manipulated to improve SSPCs regenerative capacity in older organisms.

1.7 Hypothesis

I hypothesize that decreased proliferation rate and increased cellular senescence of SSPCs are responsible for the bone loss taking place with age and the increased prevalence of bone conditions in older animals. I also hypothesize that pharmacological targeting of specific pathways involved in bone development and skeletal cell proliferation and differentiation throughout life can affect SSPCs fate decisions.

1.8 Specific aims

To test my hypothesis, I will pursue the following aims:

Aim 1: To study SSPCs proliferation and senescence in aged mice.

Bone loss is experienced in the organism as it ages. SSPCs presence in the bone does not prevent this fact. I hypothesize that SSPCs become senescent, and their proliferation rate decreases in the aging bone. To verify such a claim, I will assess EdU incorporation and SA-β-gal expression of SSPCs in aged mice in vivo and in vitro and compare the results with data collected on young mice.

Aim 2: To pharmacologically manipulate SSPCs fate decisions.

Multiple pathways and paracrine/endocrine factors are involved in bone development and growth. The pharmacological influence of these pathways and factors can change SSPCs fate decisions and alleviate age-related bone loss. In this part of the project, the effect on SSPCs of pharmacological compounds such as PTH, TAM, 20(S)-OHC, purmorphamine and cyclopamine will be assessed in young mice in vivo and in vitro.

Chapter 2: Materials and methods

2.1 Animals

The mice used in this project were approved by the Animal Care Committee of the University of Ottawa and all experiments done per the protocols submitted for review and approval to the committee.

Two mouse models were used: 1) The Sox9-CreERT; Ai14 mouse model, and 2) the C57Bl/6 mouse strain. The C57Bl/6 mice were purchased from Charles River (strain code: 027). The Sox9-CreERT: Ai14 mouse model is a transgenic mouse line generated on the C57Bl/6 background by the breeding of two mouse lines: 1) Tg(Sox9-cre/ERT2)1Msan/J; MGI:5009223[92], a driver line in which expression of the CreERT2 BAC transgenic is driven by the Sox9 promoter; and 2) B6.Cg-Gt(ROSA)26Sor$^{tm14(CAG-tdTomato)Hze}$/J; MGI : J:155793[178], a Rosa26 LoxP-STOP-LoxP fluorescent Cre-reporter mouse line. Both strains were purchased from the Jackson Laboratory (stock No.018829 and 007914, respectively).

Unless stated otherwise, the experimental samples included femurs (in vivo) and cells (in vitro) of mice of both sexes and of two age groups: young (8-week-old) and aged (1-year old). In experiments where the effect of age was assessed, samples from 8-week-old mice served as controls. Mice were housed per the Canadian Council for Animal Care guidelines on a 12-hour light/12-hour dark cycle with ad libitum access to food and water.

2.2 Genotyping

Mice of the Sox9-Cre-ERT; Ai14 model were genotyped and homo- or heterozygous mice for Cre and Ai14 were included in the study. For DNA extraction, ear punches were taken in a

1.5ml Eppendorf tube at weaning and 120 µl of lysis buffer (50mM NAOH) were added. The samples were heated at 95°C on a heat block for 20 minutes. Neutralization was achieved by adding 30µl of 1M Tris-hydrochloric acid (Tris-HCl) to the tubes. Debris and hair were separated from the mix by spinning it down in a microcentrifuge (VWR, micro star 21) at 14500 rpm (revolutions per minute) for 5 minutes. Tubes were stored at 4°C in the fridge until the polymerase chain reaction (PCR).

The PCR mix was made of 2xThermus aquaticus (Taq) master mix (FroggaBio, Cat. No. FBTAQM10), a solution of Taq DNA Polymerase, deoxynucleotide triphosphates (dNTPs), Magnesium ions (Mg2+) and reaction buffer to which were added nuclease-free water, primers (see table 2.1) and the DNA template.

Table 2.1. Primer sequences used for Cre and Ai14 genotyping.

Gene	Primer type	SEQUENCE 5' → 3'	Expected gene length
Cre	Transgene forward	GCG GTC TGG CAG TAA AAA CTA TC	~100 base pairs (bp)
	Transgene reverse	GTG AAA CAG CAT TGC TGT CAC TT	
Ai14	Wild type forward	AAG GGA GCT GCA GTG GAG TA	297bp
	Wild type reverse	CCG AAA ATC TGT GGG AAG TC	
	Mutant forward	CTG TTC CTG TAC GGC ATG G	~200bp
	Mutant reverse	GGC ATT AAA GCA GCG TAT CC	

The thermal cycler setting temperatures are presented in the next table.

Table 2.2. Thermal cycler settings for genotyping.

Gene	Initialization	Denaturation	Annealing		Elongation	Hold
Cre	1x	30x			1x	
	94°C (3mns)	94°C (30 sec)	54°C (30 sec)	72°C (1mn)	72°C (10 mns)	12°C
Ai14	1x	35x			1x	
	95°C (1mn)	95°C (30 sec)	61°C (30 sec)	72°C (1 mn)	72°C (5mns)	10°C

A 2.5% agarose gel with SYBRsafe DNA staining (Thermofisher, Cat. No. S33102) was used for electrophoresis.

2.3 Pharmacological compounds

Multiple pharmacological compounds were prepared, injected or added to cell media. For in vivo experiments exclusively, 5-ethyl-2'-deoxyuridine (EdU) (12.5mg/kg) was used for the proliferation assay and parathyroid hormone (PTH) (1-34) (400ng/g) was assessed for its potential effect on the Sox9+ cell population. For in vivo and in vitro experiments involving the Sox9;Ai14 mouse model, tamoxifen (TAM) (50mg/kg), a selective estrogen receptor modulator[179] , was injected intraperitoneally to induce tdTomato expression in Sox9+ cells (table 2.3). In C57Bl/6 mice, its effect was tested on skeletal cells proliferation and senesescence in the femur's growth plate(GP).

For in vitro experiments, compounds were added to the media during plating, at refeeding and media change time. The following were tested : PTH (1-34) (a synthetic parathyroid hormone)[180], purmorphamine (a Hh agonist)[181–185], 20(S)-hydroxycholesterol (an activator of the Smo and Hh signaling pathways)[186–189] and cyclopamine (an inhibitor of the Hh pathway)[190–192] (table 2.3).

The details about the aforementionned products (company of purchase, catalog number, vehicle, preparation condition, stock concentration, injection/seeding dosage and injection route) is presented in table 2.3. TAM necessitated stirring in a water bath at 55°C for dissolving. 20(S)-OHC and cyclopamine instantly dissolved at room temperature in EtOH whereas a sonicator (VWR Symphony™, 97043-936) was used for the dissolution of EdU and PTH (1-34) in their respective vehicles. All compounds were prepared in sterile conditions under a biosafety cabinet class 2 (BSC2) and stored in the freezer at -20°C in between uses.

Table 2.3: Pharmacological compounds

Drug	Company	Cat. No.	Vehicle	Preparation Condition	Stock concen-tration	Dose	Adminis-tration
TAM	Sigma-Aldrich	T5648	Corn Oil	Stirring in 55°C water bath	10mg/ml	50mg/kg	IP
EdU	Sigma-Aldrich	900584	PBS	RT	2.5mg/ml	12.5mg/kg	IP
PTH (1-34)	Tocris	3011	ddH_2O	RT	97µM	400ng/g 50nM	SC/ in vitro
20(S)-OHC	Tocris	4474	EtOH	RT	5mM	10µM	In vitro
Purmorpha-mine	Tocris	4551	0.5% DMSO	RT	1mM	2µM	In vitro
Cyclopamine	Tocris	1623	EtOH	RT	2.5mM	5-10µM	In vitro

TAM: Tamoxifen, IP: intraperitoneal, SC: subcutaneous, RT: room temperature, DMSO: dimethyl sulfoxide, PBS: phosphate-bufffered Saline, ddH_2O: distilled water, EtOH: ethanol, Cat. No.: catalogue number.

2.4 Bone tissue processing for in vivo experiments

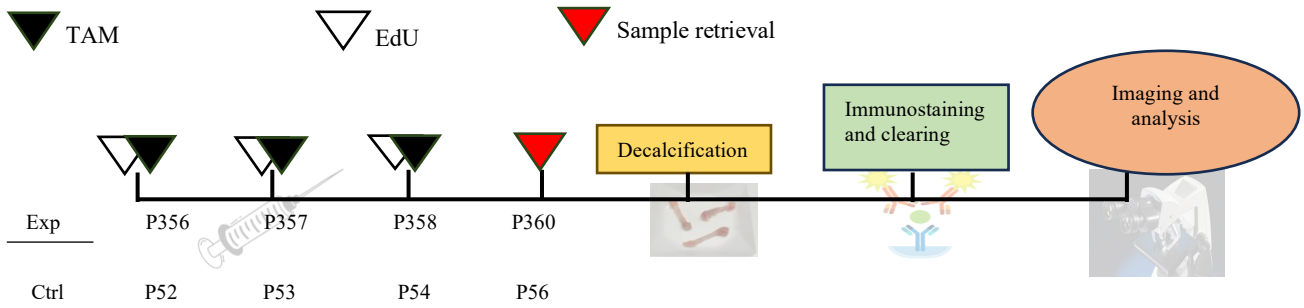

Figure 2.1. Procedural workflow for proliferation assay and senescence quantification. Mice received three TAM and EdU injections on consecutive days. Femurs were harvested two days after the last injection(s) and processed for quantitative imaging and analysis (section 2.4.1 to section 2.4.8 of methods).

2.4.1 Bone harvest and processing

When mice reached 8-week and 1-year old, they received three injections of TAM and/or EdU intraperitoneally. Two days after the last injection(s), they were euthanized with carbon dioxide (CO_2) followed by cervical dislocation. In the experiment where PTH was tested, four injections of PTH were administered concomittantly with the three doses of TAM and EdU in the three last days of injection. Euthanasia took place two days after the last injections. Dissected femurs were fixed overnight in 4% paraformaldehyde (PFA) (Electron Microscopy Sciences, Cat. No. 15710). They were washed in PBS the following day and left to decalcify in ethylenediaminetetraacetic acid (EDTA) for 14 days with solution changes three times per week.

Decalcified femurs were embedded in 4% low-gelling agarose (Fisher scientific, Cat. No. BP160-500) and cut in 300µm-thick sections on the vibratome (Leica VT 1200S) with 0.01" ceramic blades (Cadence Inc., EF-INZ10). Sections were stored in PBS at 3-8°C until needed.

2.4.2 Senescence-associated beta-galactosidase (SA-β-gal) expression detection

Before blocking and permeabilization, sections were incubated in the CellEvent™ Senescence Green Detection Kit (Invitrogen, Cat. No. C10851).) for 16-18 hours in an incubator at 37°C without CO_2 and washed before pursuing with the following staining steps. The reaction solution was prepared per the manufacturer's instructions. The buffer was left in a bath to reach 37°C and 400µl of reaction solution was prepared per section. The green fluorescent probe was added to the reaction buffer at a 1:1000 dilution.

2.4.3 Blocking and permeabilization

Sections were blocked and permeabilized with blocking buffer: 5% donkey serum and 0.3% Triton X-100 in wash buffer (0.1M Tris, 0.15M NaCl, 0.05% tween 20, 20% DMSO, pH:7.5). Blocking and permeabilization took place on a shaker at room temperature for one hour.

2.4.4 EdU proliferation assay

For the EdU proliferation assay, mice were injected with three doses of EdU as mentioned earlier and after blocking and permeabilization, sections were incubated at room temperature overnight in the EdU reaction solution prepared with components of the Click-iT™ EdU Cell Proliferation Kit for Imaging with Alexa Fluor™ 488 or 594 dye (Thermofisher, Cat. No. C10337 and C10639 respectively) (see table 2.4). The EdU reaction solution was prepared as recommended on the provider's website. The next day, sections were rinsed five times in wash buffer and further immunohistochemistry (IHC) steps pursued.

2.4.5 Immunohistochemistry

Sections were incubated in blocking buffer with diluted primary antibodies (see table 2.4 for concentration) overnight at room temperature. The following day, sections were rinsed five times in wash buffer, for one hour each, and incubated overnight at room temperature with specific secondary antibodies and 4',6-diamidino-2-phenylindole dihydrochloride (DAPI) (Thermofisher, Cat. No. D1306). DAPI was reconstituted in DMSO at 2mg/ml and used 1:500 for nuclear counterstaining.

For Sox9 signal amplification, sections were treated with the Streptavidin/Biotin Blocking Kit (Cedarlane, VECTSP2002) as per the manufacturer's guidelines.

2.4.5.1. Antibodies

Primary and secondary antibodies (see table 2.4) were reconstituted when needed as per provider's recommendations. The reconstituted volume was later mixed 1:1 in glycerol to prevent freezing at the storage temperature of -20°C, except for antibodies purchased into a liquid form and with glycerol listed as a component.

2.4.6 Histodenz clearing and slide mounting

Immunostained sections were optically cleared overnight in 88% histodenz (Sigma Aldrich, D2158-100G) in Tris-buffered saline (TBS) with 0.1% tween 20 and 0.01% sodium azide (NaN_3) (pH=8.5, RI=1.46). The refractive index (RI) was measured using a handheld refractometer (Atago). Sections were mounted in the same solution on slides (Sigma Aldrich, Cat. No. 12-550-15) with custom-designed silicone spacers (Grace Biolabs), covered with size 1.5 coverslips (Thermofisher, Cat. No. 22-050-245).

2.4.7 Confocal microscopy

Images were acquired on the Leica TCS SP8 confocal microscope with the 20× multiple immersion objective (NA 0.75) with the LAS X software. This microscope is equipped with three photomultiplier tubes (PMT), two hybrid detectors (HyD) and five lasers: blue diode (405 nm), argon (458,476, 488, 496 and 514 nm) and three helium neon (543, 594 and 633 nm). Images were taken at a 1024x1024 resolution and a frequency of 400Hz, in bidirectional mode without zoom. For imaging chondrogenic micromasses produced in vitro, , the 10x dry objective was used (NA=0.40) and images were acquired at a frequency of 200Hz.

Table 2.4. Antibodies/reagents

Antibody/reagent	Catalogue No.	Company	Clonality	Host Species	Dilution
Click-iT™ EdU Cell Proliferation Kit- Alexa Fluor™ 488	C10337	Thermofisher	-	-	-
Click-iT™ EdU Cell Proliferation Kit- Alexa Fluor™ 594	C10639	Thermofisher	-	-	-
Anti-Sox9	AF3075	R&D systems	Poly	Goat	1/50
Anti-$P16^{INK4A}$	Ab211542	abcam	Mono	Rabbit	1/200
Anti-$P16^{INK4A}$	A23882	abclonal	Poly	Rabbit	1/200
Anti-ALP	AF2910	Cedarlane/R&D	Poly	Goat	1/400
Anti-goat Alexa Fluor 633	A21082	Thermofisher	Poly	Donkey	1/200
Anti-goat biotin	A16009	Thermofisher	Poly	Donkey	1/200
Alexa Fluor 633 streptavidin- conjugate	S21375	Thermofisher	-	-	1/200
anti-rabbit Alexa Fluor 633	A21070	Thermofisher	Poly	Donkey	1/1000
BODIPY™ 493/503	D3922	Thermofisher	-	-	1/300
DAPI	D1306	Thermofisher	-	-	1/1000
anti-CD31biotin	5011513	Fisher Scientific	Mono	Rat	1/100
Anti-CD235a biotin	orb447561	Biorbyt	Poly	Rabbit	1/100

2.4.8 Image Analysis

Resulting images were transferred in Imaris v10.2.0 (Bitplane) where tdT+ cells or DAPI were segmented in the GP area as surfaces and spots respectively. The statistics (area, mean signal intensity, etc.) for each surface or spot segmented were transferred to XiT for analysis [193].There, the percentage of cells positive for every marker tested was quantified and later graphed. Accurate gating on X and Y axis was possible with fluorescence minus one (FMO) control stainings (figure 2.2).

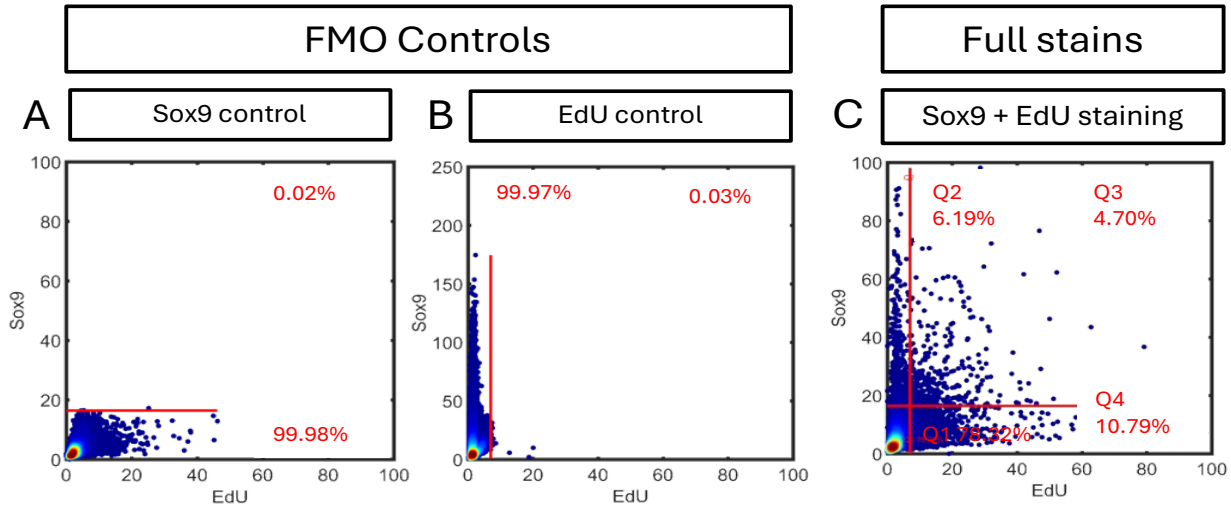

Figure 2.2 XiT plots of two fluorescence minus one (FMO) controls and a full stain. A) A Sox9 control: section was incubated in the secondary anti-goat Alexa Fluor 633 without a previous incubation in the primary anti-Sox9 antibody. B) An EdU control: section was taken from a mouse which did not receive EdU shots but whose bone sections were treated with the Click It EdU Alexa Fluor 488 or 594 reaction kit. C) A full experimental stain: the section was treated with primary and secondary antibodies in the case of Sox9 detection and the mouse of which sections were treated with Click It EdU Alexa Fluor 488 or 594 reaction kit, received three EdU shots. Double positive cells are quantified in Q3.

2.5 Skeletal cell processing for in vitro experiments

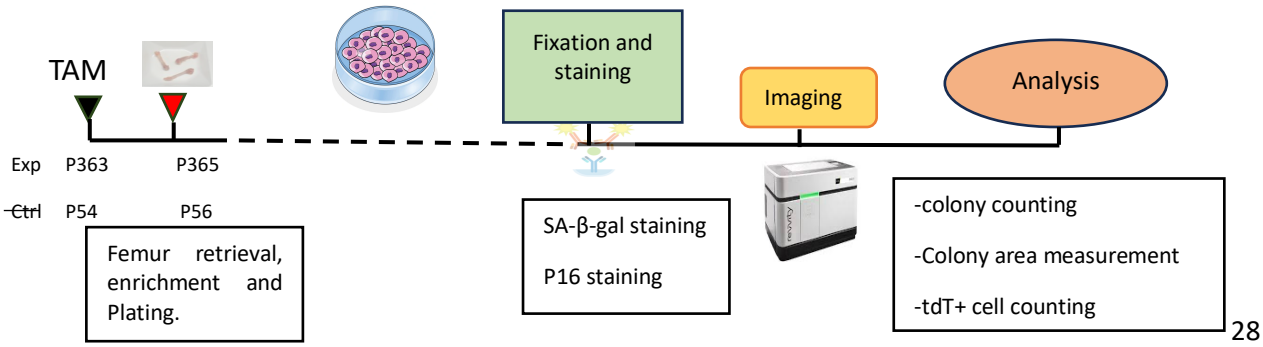

Figure 2.3. Procedural workflow for skeletal cell processing. Mice were injected with TAM, followed by femur harvest two days later. Bones were then dissociated, skeletal cells isolated and placed in culture. After fixation and staining, quantitative imaging and analysis is performed. (Section 2.5.1 to section 2.5.4 of methods)

2.5.1 Skeletal cell isolation

For in vitro experiments, mice were injected with one dose of TAM. They were euthanized two days later with CO_2 followed by cervical dislocation. Femurs were harvested. They were crushed in a mortar for mechanical dissociation and the crushed bones were later left 45 minutes on a shaker at 37°C in an enzyme mix made of 1mg/ml of STEMxyme 1 (Worthington Biochemical Corporation, LS004106), 1mg/ml of dispase II (Thermofisher, Cat. No. 17105041) and 2% volume/volume(v/v) of fetal bovine serum (FBS) in medium 199 (Thermofisher, Cat. No.11150059). The enzymatic solution with the bone fragments and cells was later passed through a 100µm cell strainer (Ultident Scientific, Cat. No. 229485) and neutralized with a neutralization mix of 3ml of FBS, 27ml of PBS and 60µl of 0.5M EDTA. The solution was centrifuged in an Eppendorf centrifuge (5810R) at 400 rcf (relative centrifugal force) at 4°C for five (5) minutes and the sediment of cells resuspended in mouse Mesencult™ basal medium (STEMCELL technologies, Cat. No. 5513).

2.5.2 Skeletal cell enrichment

The primary single cell suspension was magnetically depleted of CD45+, TER119+, CD235a+ and CD31+ hematopoietic and endothelial cells using the EasySep™ Mouse Mesenchymal Stem/Progenitor Cell Enrichment Kit (STEMCELL technologies, Cat. No. 19771) with the addition of anti-CD31(Fisher Scientific, Cat. No. 5011513) and CD235a (Biorbyt, Cat. No. orb447561) biotinylated antibodies. The solution was centrifuged at 400 rcf at 4°C for five minutes. Live cells were counted using an automatic cell counter (Invitrogen, Countess 3 FL) and plated in 24-well plate (Ibidi, #1.5H glass coverslip bottom, Cat. No. 82427) at a density of

$5x10^4/cm^2$, in mouse Mesencult^{TM} basal medium (STEMCELL technologies, Cat. No. 5513). At plating, compounds (see section 2.3) were added to the wells at the seeding concentration presented in table 2.3. For each compound, at least three biological replicates and three technical replicates were included in the study. The vehicle of each compound: PBS (metformin vehicle), ethanol (20S-hydroxycholesterol and cyclopamine vehicle) or DMSO (purmorphamine vehicle) was added to the wells that were analyzed as controls.

2.5.3 Skeletal cell senescence detection: SA-β-gal detection and $p16^{INK4A}$ staining

After seven to 13 days of culture, cells were fixed with 2% PFA (Electron Microscopy science, Cat No. 15710) in PBS for 10 minutes at room temperature, protected from light. Cells were later washed with 1% FBS in PBS to remove the fixative solution.

For SA-β-gal detection, the working solution was prepared by adding the green probe to the prewarmed (37°C) buffer (CellEvent™ Senescence Green Detection Kit, Invitrogen, Cat. No. C10851) (see table 2.4). The plates were later covered with plastic film (parafilm) and left overnight (16-18 hours) in an incubator at 37°C without CO_2. After incubation, cells were washed with PBS, blocked and permeabilized with 5% donkey serum and 0.3% Triton X-100 in PBS. When $p16^{INK4A}$ detection was pursued, cells were incubated with anti-$p16^{INK4A}$ antibody (abclonal Cat. No. A23882 or Abcam, Cat. No. ab211542, 1/200 dilution) in PBS at 4°C for 3-4 hours. They were next washed with PBST, a mix of PBS and 0.1% tween 20 (Sigma Aldrich, Cat. No. P1379) and incubated at 37°C for 1 hour with donkey anti-rabbit Alexa Fluor 633 conjugate (Thermofisher, Cat. No. A21070, 1/1000 dilution from stock concentration). Nuclei were counterstained with DAPI (Thermofisher, Cat. No. D1306, 1/1000 dilution from stock

concentration of 2mg/ml prepared in DMSO) for five minutes at room temperature. Plates were stored at 3-8°C in the fridge until imaging.

2.5.4 Skeletal cell imaging

Plates were imaged in non-confocal mode with the 20X water immersion objective of the Operetta CLS™ High-Content Analysis System (Revvity, Part # HH16000020). The 365nm, 475nm, 550nm and 630nm light emitting diodes (LEDs) were used to respectively excite DAPI, SA-β-gal, tdT and Alexa Fluor 633. Colonies, their size, cell population, tdT+, SA-β-gal+, $p16^{INK4A}$+ and double (tdT+ and $p16^{INK4A}$+, tdT+ and SA-βgal+) and triple-positive (tdT+, $p16^{INK4A}$+ and SA-β-gal+) cells were quantified in the Harmony software (V5.2, PhenoLOGIC™). The positive cells were determined with FMO controls for tdT, SA-β-gal and $p16^{INKA}$. They were, respectively, wells in which cells from Cre-; Ai14+ mice which also received one TAM injection were plated, wells incubated at 37°C without CO_2 with the CellEvent™ Senescence Green Detection Kit (Invitrogen, Cat. No. C10851) buffer solution to which the green probe was not added, and wells incubated in the secondary Alexa Fluor 633 without a previous incubation in the primary anti-$p16^{INK4A}$ antibody. Every other step of the staining process went as described for the full stains for these FMO controls. Results from cells of 8-week-old mice were analyzed and used as controls in experiments were aged and young mice were compared. The vehicle-containing wells were analyzed as controls when the pharmacological compounds were tested. The quantitative data were transferred into GraphPad Prism v.10.5.0 for statistical analysis and comparison between age and sex groups and between compounds.

2.6 In vitro differentiation potential assessment

To assess the differentiation potential of skeletal stem cells with age, mice were treated as described in section 2.5.1. Enrichment was not performed. Cells were counted using an automatic cell counter (Invitrogen, Countess 3 FL) and seeded at a density of $5x10^4/cm^2$ in triplicate, in mouse Mesencult™ basal medium (STEMCELL technologies, Cat. No. 5513) in 24-well plates, 6-well plates and 10 cm plates respectively for osteogenic, adipogenic and chondrogenic differentiation. After 14 days in culture, cells reached around 100% confluency, the mouse Mesencult™ basal medium was removed and differentiation media added to the wells. From this point forward, cells were cultured into Mesencult ™ Osteogenic stimulatory kit (STEMCELL technologies, Cat. No. 05504) and Mesencult™ adipogenic differentiation media (STEMCELL technologies, Cat. No. 05507) in their original plates for the osteogenic and adipogenic differentiation assessment experiments. In the case of chondrogenic differentiation, cells were transferred and aggregated in 15 ml tubes at the time of changing the mouse Mesencult™ basal medium to the Mesencult™-ACF chondrogenic differentiation media (STEMCELL technologies, Cat. No. 05455). All media were prepared per the manufacturer's guidelines.

After 11 days in osteogenic and adipogenic differentiation media and 21 days in chondrogenic differentiation media, cells and micromasses (in the case of chondrogenic differentiation) were fixed in 4% PFA (Electron Microscopy Sciences, Cat. No. 15710) in PBS. They were later blocked in 10% donkey serum and 0.3% triton X-100 in PBS. Cells and micromasses were later incubated in BODIPY™ (4,4-Difluoro-1,3,5,7,8-Pentamethyl-4-Bora-3a,4a-Diaza-s-Indacene) 493/503 (Thermofisher scientific, Cat. No. D3922, 1/300 dilution) and the primary antibodies against alkaline phosphatase (ALP) and Sox9 (see table 2.4) for three hours at room temperature to respectively put into evidence the adipogenic, osteogenic, and

chondrogenic differentiation potential of tdT+ cells. Cells incubated in primary antibodies were later washed twice in PBS and incubated in the secondary donkey anti-rabbit Alexa fluor 633 antibody (Thermofisher, Cat. No. A21082, 1/1000 dilution from stock concentration) for one (1) hour at room temperature in the dark. BODIPY™ and secondary antibodies excess were washed once in PBS and nuclei counterstained with DAPI (Thermofisher, Cat. No. D1306) from 2mg/ml stock at a dilution of 1/1000 in PBS. Cells and micromasses were stored in the fridge until acquisition.

Osteocytes in 24-well plates were imaged on the operetta CLS™ high content analysis system as described in section 2.5.4. Adipocytes formed in 6-well plates were imaged on the same system with the 5x Air objective, in non-confocal mode with the 475nm LED exciting BODIPY™. The ossicles were mounted in 88% Histodenz in TBS and imaged on the Leica TCS SP8 confocal microscope with the 10X dry objective, at a 200Hz speed. Images were taken at a 1024x1024 resolution. Images from both systems were qualitatively analyzed in the Harmony 5.2 software in the case of images taken by the Operetta and in Imaris v.10.2.0 (Bitplane) for images acquired on the Leica TCS SP8 confocal microscope. Double positive (tdT+ and differentiation marker positive) cells were identified. Cells from 8-week-old mice were assessed as controls.

2.7 Graphs and Statistics

Quantitative data from all experiments were analyzed in Prism v.10.5.0 (GraphPad, San Diego, CA) and the statistically significant difference per age and sex group reported. Student's t test and two-way ANOVA were used and the results reported on graphs as mean +/- standard deviation. A p value < 0.05 was used to determine significance for all statistical tests performed.

Chapter 3: Effect of sex and age on Sox9+ SSPCs proliferation and senescence

3.1 SSPCs proliferation and senescence rate with sex and age in vivo

As an organism ages, its bones become more fragile and susceptible to injuries such as fractures[163]. This is reflected in the increased prevalence of degenerative diseases and injuries in the elderly population. My objective in this part of the project was to evaluate the SSPCs population senescence level in aged (1-year-old) mice and compare with young (8-week-old) ones. I hypothesize that a decreased proliferation rate in SSPCs and their entry into senescence is responsible for these alterations in bone physiology in vivo.

For studying SSPCs proliferation and senescence in vivo in aged mice, I administered intraperitoneally 50 mg/kg of tamoxifen (TAM) and 12.5mg/kg of EdU every day for three consecutive days to 1-year-old Sox9-CreERT; Ai14 mice to induce the expression of tdT in Sox9+ cells and their progeny (see section 2.4). The mice were euthanized two days after the last injections and femurs fixed, embedded in agarose and sectioned[193]. Sections from young (8-week-old) mice were analyzed as controls.

Two sets of staining were performed. First, for evaluating the proliferation rate of SSPCs in aged and young mice of both sexes, a set of sections was treated with the Click-IT EdU Alexa Fluor 488 cell proliferation kit and stained with anti-Sox9 antibody. DAPI was used as a nuclear counterstain. Sections were later optically cleared, mounted, and imaged. The tdT+ cells of the growth plate (GP) were segmented in Imaris v10.2.0 (Bitplane) (figure 3.1 A).

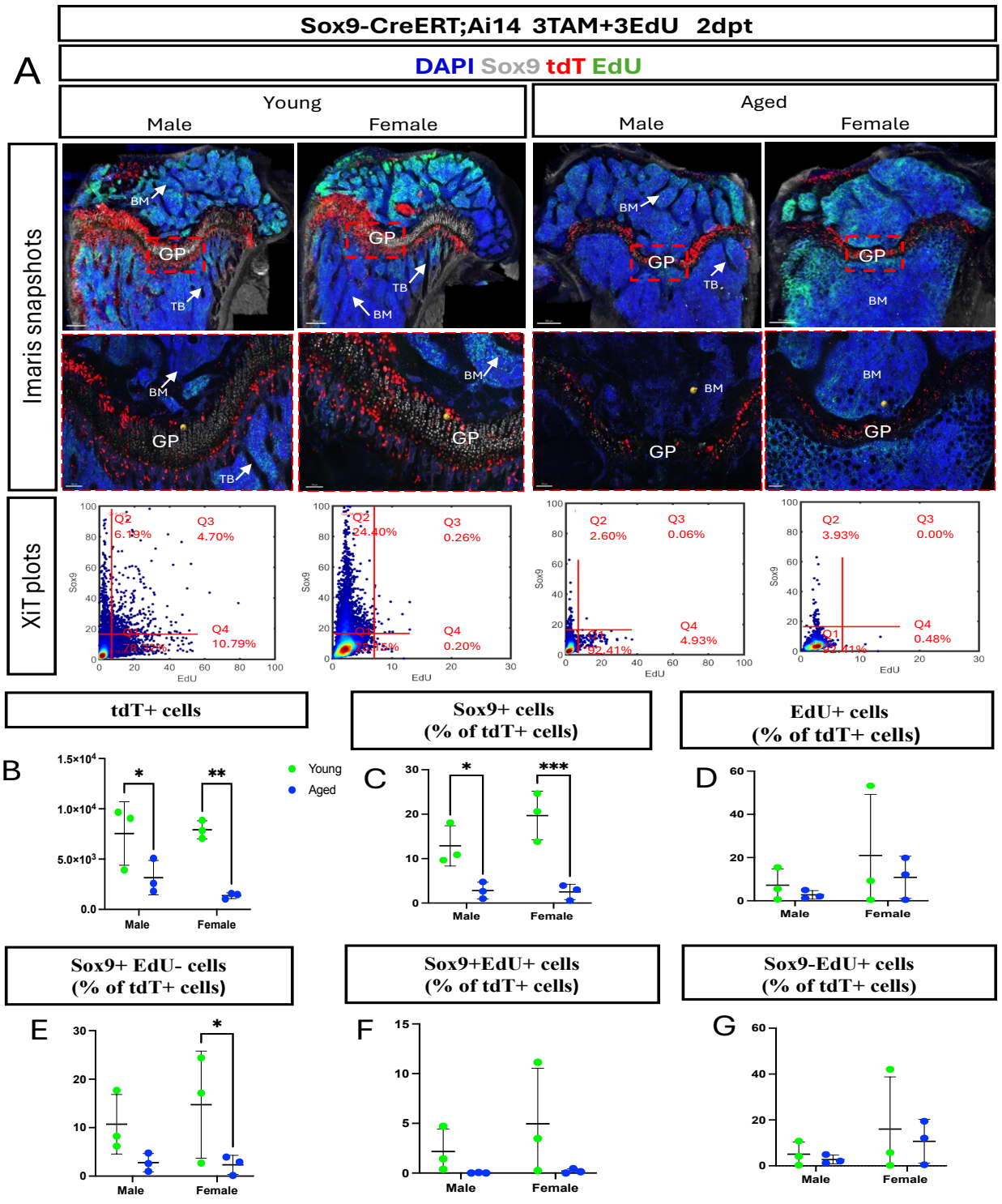

Figure 3.1. Sox9+ SSPCs population size and proliferation rate in aged male and female mice GP. Young (8-week-old) and aged (1-year-old) Sox9-CreERT; Ai14 mice were pulsed with three injections of TAM and EdU and chased for two days. 300µm-thick distal femur sections were optically cleared and imaged by confocal microscopy and tdT+, Sox9+ and EdU+ cells was assessed by imaging cytometry. A) Imaris images (+ zooms on GP) and associated XiT plots. B) Quantification of total tdT+ cells segmented, C) Graph showing the percentage of tdT+Sox9+, D) tdT+EdU+, E) tdT+Sox9+EdU-, F) tdT+Sox9+EdU+, and G) tdT+Sox9-EdU+ cells per sample. n=12 samples, n=3 per group with comparison between female and male mice of both age groups (young and aged) and between young and aged mice of the same sex group, performed by the two way-ANOVA test with a significant threshold set at p=0.05 and no correction for multiple comparisons (Fisher's LSD test). Dpt: days post-tamoxifen, GP: growth plate, TB: trabecular bone, BM: bone marrow.

Statistics about their Sox9 protein expression and EdU uptake were exported into XiT. Two FMO controls presented in figure 2.2 were used to define the gates. Each experimental and control group consisted of three males and three females. The difference between males and females of the same age group (young or aged) and between two age groups within the same sex was assessed. The results were then statistically analyzed by two-way ANOVA with a significant p-value set at 0.05.

The number of tdT+ cells segmented was significantly lower in aged mice of both sexes in comparison to their young counterparts: $3.2+/-1.7x10^3$ tdT+ cells versus $7.6+/-3.2x10^3$ in aged and young males respectively, and $1.4+/-0.3x10^3$ versus $7.9+/-0.9x10^3$ in old and young females, respectively (figure 3.1 B). The difference was more significant between females ($p=0.0025$ vs $p=0.02$). The difference in the number of tdT+ cells between males and females of the same age group was not significant. The percentage of tdT+ cells expressing detectable Sox9 protein was significantly lower in aged male and female mice in comparison to their younger counterparts of the same sex ($p= 0.011$ and $p<0.001$ respectively) (figure 3.1 C). In aged males, 2.8+/-1.9% of tdT+ cells expressed Sox9 versus 12.9+/-4.5% in young males. In females, 2.5+/-1.7% and 19.7+/-5.5% of the tdT+ cells of the GP area expressed Sox9 in aged and young mice, respectively.

The overall EdU incorporation rate did not significantly vary with age (figure 3.1 D). In males, 2.8+/-2.0% of tdT+ cells retained EdU in the aged group against 7.2+/-7.5% in the young ones. In females, these numbers were 10.9+/-9.8% in aged mice versus 21.0+/-28.3% in the young ones. Even though, the numbers seemed strikingly different in both sexes between young and aged, this was not confirmed when the statistical test was run. This might be due to a sample size too small to guarantee enough power to the analysis. The difference in EdU incorporation was not significant either between males or females of the same age group. The tdT+Sox9+EdU- cell

population percentage was significantly lower in the aged female population in comparison to the young one (2.3+/-2.0% versus 14.7+/-11.1%, p=0.047) (figure 3.1 E). The difference was insignificant between males (2.8+/-1.9% in aged ones against 10.7+/-6.1% in the young ones). The triple positive (tdT+Sox9+EdU+) cells percentage was not significantly different between sex or age groups (figure 3.1 F). The numbers were 0.02 +/-0.03% in the aged males, 2.2+/-2.3% in young males, 0.2+/-0.2% in aged females and 5.0+/-5.6% in young females. With a bigger sample size, the difference between these results likely would have been significant. The tdT+Sox9-EdU+ cell population did not particularly vary between young and aged of either sex (figure 3.1 G).

I also assessed SSPCs senescence in the GP of young and aged mice of both sexes by measuring the SA-β-gal expression in these cells. For doing so, a second set of sections from the same samples was treated with the CellEvent^{TM} Senescence Green Detection Kit and anti-Sox-9 antibody to quantify senescent and Sox9-expressing cells, respectively. 8-week-old mice were used as controls. Each experimental and control group consisted of three males and three females. The senescence rate was compared between male and female mice of the same age group (young or aged) and between young and aged of the same sex category.

As observed in the previous experiments, there was a significant decrease in the number of tdT+ cells and Sox9+ cells percentage of these tdT+ cells in the aged samples (figure 3.2 A & B). However, there was no significant difference between the senescence rate of males and females of the same age group, and between aged and young of the same sex. In aged male sections, 14.3+/-13.2% of tdT+ cells expressed SA-β-gal, and in young male ones the numbers were 29.6+/-8.5%. In females, the percentages were 36.1+/-31.1% in the aged ones and 36.6+/-7.8% in the young ones (figure 3.2 C). These results are surprising since less SA-β-gal expression was expected in young samples. This leads us to completely change our hypothesis regarding the etiology of

phenotypic changes and decreased bone regenerative capacity in aged animals. The non-significance of the difference between the numbers observed for every group could be due to the high variability of the results in most of the groups and the low number of samples analyzed, limiting the statistical power. The SSPCs SA-β-gal expression (tdT+Sox9+SA-β-gal+) statistically differ with age, both young males and females were more senescent (figure 3.2 D). The percentages of tdT+Sox9+SA-β-gal+ cells segmented in the GP area of respectively aged and young mice was in males 0.4+/-0.3% and 5.3+/-2.59% (p=0.017), and in females 2.8+/-2.7% and 8.2+/-5.2% (p=0.017).

In summary, the data collected during this part of the project show that the SSPCs (tdT+ Sox9+) population shrinks with age (figure 3.1 B and 3.2 B). Their proliferation rate decreased with age, but this decrease was determined to be statistically non-significant (figure 3.1 F). A lack of power is most likely the cause of this result of the test. This decrease in proliferation is associated with a decrease in senescence rate of GP SSPCs (figure 3.2 E) in both sexes. I can conclude that there are fewer SSPCs in the aged GP as their proliferation and senescence decreases as the organism ages. The blunted regenerative capacity of SSPCs in the aged individual is rather due to a loss of the stem cell niche than stem cell senescence in aged bones as senescence decreases while the SSPC pool shrinks. As we know that in human the GP eventually closes after puberty, a stem cell niche depletion is likely the main factor of such occurrence.

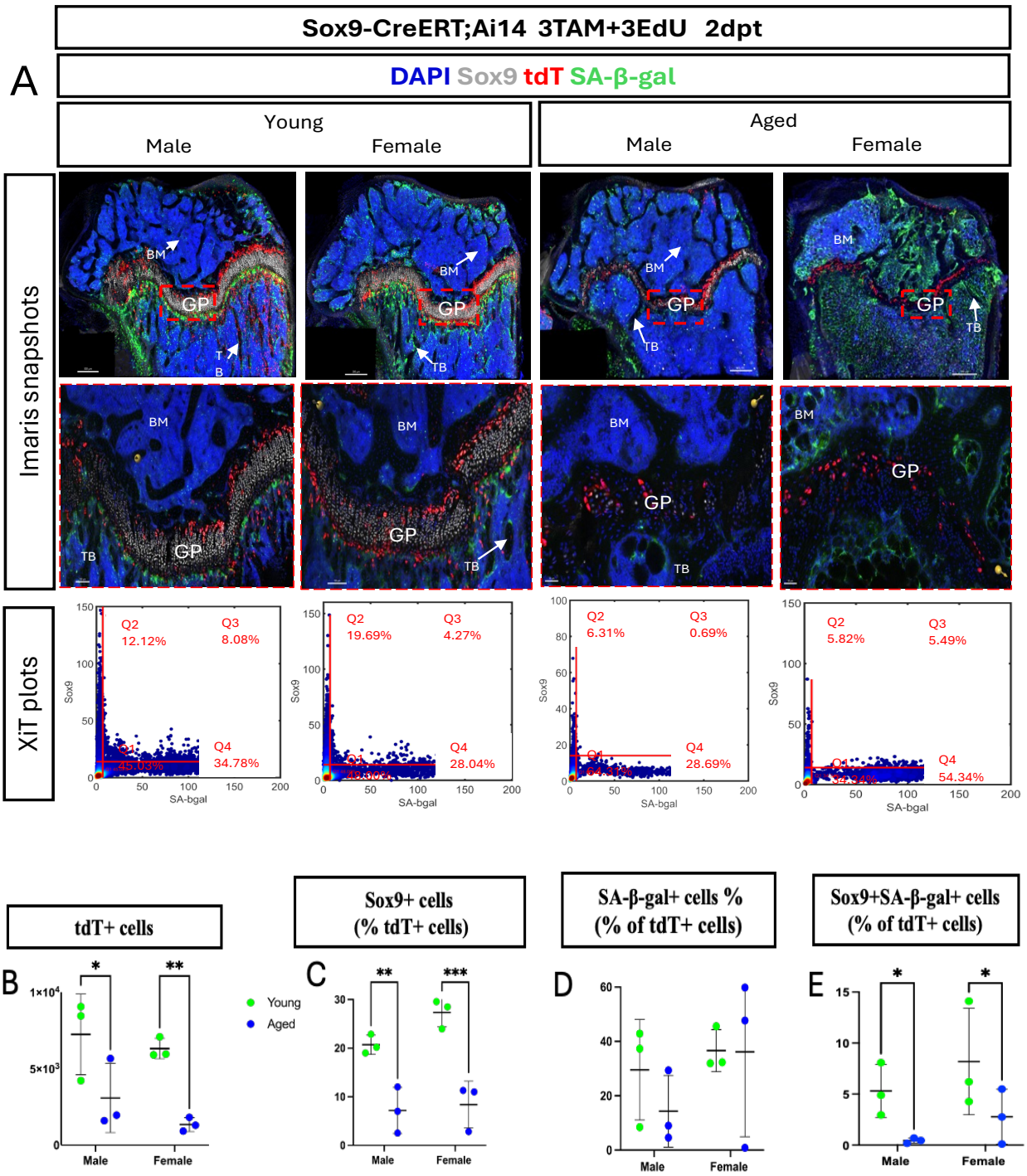

Figure 3.2. Senescence rate of Sox9+ SSPCs in young and aged mice of both sexes. Young (8-week-old) and aged (1-year-old) Sox9-CreERT; Ai14 mice were pulsed with three injections of TAM and EdU and chased for two days. 300µm-thick distal femur sections were optically cleared and imaged by confocal microscopy and tdT+, Sox9+ and SA-β-gal+ cells was assessed by imaging cytometry. A) Imaris image (+zoomed in snapshots) and XiT plots. B) Quantification of the total number of tdT+ cells segmented. C) percentages of tdT+Sox9+(C), tdT+SA-β-gal+(D), and tdT+Sox9+SA-βgal+(E) cells per sample. In this experiment, n=12 samples, n=3 per group with comparison between female and male mice of both age groups (young and aged) and between young and aged mice of the same sex group, performed by the two way-ANOVA test with a significant threshold set at p=0.05 and no correction for multiple comparisons (Fisher's LSD test). Dpt: days post-tamoxifen, GP: growth plate, TB: trabecular bone, BM: bone marrow.

3.2. SSPCs proliferation kinetics and senescence with sex and age in vitro

Understanding aging organisms' SSPCs proliferation kinetics and senescence in vitro can inspire ways to later address age-related conditions of the skeletal system by the development of stem-cell based therapies. In this part of the project, I studied the proliferation and senescence rate of aged mice' SSPCs in vitro. I expected a decreased proliferation and increased senescence rate of these cells in culture. To perform this study, femurs of 1-year-old Sox9-CreERT; Ai14 mice were harvested two days post-TAM injection (single dose), mechanically dissociated, enzymatically digested, and magnetically depleted of hematopoietic and endothelial cells (see section 2.5). Cells were counted and seeded in 24-well plates in triplicate, in mouse Mesencult^{TM} basal medium. Cells were later fixed and stained using the CellEvent™ Senescence Green Detection Kit and anti-p16^{INK4A} antibody after seven days in culture. The Operetta CLS High-Content Analysis System was used to quantify colonies, cells, tdT, p16^{INK4A} and SA-β-gal expression amongst other parameters. Cells from 8-week-old mice were analyzed and used as control. Cells from three male mice and three females were plated in each age group.

tdT+ cells isolated after a two-day TAM pulse and seeded in plates are expected to be SSPCs. After seven days in culture, tdT+ cells comprise SSPCs but also SSPC-derived cells, as some SSPCs have had the time to differentiate while keeping their tdT expression. Unfortunately, I did not perform Sox9 staining, as part of this experiment, to discriminate SSPCs from SSPC-derived cells.

Skeletal (tdT- and tdT+) cells from young female mice formed 74+/-45 colonies in vitro (figure 3.3 F). This number was significantly less than the 189+/-65 colonies formed by cells from young males ($p=0.005$). Cells from aged female mice formed 65+/-22 colonies/well whereas the

numbers were 129+/- 17 for the aged males. The difference between these two numbers was also statistically significant (p=0.005). There was no statistically significant colony size variation with sex and age. The colonies' sizes in the different wells varied between 1787 and 56 735 μm^2 across all four groups (figure 3.3 G). Single colonies from one aged female reached 142 823 μm^2 and 560 327μm^2 in two distinctive wells. These numbers did not change the interpretation of the results as showed in figure 3.3 G. A potential explanation could be that adjacent colonies merged and were measured by the Operetta as large colonies.

Also, the total number of cells counted in the wells seemed to differ across experimental and control groups, but the difference was insignificant as determined by the two-way ANOVA test: 7.2+/-2.7x10^3 in young males, 2.8+/-2.1x10^3 in young females , 12.7+/-9.8 x10^3 in aged males and 17.5+/-23.9x10^3 in aged females (figure 3.3 H).

The percentage of cells expressing tdT per well was 66.7+/-11.7% of the total cell population in the aged female group (figure 3.3 I). This number was significantly higher than the 33.0+/-11.3% obtained for cells of aged males (p=0.003) and the 30.0+/-9.0% for young females(p=0.002). 26.1+/-7.5% of the segmented cells expressed tdT in wells seeded with cells from young males. There was no significant difference between this later number and what was observed for young females or aged males.

Of the tdT+ cells segmented, 67.3+/- 9.4% were SA-β-gal+ in young males, 54.5+/-10.3% in young females, 72.5% +/-16.3% in aged males and 71.3%+/-20.3% in aged female (figure 3.3 J). The difference between these numbers were determined to be statistically non-significant. I observed that these numbers were particularly high. Skeletal cells enter senescence at a high rate in culture. Better culture media might be necessary in future attempts to study skeletal cell senescence entry in vitro.

The percentages of cells expressing SA-β-gal and $p16^{INK4A}$ (tdT+SA-β-gal+$p16^{INK4A}$+ cells) in the previously mentioned groups were: 66.6+/-9.1%, 51.3+/-8.4%, 71.7+/-16.8% and 70.0+/-20.3% respectively, with no statistically significant difference between the different groups (figure 3.3 K). Across the different technical and biological replicates, 84.2% to 99.95% of cells expressing SA-β-gal also expressed $p16^{INK4A}$.

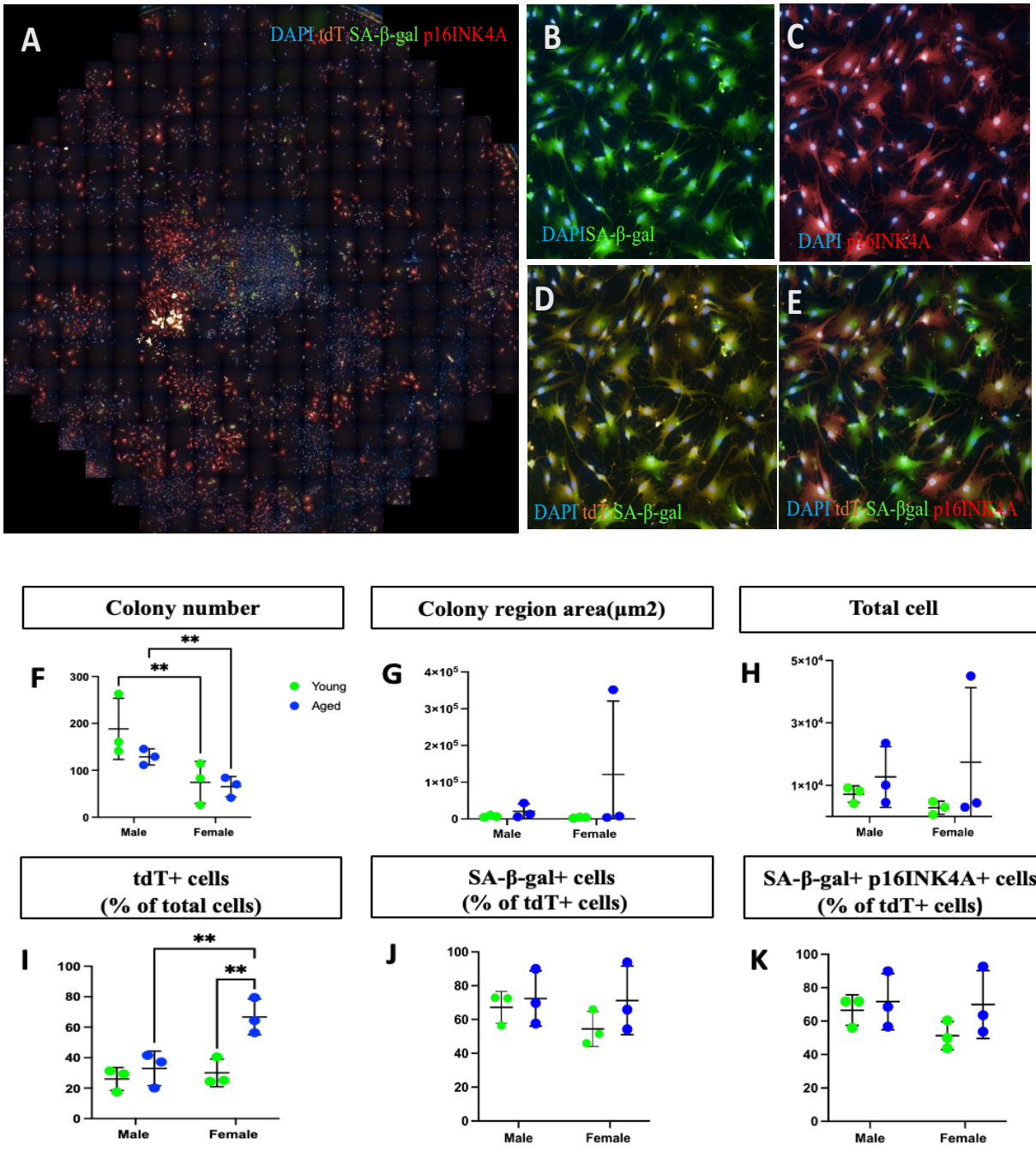

Figure 3.3. Isolation and in vitro culture of young and aged SSPCs. Sox9-CreERT; Ai14 mice were pulsed with a single TAM injection at 8-week and 1-year-old. Femurs were harvested two days post-labeling and skeletal cells isolated using enzymatic and mechanical dissociation, followed by magnetic removal of endothelial and hematopoietic cells through negative selection. A) Reconstitued image of a well with visible colonies and cells expressing tdT, SA-β-gal and $p16^{INK4A}$. In figures B), C), D) and E) we have a zoom on one field of the well. F) Quantification of the number of colonies obtained per $5x10^4$ cells/cm^2 seeded per well. G) Expansion of colonies measured and expressed as the mean colony region area in μm^2. H) Quantification of the total number of cells counted per well obtained by nuclei segmentation. I) Quantification of tdT+ cells. J) Quantification of SA-β-gal+cells. K) Quantification of the tdT+SA-β-gal+cells expressing $p16^{INK4A}$. n=12 samples, 3 biological replicates (all data points are the mean of at least three technical replicates) per group with comparison between female and male mice of both age groups (young and aged) and between young and aged mice of the same sex, performed by the two way-ANOVA test with a significant threshold set at p=0.05 and no correction for multiple comparisons (Fisher's LSD test).

In summary, skeletal cells from female mice (young and aged) show a decreased colony-forming capacity in vitro whereas these cells exhibit similar mean proliferative capacity (assessed by the total cell counts in each well) across age and sex (figure 3.3 F & H). Colony size was also similar between the four groups. On the other hand, the fraction of tdT+ cells was highest with cells from aged females (figure 3.3 I). This variation in tdT+ cells proliferation was not reflected by variation in the rate of cellular senescence. As a matter of fact, it must be noted that a high proportion of cells underwent senescence in all groups, which may have masked the effects of age or sex. The culture of SSPCs in Mesencult^{TM} basal medium seems to induce their entry into senescence as a mean of 54.5% to 72.5% of cells expressed SA-β-gal after only seven days in culture. These results suggest sex- and age-related differences in culture conditions requirements for ex vivo expansion of SSPCs and a need for culture conditions best suited for skeletal cells, in general.

3.3 Multilineage differentiation potential of SSPCs with age

To assess the differentiation potential of SSCs with age, 1-year-old Sox9-CreERT; Ai14 mice received one TAM injection, and femurs were harvested two days later. They were mechanically dissociated and enzymatically digested. Cells were counted and seeded at a density of $5x10^4/cm^2$ in triplicate, in mouse Mesencult^{TM} basal medium. Media was changed and differentiation started 14 days later. Differentiated cells were later stained for alkaline phosphatase (ALP), BODIPY and Sox9 to confirm osteogenic, adipogenic and chondrogenic differentiation, respectively. Quantification was not performed in this part of the project. Images were qualitatively evaluated for the presence of tdT+ cells also expressing differentiation markers. tdT+ cells from 8-week-old mice, differentiating into osteoblast, chondrocytes and adipocytes as evidenced by their expression of ALP, Sox9 and BODIPY were used as controls.

SSPCs from aged female and male mice successfully differentiated into osteoblasts as evidenced by the presence of tdT+ALP+ cells (figure 3.4). In adipogenic conditions, tdT+ also stained positive for BODIPY in lipid droplets, confirming their adipogenic potential (figure 3.5).

To assess chondrogenic potential, cells were aggregated into micromasses and placed in chondrogenic medium. Imaging of the chondrogenic micromasses confirmed the presence of tdT+Sox9+ cells (figure 3.6).

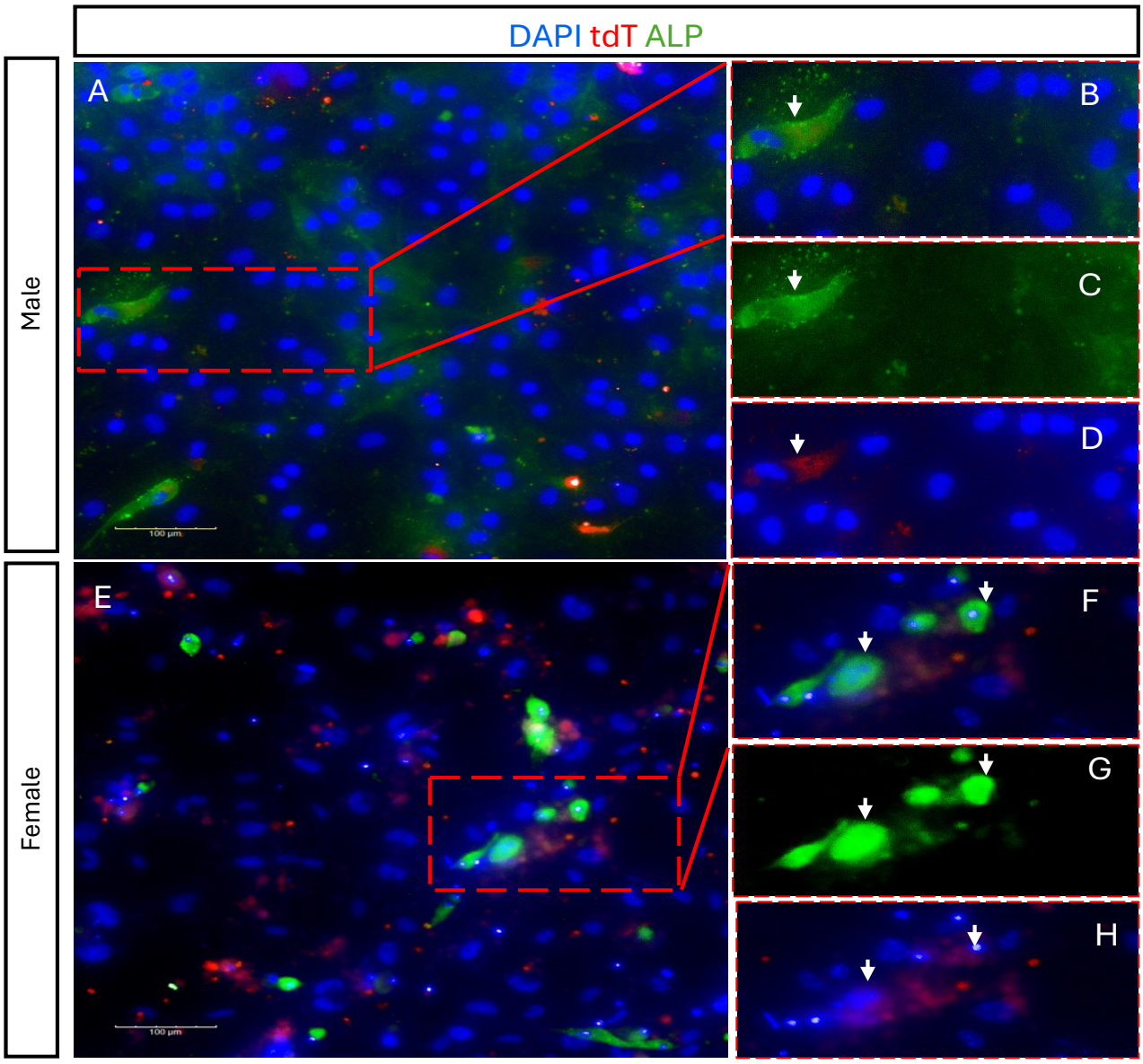

Figure 3.4. Osteogenic differentiation potential of SSPCs in aged mice. Sox9-CreERT; Ai14 mice were pulsed with a single TAM injection at 8-week and 1-year-old. Femurs were harvested two days post-labeling and skeletal cells isolated using enzymatic and mechanical dissociation and plated. Cells were assessed in osteogenic conditions. The assay was performed on n=19 samples (six aged males, four aged females, five young males and four young females). Four technical replicates were assessed per biological ones. Osteogenic differentiation was assessed using anti-ALP antibody staining and the presence of osteoblasts (B & F) was qualitatively assessed. Arrows are pointing at tdT (D & H) and ALP (C & G) signals. ALP: alkaline phosphatase

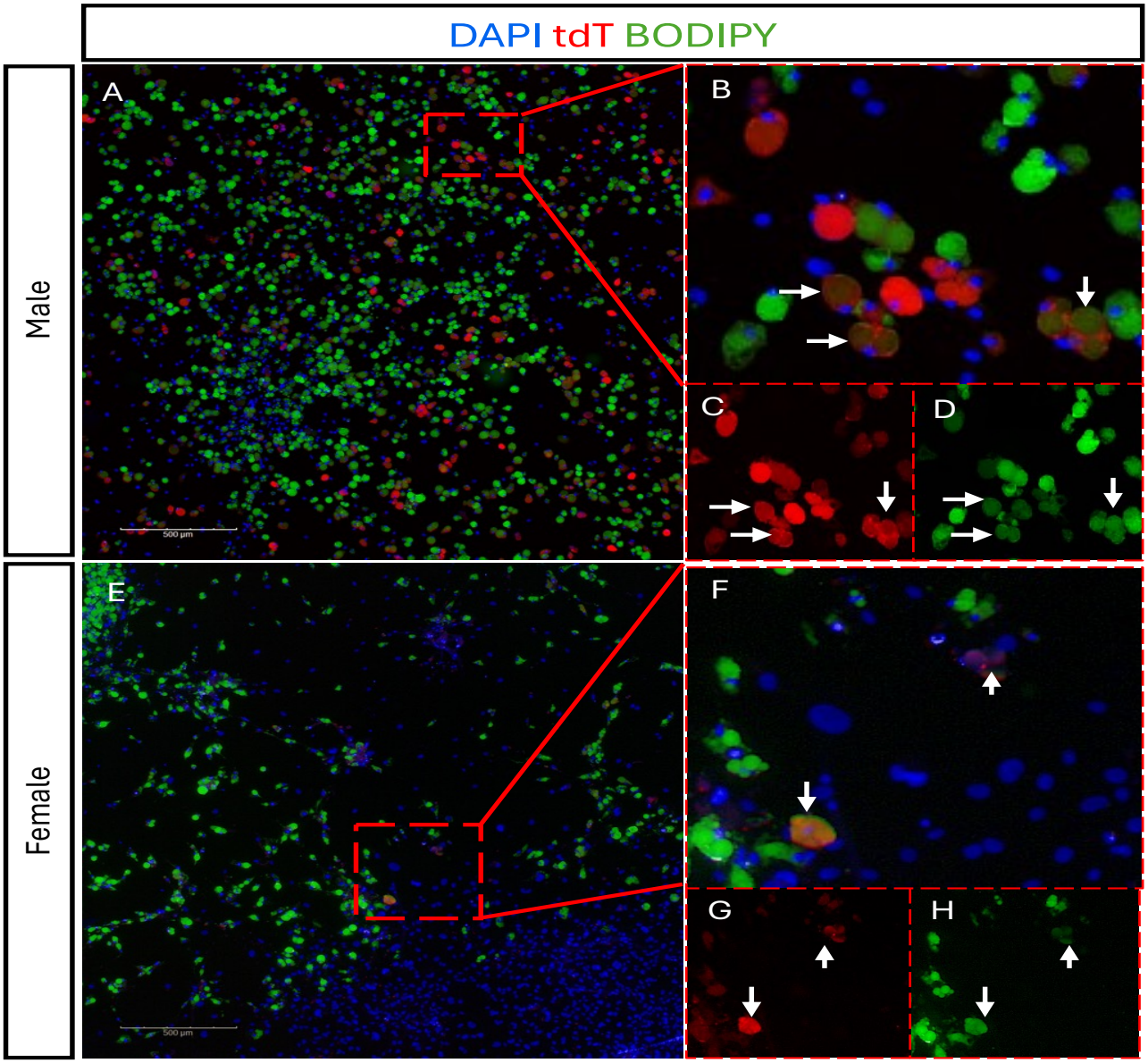

Figure 3.5. Adipogenic differentiation potential of SSPCs in aged mice. Sox9-CreERT; Ai14 mice were pulsed with a single TAM injection at 8-week and 1-year-old. Femurs were harvested two days post-labeling and skeletal cells isolated using enzymatic and mechanical dissociation and plated. Cells were later subjected to differentiation into adipocytes. The assay was performed on n=19 samples (six aged males, four aged females, five young males and four young females). Three technical replicates were assessed per biological ones. Adipogenic differentiation was assessed by BODIPY staining of lipid droplets. Numerous tdT+ cells(red) (C & G) stained positive for BODIPY (green) (D & H). The adipocytes' pinkish appearance (B & F) is due to the additions of blue (DAPI), red (tdT) and green (BODIPY).

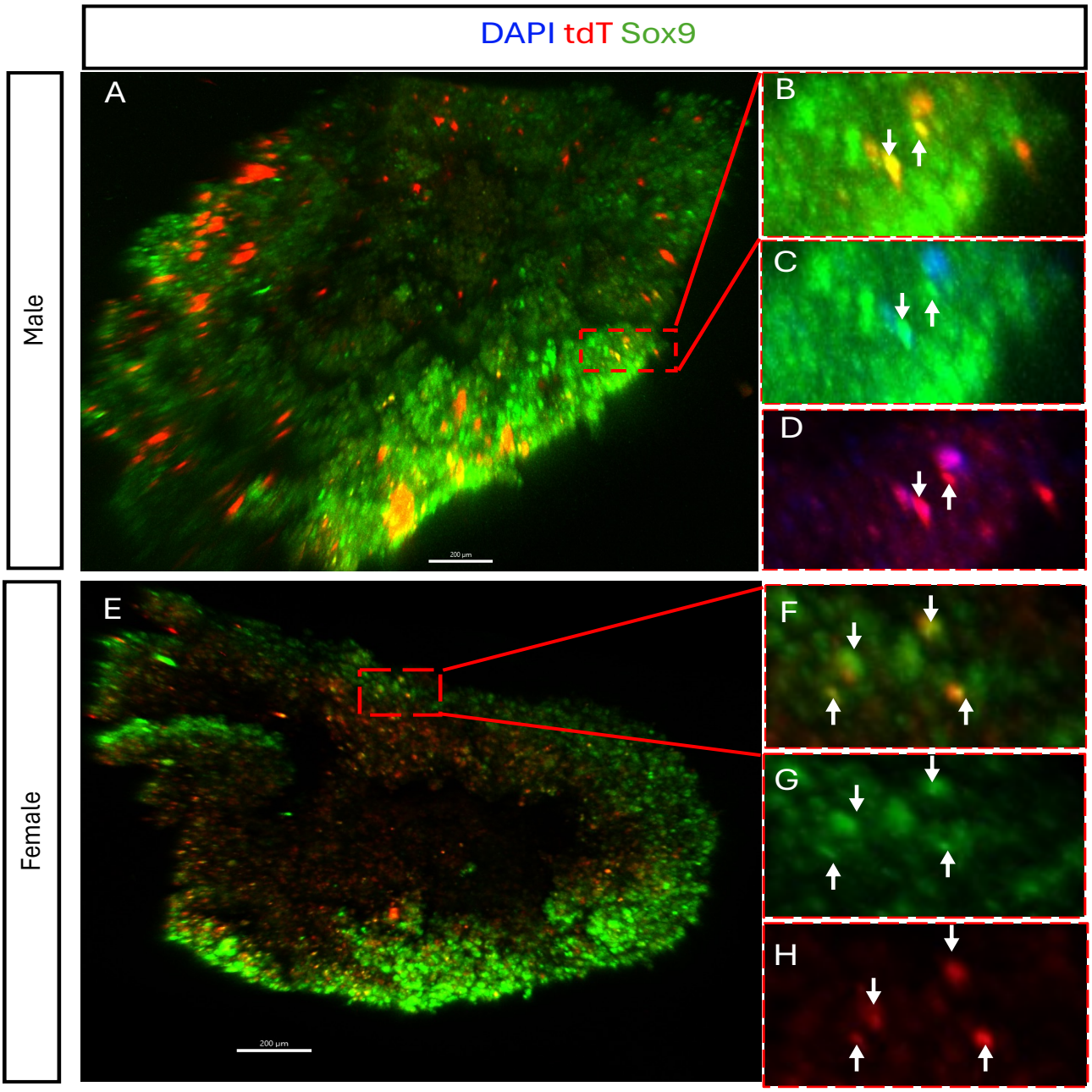

Figure 3.6. Chondrogenic differentiation potential of SSPCs in aged mice. Sox9-CreERT; Ai14 mice were pulsed with a single TAM injection at 8-week and 1-year-old. Femurs were harvested two days post-labeling and skeletal cells isolated using enzymatic and mechanical dissociation and plated. Cells were later subjected to differentiation into chondrocytes. The assay was performed on n=19 samples (six aged males, four aged females, five young males and four young females). Two technical replicates were assessed per biological ones. Chondrogenic differentiation was assessed using anti-Sox9 antibody staining (C & G) and the presence of tdT+ chondrocytes (D & H) was qualitatively assessed. Chondrocytes appeared yellow (B & F)) due to the superposition of red (tdT) and green (Sox9).

3.4 Summary

In this first part of the project, I put into evidence that SSPC pool shrinks with age as senescence and proliferation decrease (figure 3.1 B, C, F et E). These results infirm the hypothesis of senescence as the etiology of bones' age-related diseases and blunted regenerative capacity and shift our focus toward stem cell niche depletion as the main causal mechanism in these cases. Less SSPCs are available to participate in repair and these cells proliferate less, putting elderly individuals at risk of injuries and a higher injury-related morbidity due to a particularly longer repair process in comparison to young individuals. This decreased proliferation and senescence rate of SSPCs in vivo is likely driven by local factors affecting these cells fate in the tissue, as skeletal cells maintain their proliferative and differentiation capacity in vitro. No significant difference was observed between young and aged mice cells of either sex, in terms of total cells count and cells from aged mice differentiated into osteoblast (figure 3.4), adipocytes (figure 3.5) and chondrocytes (figure 3.6) in vitro. On the contrary, the colony-forming capacity of skeletal cells decreased in females, independently of age (figure 3.3 F) and aged female mice tdT+ cells showed a significantly higher proliferation rate than any other group (figure 3.3 I). This could suggest sex- and age-related differences in skeletal cells response to culture media.

Chapter 4. Pharmacological manipulation of SSPCs fate decisions

Understanding the hormones, transcription factors and signaling pathways involved in bone development and SSPCs proliferation can provide leverage to influence their fate decisions. The Hedgehog (Hh) pathway is activated during endochondral ossification and regulates chondrocyte proliferation[29,30]. Parathyroid hormone (PTH) stimulates osteogenic differentiation of growth plate (GP) chondrocytes[194]**.** A CellChat analysis performed in the lab, demonstrated molecular crosstalk between several cell types and resting zone chondrocytes (RZ-Ch), which comprise most SSCs[58]. The RZ-Ch receives canonical and non-canonical Wnt signaling from hypertrophic chondrocytes. Perichondral cells, osteoblasts, and fibroblasts send Hh, Fibroblast Growth Factor and PTH signals to the resting zone chondrocytes, respectively (figure 1.3).

Based on a review of the literature and the scRNA-seq analysis data previously mentioned (section 1.3.1.2). I decided to screen several pathways involved in bone development and postnatal homeostasis by influencing them with agonists and antagonists hoping to identify pathways that could be targeted for SSPCs proliferation while avoiding cellular senescence with the aim of being able to use them for future stem-cell based therapies. Candidate compounds included PTH (1-34) [195–197], purmorphamine (a Hh agonist)[182–185,198,199], 20(S)-hydroxycholesterol (20(S)-OHC) (an activator of the Smo and Hh signaling pathways)[186–189], cyclopamine (an inhibitor of the Hh pathway)[190–192] and tamoxifen (TAM) (a selective estrogen receptor modulator)[179,200–202]. Dosage and administration times for most of these compounds have been established (see table 2.1). The Hh pathway regulators (20(S)-OHC, purmorphamine and cyclopamine) were tested in vitro only, PTH in vitro and vivo, and TAM in vivo.

4.1. Effect of PTH and Hh pathway regulators on SSPCs proliferation and senescence in vitro

Five compounds were assessed for their ability to stimulate SSPCs expansion in vitro while avoiding cellular senescence: 20(S)-OHC (10μM), PTH (1-34) (50nM), purmorphamine (2 μM), cyclopamine (5mM).

8-week-old Sox9-CreERT; Ai14 mice (n=4, two males and two females) were pulsed with a single TAM injection. Femurs were harvested two days later and skeletal cells isolated using enzymatic and mechanical dissociation, followed by magnetic removal of endothelial and hematopoietic cells by negative selection. For this initial screening, cells from male and female mice were used indiscriminately. Cells were seeded in 24-well Ibidi plates at a density of 10^5 cells/cm^2 in at least three technical replicates per biological replicate in mouse Mesencult^{TM} basal medium supplemented with the indicated compounds at the time of plating. In the control wells, medium was supplemented with ethanol (vehicle for 20(S)-hydroxycholesterol and cyclopamine) or DMSO (vehicle for purmorphamine). PTH was reconstituted in water. In control wells for PTH, cells grew in media only. The media was changed every two to three days. The cells were not further stimulated with the compounds as the first goal was to measure any variation in the effects of every compound in comparison to their controls. After 13 days of culture, the colonies and their size, total cells, tdT+ cells and their SA-β-gal expression was quantified and comparison made between compounds and their controls.

When the skeletal (tdT- and tdT+) cells were stimulated with PTH (1-34) in vitro, 28+/-8 colonies (vs 28+/-11 for the control) were formed into the wells, and they measured 29.5+/-18.2x 10^5 μm^2 (vs 28.3+/-23.17 x10^5 for the control) (figure 4.1 A). 21.3+/-15.0 x10^3 cells (vs 14.8+/-

12.1x 10^3 for the controls) were counted. 14.1+/-16.3 x10^3 of these cells expressed tdT (vs 11.2+/-10.3 x10^3 for the controls) and of these tdT+ cells 60.4+/-30.1% expressed SA-β-gal (vs 47.3+/-31.6% for the controls). The differences observed with all the measured parameters were determined to be statistically non-significant.

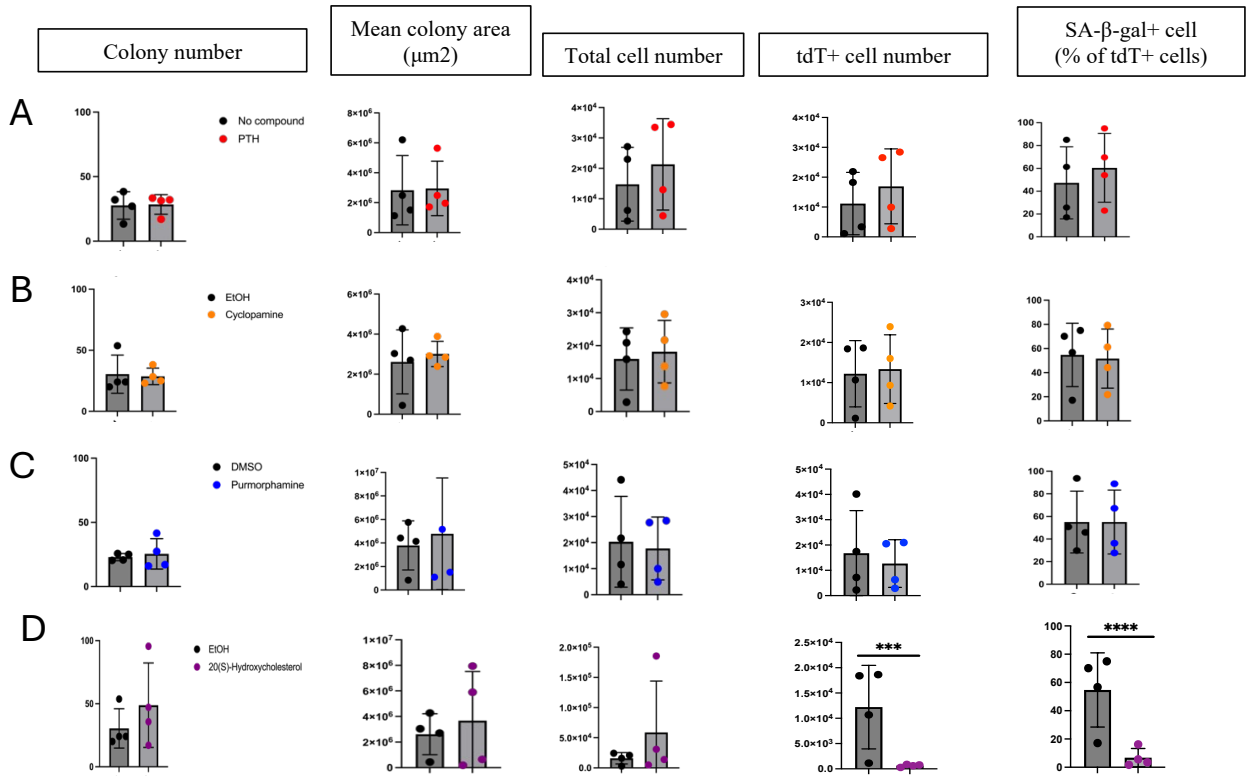

Figure 4.1. In vitro assays in basal medium with supplementation of PTH, cyclopamine, purmorphamine and 20(S)-OHC. Male and female 8-week-old Sox9-CreERT; Ai14 mice (n=4, two males and two females) received a single injection of tamoxifen. Femurs were harvested two days later and skeletal cells isolated by enzymatic and mechanical dissociation, followed by magnetic removal of endothelial and hematopoietic cells by negative selection. Cells were seeded in 24-well plates at a density of 10^5 cells/cm^2 in at least three technical replicates/biological replicate in mouse Mesencult^{TM} basal medium supplemented once with PTH, cyclopamine, purmorphamine and 20(S)-OHC or their respective vehicle. The statistical test performed to compare result of compounds and vehicles was the student t-test, with a significant threshold set at p=0.05.

For cyclopamine and purmorphamine, the mean number of colonies counted, and their size was similar to what was quantified in the wells where their vehicle was added. The total number of cells counted per well, the number of tdT+ cell and the SA-β-gal expression was also similar between experimental and control wells (figure 4.1 B &C).

There was no significant difference in colony-forming capacity between skeletal (tdT- and tdT+) cells treated with 20(S)-OHC and the EtOH control (figure 4.1 D). 30+/-16 colonies were formed in the presence of EtOH and 49+/-34 when 20(S)-OHC was added. The colonies were not significantly bigger when 20(S)-OHC was added to the media at plating (26.1+/-16.0x10^5 μm^2 in the presence of 20(S)-OHC and 36.7+/-38.5x10^5 μm^2 with EtOH). The total number of skeletal cells counted did not significantly change with the compound (EtOH: 16.0+/-9.4x10^3 cells, 20(S)-OHC: 58.8+/-85.1x10^3 cells). On the other hand, the number of tdT+ cells (mostly SSPCs) significantly decreased with exposure to 20(S)-OHC. The number changed from 10.0+/-9.5 x10^3 to 0.7+/-0.6 x10^3 ($p<0.001$). Also, the percentage of senescent tdT+ (tdT+SA-β-gal+) cells percentage decreased with 20(S)-OHC. 54.7+/-26.3% of tdT+ cells expressed SA-β-gal in the control wells against 6.8+/-6.7% in the experimental wells ($p<0.0001$).

In summary, of the four compounds tested, 20(S)-OHC, an Hh agonist, is the only one with a significant effect on the SSPCs after 13 days in culture (figure 4.1 D). It keeps SSPCs quiescent/non-proliferative. Their number decreases when 20(S)-OHC is added to the media while the total cell population proliferation and colony-forming capacity is similar to what is quantified when the vehicle is added. I can conclude that a one-dose 20(S)-OHC has no effect on the tdT- cell population but, keeps SSPCs in a non-proliferative state, at the same time reducing their colony-forming capacity and their entry into senescence.

4.2 Effect of prolonged stimulation with 20(S)-OHC on SSPCs proliferation and senescence in vitro

A single dose of 20(S)-OHC had a substantial effect on SSPCs proliferation and colony-forming capacity. Initially, I wanted to confirm this effect and detect any other effects for which a

single stimulation would not have been sufficient. I repeated this experiment, but this time with continuous stimulation of the cells with this compound. 20(S)-OHC (10 μM) was added at plating, at refeeding three days later and during media change two days post-refeeding. Subsequently, I wanted to confirm that 20(S)-OHC affected the SSPC population via activation of the Hh pathway. Therefore, cells were also exposed to 20(S)-OHC (10 μM) in combination with cyclopamine (10 μM), an Hh antagonist. Finally, I sought to determine whether the effect of 20(S)-OHC on SSPCs was sex-dependent. This experiment was then conducted on seven mice (n=7), four male and three female mice.

Plates were imaged after seven days in culture. Cell confluency exceeded 80% at that point. Colonies, their size, total cell per well, tdT+ cells and their SA-β-gal expression was quantified and comparison made between the agonist (20(S)-OHC), the combination agonist (20(S)-OHC)-antagonist (cyclopamine) and their vehicle (EtOH). Because of the low viability of the isolated cells, only one technical replicate was possible per biological replicate.

In wells where the vehicle was added, 443+/-43 and 304+/-45 colonies were formed in males and females, respectively (figure 4.2 A). The colonies measured 13.0+/-5.3x10^3 μm^2 in males and 9.2+/-5.9x10^3 μm^2 in females (figure 4.2 B). When 20(S)-OHC was added, cells from male and female mice formed 9+/-4 colonies and 8 +/-3 colonies, respectively and measured 1.9+/-0.9x10^3 μm^2 in males and 1.4+/-0.2x10^3 μm^2 in females. In the presence of the 20(S)-OHC-cyclopamine combination, 0+/-1 was formed in males and 14+/-23 colonies in females. The colonies' sizes were 0.7+/-1.3x10^3 μm^2 in males and 2.1+/-2.7x10^3 μm^2 in females (figure 4.2 A & B). The colonies were significantly smaller when 20(S)-OHC was added on male ($p<0.001$) and female cells ($p=0.034$) (figure 4.2 B). Therefore, continuous 20(S)-OHC stimulation greatly

reduced colony formation and cell proliferation independent of age, and this effect was surprisingly not blocked by cyclopamine.

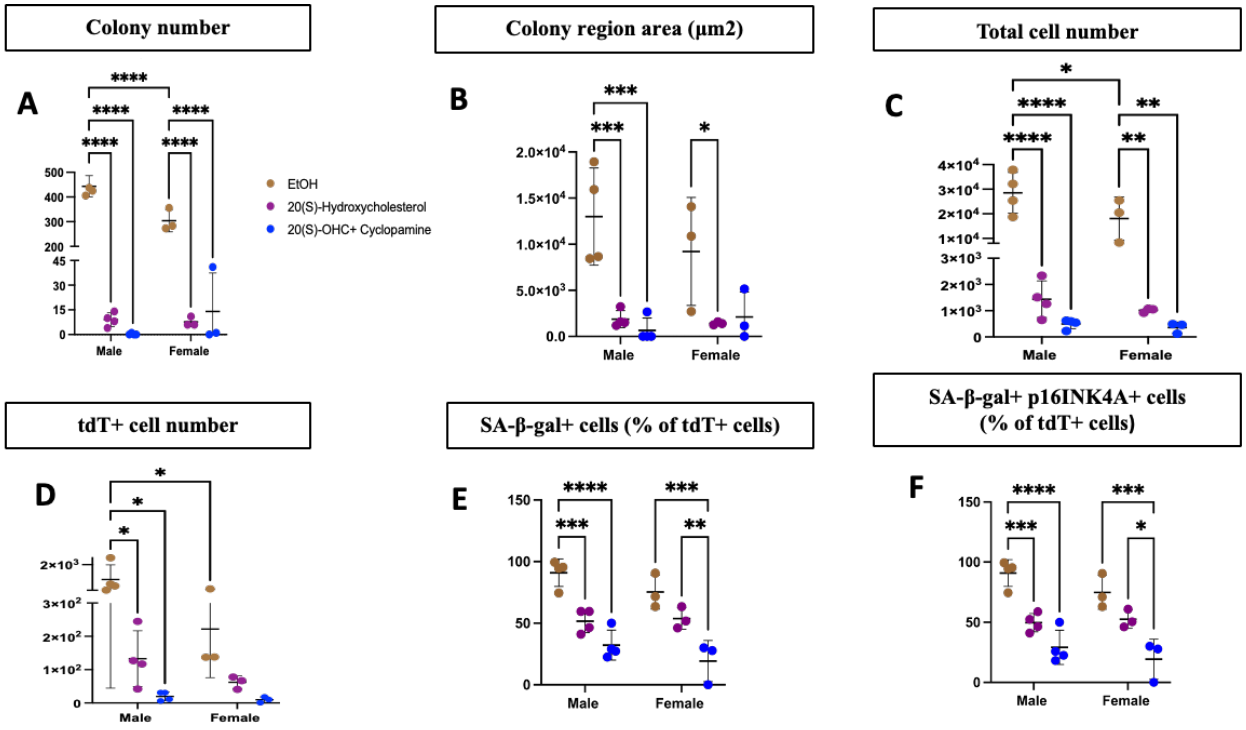

Figure 4.2. In vitro colony assays in basal medium with supplementation with 20(S)-OHC and its combination with cyclopamine. SSPCs were isolated and enriched from 8-week-old Sox9-CreERT; Ai14 mice (n=7, four males and three females) 48h after a single injection of tamoxifen. Cells were seeded in 24-well plates at a density of $5x10^4$ cells/cm^2 basal medium supplemented with 20(S)-OHC, 20(S)-OHC + cyclopamine, or EtOH (vehicle control). The compounds were added at every media change. Cells were left in culture for seven days then analyzed on the Operetta CLS High-Content analysis system. A) Quantification of the total number of colonies obtained per condition and B) their region area in μm^2. C) Quantification of the total number of cells counted per well obtained by nuclei segmentation. E) The number of tdT+ cells counted per well. F) Quantification of the tdT+SA-β-gal+ cells expressed as the percentage of total tdT+ cells. G) Quantification of the tdT+SA-β-gal+$p16^{INK4A}$+ cells expressed as the percentage of total tdT+ cells. The statistical test performed was the two-way ANOVA test, p=0.05. Results were corrected for multiple comparisons using the Tukey's test.

When 20(S)-OHC was added to the media, a mean of 1.4+/-0.7$x10^3$ (males) and 1.0+/-0.1$x10^3$ cells (females) were counted, of which 0.1+/-0.08$x10^3$ and 0.06+/-0.02$x10^3$ expressed tdT in males and females, respectively (figure 4.2 C & D). With the vehicle, 28.5+/-8.3$x10^3$ (males) and 18.1+/-8.8$x10^3$ total cells (females) were counted, with 1.0+/-0.9$x10^3$ and 0.2+/-0.1$x10^3$ of this cells expressing tdT in males and females, respectively. When 20(S)-OHC was combined with cyclopamine, these numbers changed to 0.5+/-0.2$x10^3$ and 0.4+/-0.2x 10^3 total cells counted in

males and females respectively and 20+/-13 and 10+/-9 expressed tdT. The differences in the total cells counted between 20(S)-OHC and the vehicle and between the vehicle and the combination of 20(S)-OHC and cyclopamine were statistically significant as determined by the two-way ANOVA test (males: $p<0.0001$ in both cases and females: $p=0.002$ and 0.001). The SA-β-gal expression gradually decreased between the pairs EtOH-20(S)-OHC and EtOH-(20(S)-OHC-cyclopamine) combination in males ($p<0.001$ and $p<0.0001$, respectively) (figure 4.2 E). The percentages went from 91.0+/-11.2% (EtOH) to 51.7+/-9.4% (20(S)-OHC) and 32.2+/-12.2% (20(S)-OHC-cyclopamine combination). In females, there was no significant difference between the percentage of tdT+SA-β-gal+ cells when the vehicle or 20(S)-OHC was added (75.3+/-13.8% and 53.8+/-8.8% respectively). The percentages obtained with the vehicle and 20(S)-OHC were both individually significantly higher than the numbers obtained for the 20(S)-OHC-cyclopamine combination (19.3+/-16.7%) ($p=0.0001$ and 0.008). The same pattern was observed between the three experimental conditions in the case of the triple positive (tdT+SA-β-gal+$p16^{INK4A}$+) cell population (figure 4.2 F).

In summary, a single dose of 20(S)-OHC has no effect on tdT- cell proliferation, colony number and size and but inhibited tdT+ (SSPCs) proliferation, colony-forming ability and senescence (figure 4.1 D). Continuous stimulation with 20(S)-OHC, on the other hand, inhibited all skeletal cells proliferation, colony-forming capacity and expansion (figure 4.2 A, B &C). And its effect is not counteracted by the presence of cyclopamine. In both sexes, the exposure to multiple doses of 20(S)-OHC appears to inhibit SSPCs cell proliferation while inhibiting cellular senescence (the analysis lacked the power to detect a significance in female). Cyclopamine failed to reverse these effects.

4.3 Effect of PTH on the SSPCs population size in vivo

PTH is involved in bone homeostasis. It is used in the treatment of osteoporosis in menopausal women. At the cellular level, it has been reported to induce an increase in the number of Sox9-expressing cells in mouse bone and their differentiation into osteoblasts [194]. This effect took place after a seven-day pulse. PTH was also shown to activate the Hh pathway in chondrogenic ATCD5 cells.[196]. I wanted to test its effect on the Sox9+ SSPC population, because if a proliferation-promoting effect was observed, it could then be used to induce SSPCs proliferation for stem-cell based therapies. In this part of the project, TAM was administered intraperitoneally every day for three days and 400ng/g of PTH subcutaneously during four days to 56 to 66-week-old Sox9-CreERT; Ai14 mice to respectively induce the expression of tdT in Sox9+ cells and their progeny and assess PTH's effect on this cell population. The mice were euthanized two days after the last injections. Femur sections were stained for Sox9, imaged and analyzed (figure 4.3 A). Mice injected with the PTH vehicle were processed as controls. Each experimental and control group consisted respectively of four and three mice of both sexes.

In bone sections from vehicle-treated mice, $3.2+/-0.8x10^3$ tdT+ cells were segmented, of which 89.2+/-8.6% expressed Sox9. In the PTH-treated mice bone sections, $3.1+/-1.3x10^3$ tdT+ cells were counted and 75.7+/-19.5% of these were Sox9+. As determined by the Student's t-test, the difference between experimental and control group regarding tdT+ cell number and Sox9+ cells percentage was not statistically significant (figure 4.3 B & C).

In summary, a four-day PTH pulse has no significant effect on the SSPC population in vivo.

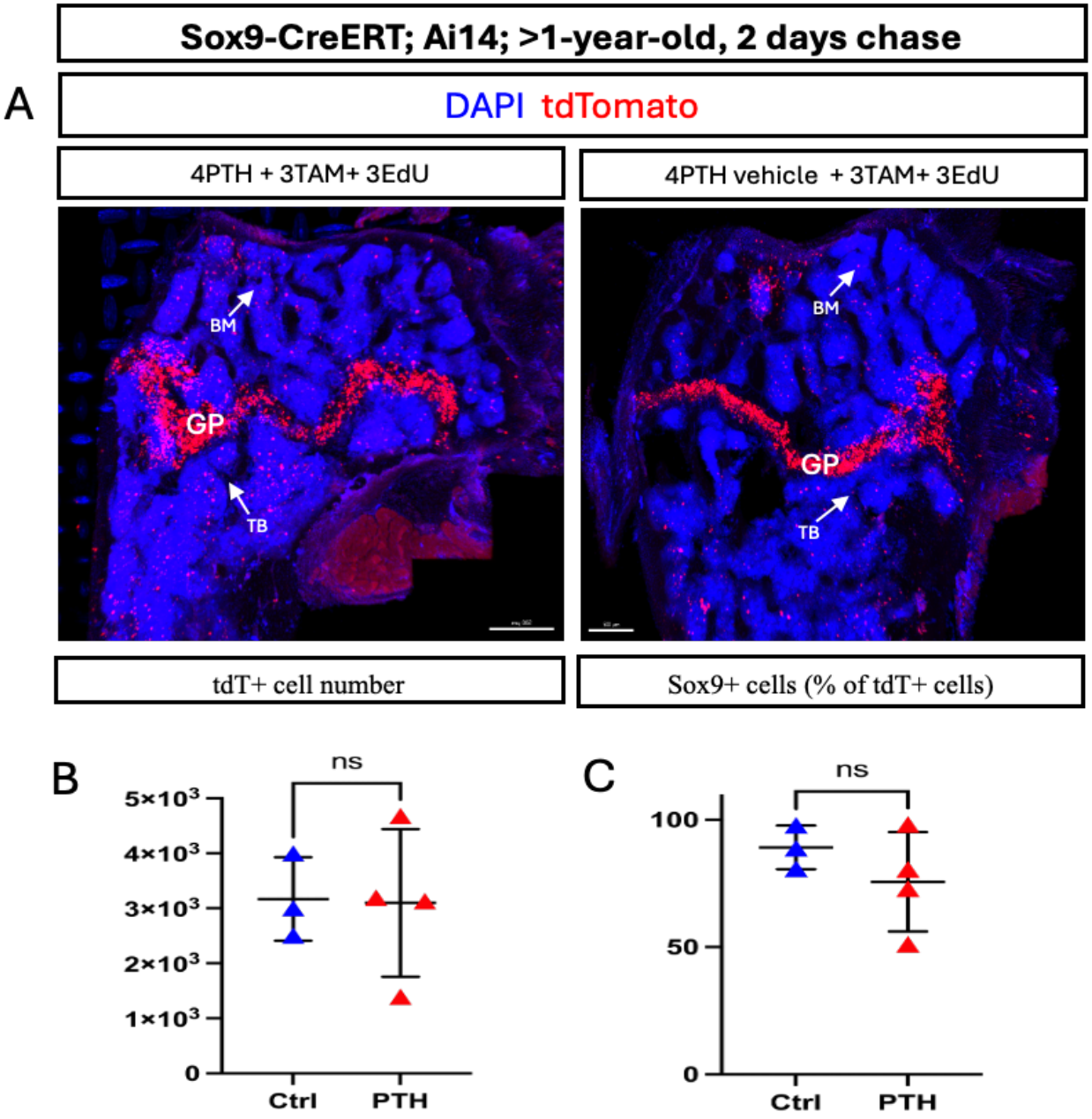

Figure 4.3. Quantification of Sox9+ SSPCs in mouse femur sections exposed to PTH. Male and female aged mice (56 to 66-week-old) were injected four doses of PTH and three doses of TAM and EdU. Femurs were harvested two (2) days post-labeling and the effect of PTH on the Sox9+ SSPCs assessed. A) Confocal image of two distal femur sections (Sox9 stainings are not shown). B) Quantification of tdT+ cells. C) Quantification of Sox9+ cells expressed as the percentage of Sox9+ cells in the tdT+ cell population. n=7, n=4 in the experimental group and n=3 in the control group. All sections were obtained from male mice. The significance of the difference level between the means of both groups was determined by the student's t-test. The significant threshold was set at p=0.05. GP: growth plate, TB: trabecular bone, BM: bone marrow, ctrl: control.

4.4. Sex-dependent effects of tamoxifen (TAM) on growth plate chondrocytes proliferation and senescence

TAM is a selective estrogen receptor modulator. In the uterus and the postmenopausal bones, it acts as an estrogen receptor agonist whereas its effect is antagonistic in tissues such as the breast. It has been used in the treatment of precocious puberty in the McCune-Albright syndrome, a disease associated with short stature in affected male individuals[179]. Also, TAM is used in multiple lineage tracing and conditional knockout studies in the skeleton[203,204]. It activates the CreERT recombinase to excise a gene or stop codon, conditionally deleting a gene or allowing the expression of a reporter. Due to its widespread use in skeletal studies and its possible side effects on bone physiology when used long-term, I wanted to assess its effect in the GP of postnatal mice at the cellular level, but only over a period similar to that generally chosen in our studies. My results could also be extended to future studies in regenerative orthopedics.

The following experiments were conducted in C57Bl/6 mice to specifically study the effects of TAM on the proliferation and senescence of cells within the postnatal GP. Since I did not use the Sox9-CreERT; Ai14 model, I will refer to the cells analyzed as GP chondrocytes rather than SSPCs. Here, I relied on a spatial gating of the GP and included the broad chondrocytic population of this region of the bone. When Sox9 antibody staining was performed and quantified, in the description of the results I will refer more specifically to the SSPC population.

8-week-old C57Bl6 mice were given three pulses of TAM and EdU intraperitoneally and euthanized two days later. The control group only received three pulses of EdU before euthanasia. Femurs were processed and 300µm-thick sections treated with the CellEvent™ Senescence Green Detection Kit, click IT EdU Alexa Fluor 488 kit and stained with anti-Sox9 antibody. DAPI was

used as a nuclear counterstain. Sections were later cleared, mounted and images acquired (figure 4.4 A). The DAPI spots of the distal femur were segmented in Imaris v10.2.0 (Bitplane) and the software permitted the selection of spots localized in the GP area. Statistics about the GP area cells' SA-β-gal and Sox9 protein expression and their EdU uptake was transported into XiT (figure 4.4 A) [193]. Statistics of the FMO controls were used in XiT for defining the gates on the axes (figure 2.2).

In general, there was no significant difference between males and females in terms of EdU incorporation and SA-β-gal expression before TAM injection (figure 4.4 B & C). In the presence of TAM, 20.0+/-15.2% of cells in male mice bone sections were EdU+, a significantly higher number than the 0.5+/-1.0% quantified in the absence of TAM ($p=0.002$) (figure 4.4 B). In females, the numbers were 2.6+/-3.5% and 0.7+/-0.5% in the presence and absence of TAM respectively. This incorporation rate of EdU in female mice exposed to TAM was significantly lower than what is observed in males under the same conditions ($p=0.004$).

When SA-β-gal expression was quantified, there was no significant difference between the mean percentages of SA-β-gal+ cells with and without TAM in males (18.3+/-3.4% vs 22.5+/-5.2%) (figure 4.4 C). In females, on the contrary, the SA-β-gal+ cell population percentage significantly decreased from 29.8+/-6.4% before TAM injection to 13.2+/-5.6% when TAM was injected ($p<0.001$). The percentage of senescent proliferating cells (EdU+SA-β-gal+) followed the same pattern as the total EdU-incorporating cells (figure 4.4 B & D). Their percentage increases in males when TAM is injected ($p=0.0001$) and the number is significantly higher than what is observed in females under the same conditions ($p<0.001$). The EdU-SA-β-gal+ cells followed the trend of the total senescent cells (SA-β-gal+) (figure 4.4 C & E).

A mean percentage of 8.1+/-1.7% of cells expressed Sox9 in male mice injected with TAM against 16.4+/-2.7% when corn oil was injected (figure 4.4 F). The difference between these two numbers was determined to be statistically significant ($p=0.023$). For female mice, these numbers were 9.7+/-3.5% with TAM injection and 8.3+/-5.5% in the case of corn oil. There was a significant difference in the Sox9 expression between male and female mice injected with corn oil, less cells expressed Sox9 in females ($p=0.025$) (figure 4.4 F).

In summary, young male and female mice present a similar baseline proliferation and senescence rate (figure 4.4 B & C). TAM stimulates chondrocyte proliferation in young male mice but not in young females (figure 4.4 B). This phenomenon is concomitant with a decreased Sox9 expression in males and a steady Sox9 expression in females (figure 4.4 F). TAM likely induce male Sox9+ SSPCs commitment toward proliferation and/or differentiation, an effect not observed in females. This TAM-induced chondrocyte proliferation in males is concomitant with an expected induction of senescence in the proliferating chondrocytes (figure 4.4 D) while the overall senescence of the tissue stays unchanged (figure 4.4 C). TAM appears to have a sex-dependent effect on GP chondrocytes, inducing their proliferation (with concomitant senescence in males) and protecting them from senescence in females while their proliferation rate stays the same.

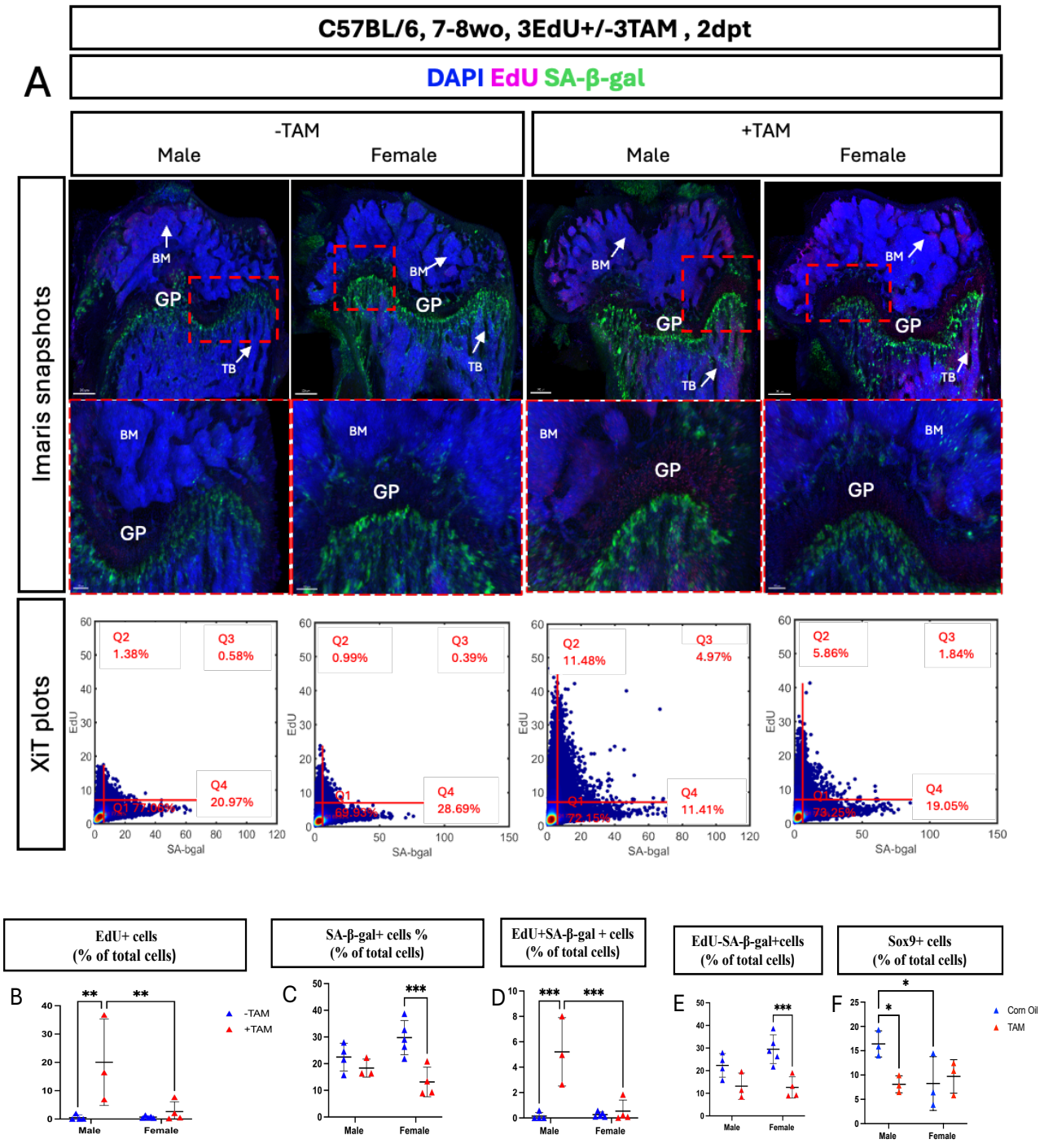

Figure 4.4. Tamoxifen effect on growth plate chondrocytes. 8-week-old C57Bl6 mice (n=16, seven males and nine females) received three injections of tamoxifen and EdU while controls were injected with either EdU only or EdU and corn oil (TAM vehicle). Femurs were harvested two (2) days after the last injection, processed and analyzed. A) Confocal images of the distal femur of mice of both sexes which have received either tamoxifen and EdU or EdU only. B) Quantification of EdU+ cells in the total cell population. C) Quantification of SA-β-gal+ cells in the total cell population, D) Quantification of double positive (EdU+SA-β-gal+) cells in the total cell population. E) Quantification of EdU-SA-β-gal+ cells in the total cell population. F) Quantification of Sox9+cells in the total cell population. All results are expressed as the percentage of the total cell population. comparison between the four groups was performed by the two way-ANOVA test with a significant threshold set at p=0.05 and no correction for multiple comparisons (Fisher's LSD test). Dpt: day post-tamoxifen, GP: growth plate; TB: trabecular bone; BM: bone marrow.

Chapter 5: Discussion, limitations, future directions and conclusion

5.1 Discussion

Multiple diseases affecting the elderly are particularly rare during youth. In the skeletal system, the high prevalence of conditions such as osteoarthritis, osteoporosis and fractures in the aging population constitutes a huge socio-economic burden. Since stem cells are responsible for homeostatic maintenance and repair of most tissues, including the skeleton, a better understanding of stem cell physiology in the elderly would provide novel therapeutic avenues to prevent, cure, or stop the progression of age-related diseases. Studies performed in our lab showed that putative self-renewing SSCs are present in the skeleton[58]. As this cell population was present in aged mice bone, we favored the senescence hypothesis as a potential etiologic mechanism in age-related conditions and aged bone blunted regenerative capacity over, for instance, an eventual depletion of the SSC niche. We hypothesized that a decrease in SSPCs proliferation rate and their entry into senescence was responsible for the advent of these conditions in the aged skeleton and that influencing pathways involved in bone development can change SSPCs fate decisions and provide insights to address these age-related conditions in the future.

5.1.1 SSPCs proliferation and senescence rate with sex and age in vivo

Bone mass decreases with age[163]. However, the constant presence of stem and progenitor cells has been proven in mouse growth cartilage. Changes in the fate decision of these cells are certainly involved in the onset of bone loss with age. My hypothesis was that there is an increase in senescence and a decrease in the proliferation of these cells with age. To study these two

processes in SSPCs, 1-year-old Sox9-CreERT; Ai14 mice were used in the study. With regards to skeletal development and maturity, 1-year-old mice correspond to mid-forty/early 50-year-old humans[205]. 8-week-old mice were analyzed as controls. 8 weeks for a mouse correspond to between 11.5 and 20 years for a human.

The data collected in these experiments showed a decrease in the abundance of the tdT+Sox9+ (SSPCs) cell population with a decreased proliferation and decreased senescence with age (figure 3.1 & 3.2). The decrease in proliferation was not statistically significant likely due to the study being underpowered. At some point between the 8th week and 1st year of the mice's lives (11.5-yo and 50-yo for humans), tdT+ SSPCs decrease from a mean of 19.7% to 2.5% of total cells of the GP. During this period, the GP fuses completely in humans and incompletely in mice. As SSCs reside in the GP, the stem cell niche is lost in humans and shrinks in animals. Therefore, the GP of older animals houses less SSPCs, which are also proliferating at a slower rate. As SSPCs proliferation decreases, their senescence level follows the same trend. In murine and human bones, Farr et al., 2016, showed a higher p16^{INK4A} expression in osteocytes, osteoblasts and their progenitors in aged individuals in comparison to young ones[175]. That would suppose that while Sox9+ SSPCs proliferate less, their progeny cells keep proliferating, eventually leading to an increased senescence level, as put into evidence by Farr. *et al.,* 2016. Bone remodelling in the aged individuals is likely sustained by the few Sox9+ SSPCs remaining in the aged skeleton GP (mice) and Sox9+ SSPCs in the periosteum (mice and humans). An alternative explanation for the decrease in the number of SSPCs could be that they undergo apoptosis. I did not test for apoptosis, and it should be further investigated in the future.

It is worth to add that senescence could still be at play in the SSPCs loss in mice with age. I might have miss the time frame in which senescence was the highest in this cell population. Such

state could be followed by the apoptosis of SSPCs of the GP by the interplay of endocrine and paracrine factors such as interleukins present in the senescence-associated secretory phenotype (SASP)-induced inflammatory environment. Future analysis should be performed in mice younger than 1-year-old.

5.1.2 SSPCs proliferation kinetics and senescence with sex and age in vitro

The capacity of SSPCs to proliferate, form colonies and their senescence rate in vitro was also assessed.

The skeletal cells (tdT- and tdT+) from males and females of both age groups proliferated the same, but cells from young and aged male mice formed more colonies than their female counterparts (figure 3.3 F & H). One data point in the aged female group is extremely higher than all the other data point but it didn't reflect in the colony counting since cells proliferated so much that colonies fused, decreasing the number of colonies counted by the Harmony software. That constitutes a limitation in the interpretation of this data. Puberty in males starts later but lasts longer and bones grow faster, reaching thicker and stronger bones as the cortical deposition is higher in this sex. Male cells retained their greater colony-forming ability in vitro likely due to sex-based epigenetic imprinting of genes regulating cells proliferation in vivo [206]. Higher proliferation capacity in vivo in males likely expresses itself as a higher individual clonogenicity of SSPCs in vitro. Further investigations about the epigenetic profile of male cells in comparison to female ones is necessary to verify such claims. Also, time-lapse microscopy could be envisaged as it would help investigate this finding further without the limitations of imaging and analyzing fixed cell.

SSPCs (tdT+) percentage reached a mean of 66.7% of the total cells (tdT- and tdT+) in vitro for aged females (figure 3.3 I). This number varied from 26% to 33% for young males and females and for aged males in vitro. The total number of cells being similar across age and sex groups, SSPCs (tdT+) of aged females have a higher ratio relative to the total cell count than committed tdT- cells in vitro. These cells are likely targeted by hormones and factors affecting their proliferation in vivo. This property of aged female cells could be used in cell-based therapies aimed to address bone loss in postmenopausal women. A limitation is the increased senescence level. 71.3 % of the SSPCs were senescent under these culture conditions.

In general, the mean senescence rate of SSPCs in vitro varied from 54.5 to 72.5% (figure 3.3 J) whereas this number ranged from 0.5 to 8.2% in vivo (figure 3.2 D). The culture conditions used in this study are not favorable for long-term expansion of this cell population in vitro. Optimization of culture conditions to favor expansion of Sox9+ SSPCs while avoiding replicative senescence will likely be required for the future development of culture-expanded stem cell products for therapeutic use in regenerative orthopedic surgery.

5.1.3 Multilineage differentiation potential of SSCs with age

I next assessed the multilineage differentiation potential of aged 1-year-old SSPCs in vitro. Cells were placed in osteogenic, adipogenic and chondrogenic conditions. Cells from 8-week-old mice cells were analyzed as controls.

My analysis shows that SSPCs maintained their multilineage differentiation ability in aged mice. tdT+ osteoblasts, chondrocytes and adipocytes were identified in aged samples (figure 3.4, 3.5 & 3.6). The SSPC population decreases in vivo but can still be isolated from bone tissue. Under differentiation conditions, they undergo multilineage differentiation. SSPCs transplantation

studies showed that adipogenic differentiation is favored in aged mice at the expense of osteogenic differentiation[207]. Since we only performed a qualitative analysis of the differentiation potential of tdT+ cells, we cannot draw conclusion on a potential lineage bias with age. Further quantitative analysis should be carried out.

5.1.4 Effect of PTH and Hh pathway regulators on SSPCs proliferation and senescence in vitro.

A second hypothesis for this work was that influencing pathways activated during bone development and in putative SSCs in the resting zone of the growth plate (GP) can change SSPCs fate decisions. PTH is involved in bone homeostasis in the organism. It is used in the treatment of osteoporosis in postmenopausal women[208]. At the cellular level, it has been reported to induce an increase in the number of Sox9-expressing cells in mouse bone and their differentiation into osteoblasts [194]. A CellChat analysis performed in the lab, demonstrated molecular crosstalk between several bone cell types and resting zone chondrocytes (RZ-Ch), which constitute the SSCs [58]. The RZ-Ch receive canonical and non-canonical Wnt signaling from hypertrophic chondrocytes. Perichondral cells, osteoblasts, and fibroblasts send Hh, FGF and PTH signals to the resting zone chondrocytes, respectively.

First, I assessed the effect of PTH (1-34), purmorphamine, cyclopamine and 20(S)-OHC in vitro. the compounds were added to the cell media at the moment of plating skeletal cells of 8-week-old Sox9-CreERT; Ai14 mice. These mice were euthanized two days post-TAM injection. Of the compounds tested, three did not have any effect in vitro: PTH (1-34), purmorphamine, and cyclopamine. 20(S)-OHC did not influence skeletal cells (tdT- and tdT+) proliferation, colony formation and expansion but decreased tdT+ cell proliferation and senescence. SSPCs were kept

quiescent/non-proliferative by 20(S)-OHC. 20(S)-OHC is known to stimulate osteogenic differentiation in murine MSCs, but in the setting of this work the cells were not under differentiation conditions and no sign of mineralization was observed. To my knowledge, no studies have reported on the effect of PTH, 20(S)-OHC, purmorphamine and cyclopamine on Sox9+ SSPCs in vitro, specifically.

It has been reported that 20(S)-OHC, purmorphamine and PTH promote osteogenic differentiation of MSCs through activation of the Hh pathway[183,185,188,198,199]. Only 20(S)-OHC influenced the Sox9+ SSPCs in the first assay. This prompted me to question whether this observed effect of 20(S)-OHC on SSPCs was indeed through a Hh pathway activation. 20(S)-OHC was tested again. Cell stimulation with 20(S)-OHC would be continuous in this second assay. Also, cyclopamine—a Hh antagonist—was added to the medium to test for an activation of the Hh pathway in SSPCs by 20(S)-OHC. The previously mentioned effects (decreased tdT+ cell proliferation and senescence) would be inhibited by the addition of cyclopamine to the medium.

Continuous stimulation with 20(S)-OHC had a striking inhibiting effect on the total (tdT+ and tdT-) cell population expansion, their colony-forming capacity and colony expansion. These parameters decreased considerably in the presence of cyclopamine (figure 4.2). Also, the number of tdT+ (SSPCs) cells decreased (figure 4.2 D). 20(S)-OHC has a similar effect on SPPCs (tdT+) and total (tdT- and tdT+) cells (figure 4.2 C & D). Both cell types were kept quiescent/non-proliferative. However, continuous stimulation was needed to inhibit proliferation of tdT- cells (figure 4.1 H). This decreased proliferation in tdT- and tdT+ is reflected by a decrease in replicative senescence (figure 4.2 E & F). The effect of 20(S)-OHC on tdT- and tdT+ cells is likely exerted through the same pathway as proliferation and senescence are similarly inhibited in both cell populations.

Cyclopamine did not reverse the effect of 20(S)-OHC on any of the measured parameters, whereas this effect was expected[209]. One explanation could be that the media contained some Hh family proteins that activated the Patched 1 (Ptch1) receptor. Together with the 20(S)-OHC, these Hh proteins triggered the transmembrane protein Smoothened (Smo) relocation to the primary cilium[210]. In the case of such occurrence, the cyclopamine dose added would be insufficient for an effective antagonistic effect.

Also, cyclopamine's modulation of Smo is binding site-dependent[211]. It acts as an Hh pathway agonist when it binds the extracellular cysteine-rich domain (CRD) of Smo, and as an Hh antagonist only when binding to the heptahelical transmembrane domain (TMD). The exact Smo domain through which cyclopamine binds on SSPCs is not known. The effect of cyclopamine on SSPCs necessitate further investigations. Thus far, I could not determine if 20(S)-OHC acts through the Hh pathway to exert its effects on SSPCs. Future studies will also be required to answer this important question.

In vivo Hh activation in PTHrP+ resting zone chondrocytes stimulated an exaggerated proliferative response described as "patched roses" (concentric, potentially clonal population of PTHrP+ chondrocytes in the metaphysis) and their migration to the trabecular bone where they differentiated into osteoblasts[231]. By this report, the PTHrP+ chondrocytes are SSPCs which include the SSC population. These PTHrP+ SSPCs exited the quiescence stage upon Hh activation. I observed a reverse effect on Sox9+ SSPCs and skeletal (tdT- and tdT+) cells in vitro (figure 4.2 C & D). In general, no reports on the effect of Hh activation in Sox9+ SSPCs is available in the literature. This report is the first of its kind. It lays the foundation for the use of Hh agonists in attempts to inhibit skeletal (total tdT+ and tdT-) cell proliferation. Further steps could involve studying the effect of Hh activators on SSPCs quiescence, proliferation and self-renewal in vivo.

5.1.5 Effect of PTH on the SSPC population size in vivo

I also tested the ability of PTH (1-34) to influence SSPCs fate decision.

Intermittent PTH administration increases bone mass by stimulating new bone formation (cortical, trabecular, endosteal and periosteal bone apposition) in humans, rabbits, monkeys and rodents [212–218]. At low concentrations, PTH stimulates osteoblastic activation and bone formation [194]. It is believed that the rapid degradation of the hormone prevents osteoclast activation and bone resorption. Daily low-dose PTH is currently used in the treatment of osteoporosis in postmenopausal woman[208]. I wanted to test its effect on the Sox9+ SSPCs.

A PTH (1-34) concentration of 400ng/g was injected every day over a four-day period to aged Sox9-CreERT; Ai14 mice, and the SSPC population in the GP compared between PTH-treated samples and controls. No significant difference was observed between experimental and control groups (figure 4.3 C). This result echoed what was observed in a report by the Kronenberg group[194] . In 6-week-old mice, a three-day pulse had no effect on the Sox9+ SSPCs in the metaphysis (GP included). On the other hand, a seven-day pulse of PTH increased the Sox9+ cell population and their differentiation into osteoblasts. The establishment of PTH's effect takes place only after sustained stimulation— for at least a week—of Sox9+ cells. This experiment should be repeated with a similar pulse period. This property of PTH could be exploited in future attempts to induce SSPCs proliferation in vitro for future transplantation in the setting of stem cell-based therapies.

5.1.6 Sex-dependent Tamoxifen (TAM) effect on growth plate (GP) chondrocytes proliferation and senescence in C57Bl/6 mice

In experiments aimed at testing the effect of TAM in vivo, chondrocytes from young male and female mice presented a similar baseline proliferation and senescence rate when treated with the TAM vehicle (figure 4.4 B & C). Based on EdU incorporation, TAM stimulated chondrocyte proliferation in young males but not in young females (figure 4.4 B). This TAM-induced chondrocyte proliferation is concomitant with an expected induction of senescence in a small fraction of males' proliferating chondrocytes, based on SA-β-gal expression (figure 4.4 D). As previously mentioned, proliferation is often followed by replicative senescence. Male mice also had a higher Sox9+ SSPC proportion in the distal femoral GP before TAM injection (figure 4.4 F). This level was decreased to the female level after TAM. Therefore, in male mice, TAM likely induced SSPCs commitment toward proliferation (with concomitant senescence entry), and/or differentiation. It would be interesting to investigate the relationship between transcription factors such as Sox9 and TAM and identify the type of progeny coming out of this stimulation.

Female chondrocytes exposed to TAM were protected from proliferation and senescence in mice (figure 4. 4 B & C). In post-menopausal women TAM has been shown to only slightly increase bone mineral density when compared to estrogen and bisphosphonate therapy[219]. In practice, TAM is unlikely to be effective as a growth stimulant in females and could be used in the treatment of senescence-associated skeletal conditions of the elderly women.

In general, these results could change our perception of aging, particularly in the skeletal system. SSPCs population decreases while proliferating less. The sexual dimorphism observed in

vivo with TAM complicates the development of drugs capable of addressing diseases indiscriminately in both sexes.

Also, I gathered more proof regarding the pitfalls of the use of TAM in the inducible Cre-recombinase system widely used in bone research. In the field of SSPCs, researchers who inject TAM into their mice to induce the expression of a reporter of interest, should consider the possible effects of this drug on this cell population, include information on this subject in their reports and, if possible, choose a mouse genetic construct other than the TAM-inducible Cre, i.e., not requiring TAM injection (see section 1.3.1).

The main goal with this work was to contribute to the theorical basis for the future development of stem-cell based therapies addressing diseases of the aged individual. The hypothesis that senescence was the main culprit in the latter cases has been put forward. The decrease of the SSPC population with a decrease in their proliferation and senescence force us to consider other angles in future studies.

5.2 Limitations and future directions

Some limitations of the work I presented in this thesis should be mentioned. Senescence was assessed with SA-β-gal as the sole marker in vivo (figure 3.2 & 4.4). The international cell senescence association (ICSA) recommends the confirmation with a second marker. In vitro, $p16^{INK4A}$ successfully labeled between 84.2% and 99.95% of the SA-β-gal expressing cells (figure 3.3 K). Anti-$p16^{INK4A}$ antibody that can be used on tissue sections are scarce, and none of those I screened showed any overlapping staining with SA-β-gal in vivo. It would be important to repeat these experiments with other senescence markers such as lamin B1[220–223].

Multiple trends observed in this study were not confirmed by the statistical tests performed (figure 3.1 D & F, 4.4 C &E). The small sample size in my experiment limited my statistical power. These studies should be repeated with a larger sample size to uncover suspected differences hidden by an underpowered analysis in the case of the present study.

In this thesis, I addressed the Sox9+ SSPCs in the GP. The same assessment should be made for Sox9+SSPCs of the periosteum. Any kinetic and dynamic change of this cell population would complete the story and further the understanding of Sox9+ SSPCs fate decision with age.

I missed on the opportunity to show an effect of PTH (1-34) on the SSPCs in vivo (figure 4.3). This experiment should be repeated with a seven-day pulse and quantification of self-renewal and multilineage differentiation of Sox9+ SSPCs should be made.

The extrapolation of the results of TAM stimulation on the chondrocytes of the GP has its limits (figure 4.4). I am uncertain that the observed effect applies to the Sox9+ cell population. This uncertainty can be addressed by performing anti-Sox9 antibody staining along with the other parameters studied (EdU incorporation, senescence).

In general, in all in vivo experiments, testing for the self-renewal of the Sox9+ SSPCs would be particularly interesting as it would narrow down and focus on the Sox9+ SSCs. Identification and influencing of SSCs can provide ways for addressing multiple age-related skeletal condition with stem-cell based therapies.

In vitro, SSPCs culture in Mesencult^{TM} basal media showed an elevated senescence rate (figure 3.3 J & K, 4.1 A, B, C & D EtOH, 4.2 E &F). This should be addressed in future assays. For example, medium supplement with FGF-2 could be used to culture these cells and prevent these pitfalls[224,225]. Also, A time-course analysis of the lysosomal *galactosidase β 1* (*GLB1*) gene

expression should be considered in the future as it can provide thorough information about the dynamics at play over the seven-day period of the culture.

As the work with cyclopamine and 20(S)-OHC was repeated. I did multiple stimulations of 20(S)-OHC alone and 20(S)-OHC associated with cyclopamine, but I did not retest cyclopamine alone. This should be considered in the future. Also, further works should be carried out to confirm Gli activation in the presence of Hh pathway activators such as 20(S)-OHC and, activators of other pathways on which 20(S)-OHC stimulation might occur should be tested. Compounds of the same group have been reported as Liver X Receptor (LXR) agonist[226,227]. LXRs are present in pre-hypertrophic and resting zone chondrocytes [228] .Stimulating these receptors with compounds such as WAY 252623 (LXR agonist) and GSK 2033 (LXR antagonist) should be done in SSPCs[226,229]. In parallel, 20(S)-OHC administration in vivo could also be attempted in young mice, aged mice and mice with bone injuries or pathological conditions.

A quantitative SSPCs multilineage differentiation potential assessment in vivo and in vitro should also be envisaged. As I did a qualitative analysis, there is a lack of information on a possible lineage bias of the SSPCs as the organism ages.

In summary, multiple avenues can be taken to complete this work.

5.3 Conclusion

SSPCs are present in the mature skeleton. Unlike in young individuals, they are less likely to ensure perfect bone maintenance in the elderly. We proposed to evaluate the behavior of SSPCs in aged mice, and to influence them using different compounds mimicking bone-anabolic hormones and/or activating pathways known to play a role in bone development and growth. The data revealed a shrinking of the SSPC population, while their proliferation rate and senescence

level decreased. In vitro, 20(S)-OHC preserved SSPCs quiescence while protecting them from senescence. In vivo, TAM stimulated male chondrocyte proliferation and senescence while protecting female chondrocytes from senescence. These compounds could be tested as therapies in senescence-associated skeletal conditions, although further assessment of the pathways activated by these compounds is necessary. These studies brought us a step closer to our goal of addressing acute and chronic skeletal system conditions affecting the elderly with skeletal stem cell-based therapies.

Chapter 6: References

1. Weatherholt, A. M., Fuchs, R. K. & Warden, S. J. Specialized connective tissue: Bone, the structural framework of the upper extremity. *Journal of Hand Therapy* 25(2):123-31 (2012).

2. Jensen, A. L., Copp, D. H., Shim, S. S. The homeostatic function of bone as a mineral reservoir. *Oral Surg Oral Med Oral Pathol.* 16:738-44 (1963).

3. Khan, I. M. *et al.* The Development of Synovial Joints. *Current Topics in Developmental Biology* 79:1-36 (2007).

4. Nishimoto, S. & Logan, M. P. O. Subdivision of the lateral plate mesoderm and specification of the forelimb and hindlimb forming domains. *Seminars in Cell and Developmental Biology* 49:102–8 (2016).

5. Roth, D. M., Bayona, F., Baddam, P. & Graf, D. Craniofacial Development: Neural Crest in Molecular Embryology. *Head and Neck Pathology* 15(1):1-15 (2021).

6. Blumer, M. J. F. Bone tissue and histological and molecular events during development of the long bones. *Annals of Anatomy* 235:151704 (2021).

7. Mackie, E. J., Ahmed, Y. A., Tatarczuch, L., Chen, K. S. & Mirams, M. Endochondral ossification: How cartilage is converted into bone in the developing skeleton. *International Journal of Biochemistry and Cell Biology* 40(1):46–62 (2008).

8. Hall, B. K. & Miyake, T. All for one and one for all: Condensations and the initiation of skeletal development. *BioEssays* 22(2):138–47 (2000).

9. Zhao, Q., Eberspaecher, H., Lefebvre, V. & De Crombrugghe, B. Parallel expression of Sox9 and Col2a1 in cells undergoing chondrogenesis. *Developmental Dynamics* 209(4):377–86 (1997).

10. Yang, L., Tsang, K. Y., Tang, H. C., Chan, D. & Cheah, K. S. E. Hypertrophic chondrocytes can become osteoblasts and osteocytes in endochondral bone formation. *Proc Natl Acad Sci U S A* 111(33):12097–102 (2014).

11. Zhou, X. *et al.* Chondrocytes Transdifferentiate into Osteoblasts in Endochondral Bone during Development, Postnatal Growth and Fracture Healing in Mice. *PLoS Genet* 10(12):e1004820 (2014).

12. Park, J. *et al.* Dual pathways to endochondral osteoblasts: A novel chondrocytederived osteoprogenitor cell identified in hypertrophic cartilage. *Biol Open* 4(5):608–21 (2015).

13. Jing, Y. *et al.* Chondrocytes directly transform into bone cells in mandibular condyle growth. *J Dent Res* 94(12):1668–75 (2015).

14. Hojo, H., Ohba, S., He, X., Lai, L. P. & McMahon, A. P. Sp7/Osterix Is Restricted to Bone-Forming Vertebrates where It Acts as a Dlx Co-factor in Osteoblast Specification. *Dev Cell* 37(3):238–53 (2016).

15. Otto, F. *et al.* Cbfa1, a Candidate Gene for Cleidocranial Dysplasia Syndrome, Is Essential for Osteoblast Differentiation and Bone Development. *Cell* 89(5):765-71. (1997).

16. Nakashima, K. *et al.* The Novel Zinc Finger-Containing Transcription Factor Osterix Is Required for Osteoblast Differentiation and Bone Formation Blasts Derive from a Common Precursor. *Cell* vol. 108 (1):17-29 (2002).

17. Wright, E. M., Snopek, B. & Koopman, P. Seven New Members of the Sox Gene Family Expressed during Mouse Development. *Nucleic Acids Research* vol. 21(3):744 (1993).

18. Bi, W., Deng, M., Zhang, Z., Behringer, R. R. & De Crombrugghe B. Sox9 Is Required for Cartilage Formation. *Nat Genet.* 22(1):85-9 (1999).

19. Wright, E. *et al.* The Sry-Related Gene Sox9 Is Expressed during Chondrogenesis in Mouse Embryos. *Nat Genet.* 9(1):15-20 (1995).

20. Huang, W., Zhou, X., Lefebvre, R. & De Crombrugghe, B. Phosphorylation of SOX9 by Cyclic AMP-Dependent Protein Kinase A Enhances SOX9's Ability to Transactivate a Col2a1 Chondrocyte-Specific Enhancer. *Molecular and cellular biology* vol. 20(11):4149-58. (2000).

21. Ronique Lefebvre, V., Huang, W., Harley, V. R., Goodfellow, P. N. & De Crombrugghe, B. SOX9 Is a Potent Activator of the Chondrocyte-Specific Enhancer of the Pro1(II) Collagen Gene. *Molecular and cellular biology* 17(4):2336-46. (1997).

22. Akiyama, H., Chaboissier, M. C., Martin, J. F., Schedl, A. & De Crombrugghe, B. The transcription factor Sox9 has essential roles in successive steps of the chondrocyte differentiation pathway and is required for expression of Sox5 and Sox6. *Genes Dev* 16(21):2813–28 (2002).

23. Akiyama, H. *et al.* Osteo-Chondroprogenitor Cells Are Derived from Sox9 Expressing Precursors. *Proc Natl Acad Sci U S A.* 102(41):14665-70 (2005).

24. Kawanami, A., Matsushita, T., Chan, Y. Y. & Murakami, S. Mice expressing GFP and CreER in osteochondro progenitor cells in the periosteum. *Biochem Biophys Res Commun* 386(3):477–82 (2009).

25. Liu, C. F. & Lefebvre, V. The transcription factors SOX9 and SOX5/SOX6 cooperate genome-wide through super-enhancers to drive chondrogenesis. *Nucleic Acids Res* 43(17):8183–203 (2015).

26. Lefebvre, V., Li, P. & De Crombrugghe, B. A New Long Form of Sox5 (L-Sox5), Sox6 and Sox9 Are Coexpressed in Chondrogenesis and Cooperatively Activate the Type II Collagen Gene. *The EMBO Journal* 17(19):5718-33 (1998).

27. Huang, W., Chung, U.-I., Kronenberg, H. M., De Crombrugghe, B. & Rosenfeld, M. G. The Chondrogenic Transcription Factor Sox9 Is a Target of Signaling by the Parathyroid Hormone-Related Peptide in the Growth Plate of Endochondral Bones. *Proc Natl Acad Sci U S A.* 98(1):160-5 (2001).

28. Day, T. F., Guo, X., Garrett-Beal, L. & Yang, Y. Wnt/β-catenin signaling in mesenchymal progenitors controls osteoblast and chondrocyte differentiation during vertebrate skeletogenesis. *Dev Cell* 8(5):739–50 (2005).

29. Ohba, S. Hedgehog signaling in skeletal development: Roles of Indian hedgehog and the mode of its action. *International Journal of Molecular Sciences* 21(18):6665 (2020).

30. Yang, J., Andre, P., Ye, L. & Yang, Y. Z. The Hedgehog signalling pathway in bone formation. *International Journal of Oral Science* 7(2):73–9 (2015).

31. Lanske, B. *et al.* PTH/PTHrP Receptor in Early Development and Indian Hedgehog-Regulated Bone Growth. *Science* 273(5275):663-6 (1996).

32. Vortkamp, A. *et al.* Regulation of Rate of Cartilage Differentiation by Indian Hedgehog and PTH-Related Protein. *Science* 273(5275):613-22 (1996).

33. Guo, J. *et al.* PTH/PTHrP receptor delays chondrocyte hypertrophy via both Runx2-dependent and -independent pathways. *Dev Biol* 292(1):116-28 (2006).

34. St-Jacques, B., Hammerschmidt, M. & Mcmahon, A. P. Indian Hedgehog Signaling Regulates Proliferation and Differentiation of Chondrocytes and Is Essential for Bone Formation. *Genes Dev.* 13(16):2072-86 (1999).

35. Ornitz, D. M. & Marie, P. J. Fibroblast growth factor signaling in skeletal development and disease. *Genes Dev.* 29(14):1463-86. (2015)

36. Sahni, M. *et al.* FGF Signaling Inhibits Chondrocyte Proliferation and Regulates Bone Development through the STAT-1 Pathway. *Genes Dev.* 13(11):1361-6 (1999).

37. Minina, E., Kreschel, C., Naski, M. C., Ornitz, D. M. & Vortkamp, A. Interaction of FGF, Ihh/Pthlh, and BMP Signaling Integrates Chondrocyte Proliferation and Hypertrophic Differentiation. *Developmental Cell* 3(3):439-49 (2002).

38. Ohbayashi, N. *et al.* FGF18 is required for normal cell proliferation and differentiation during osteogenesis and chondrogenesis. *Genes Dev.* 16(7):870–9 (2002).

39. Liu, Z., Xu, J., Colvin, J. S. & Ornitz, D. M. Coordination of chondrogenesis and osteogenesis by fibroblast growth factor 18. *Genes Dev.* 16(7):859–69 (2002).

40. Takimoto, A., Nishizaki, Y., Hiraki, Y. & Shukunami, C. Differential actions of VEGF-A isoforms on perichondrial angiogenesis during endochondral bone formation. *Dev Biol.* 332(2):196–211 (2009).

41. Maes, C. *et al.* Impaired Angiogenesis and Endochondral Bone Formation in Mice Lacking the Vascular Endothelial Growth Factor Isoforms VEGF 164 and VEGF 188. *Mech Dev.* 111(1-2):61-73 (2002).

42. Dai J, Rabie AB. VEGF: an essential mediator of both angiogenesis and endochondral ossification. *J Dent Res.* 86(10):937-50 (2007)

43. Pizette, S. & Niswander, L. BMPs are required at two steps of limb chondrogenesis: Formation of prechondrogenic condensations and their differentiation into chondrocytes. *Dev Biol* 219(2): 237–49 (2000).

44. Xie, H. *et al.* PDGF-BB secreted by preosteoclasts induces angiogenesis during coupling with osteogenesis. *Nat Med* 20(11):1270–8 (2014).

45. Wu, M., Wu, S., Chen, W. & Li, Y. P. The roles and regulatory mechanisms of TGF-β and BMP signaling in bone and cartilage development, homeostasis and disease. *Cell Research* vol. 34:101–23 (2024).

46. Hosaka, Y. *et al.* Notch signaling in chondrocytes modulates endochondral ossification and osteoarthritis development. *Proc Natl Acad Sci U S A* 110(5):1875-80 (2013).

47. Mead, T. J. & Yutzey, K. E. Notch Pathway Regulation of Chondrocyte Differentiation and Proliferation during Appendicular and Axial Skeleton Development. *Proc Natl Acad Sci U S A.* 106(34):14420-5 (2009).

48. Hosaka, Y. *et al.* Notch signaling in chondrocytes modulates endochondral ossification and osteoarthritis development. *Proc Natl Acad Sci U S A* 110(5):1875-80 (2013).

49. Yakar, S. *et al.* Circulating levels of IGF-1 directly regulate bone growth and density. *Journal of Clinical Investigation* 110(6):771–81 (2002).

50. Jin, S. W., Sim, K. B. & Kim, S. D. Development and growth of the normal cranial vault: An embryologic review. *Journal of Korean Neurosurgical Society* 59(3):192–6 (2016).

51. Abad, V. *et al.* The Role of the Resting Zone in Growth Plate Chondrogenesis. *Endocrinology* 143(5):1851–7 (2002).

52. Voller, T., Cameron, P., Watson, J. & Phadnis, J. *The Growth Plate: Anatomy and Disorders*. *Orthopaedics and trauma* 34(3):135-40 (2020).

53. Noonan, K. J., Hunziker, E. B., Nessler, J. & Buckwalter, J. A. Changes in cell, matrix compartment, and fibrillar collagen volumes between growth-plate zones. *Journal of Orthopaedic Research* 16(4):500–8 (1998).

54. Mackie, E. J., Ahmed, Y. A., Tatarczuch, L., Chen, K. S. & Mirams, M. Endochondral ossification: How cartilage is converted into bone in the developing

skeleton. *International Journal of Biochemistry and Cell Biology* 40(1):46–62 (2008).

55. Trompet, D., Melis, S., Chagin, A. S. & Maes, C. Skeletal stem and progenitor cells in bone development and repair. *Journal of Bone and Mineral Research* 39(6):633–654 (2024).

56. Bianco, P. & Robey, P. G. Skeletal stem cells. *Development* 142(6):1023-7 (2015).

57. Blanpain, C. & Simons, B. D. Unravelling stem cell dynamics by lineage tracing. *Nature Reviews Molecular Cell Biology* 14(8):489–502 (2013).

58. Farhat, S. *et al.* Title: Self-renewing Sox9+ osteochondral stem cells in the postnatal skeleton Authors. https://doi.org/10.1101/2023.12.07.570646 doi:10.1101/2023.12.07.570646.

59. Gratzner, H. G. Monoclonal Antibody to 5-Bromo- and 5-Iododeoxyuridine: A New Reagent for Detection of DNA Replication. *Science* 218(4571):474-5 (1982).

60. Angelozzi, M., de Charleroy, C. R. & Lefebvre, V. EdU-Based Assay of Cell Proliferation and Stem Cell Quiescence in Skeletal Tissue Sections. *Methods in Molecular Biology* 2230:357–65 (2021).

61. Mead, T. J. & Lefebvre, V. Proliferation assays (BrdU and EdU) on skeletal tissue sections. *Methods in Molecular Biology* 1130:233–43 (2014).

62. Kerney, R. R., Brittain, A. L., Hall, B. K. & Buchholz, D. R. Cartilage on the move: Cartilage lineage tracing during tadpole metamorphosis. *Dev Growth Differ* 54(8):739–752 (2012).

63. Gossen, M. & Bujardt, H. Tight Control of Gene Expression in Mammalian Cells by Tetracycline-Responsive Promoters. *Proc Natl Acad Sci U S A.* 89(12):5547-51 (1992).

64. Das, A. T., Tenenbaum, L. & Berkhout, B. Tet-On Systems For Doxycycline-inducible Gene Expression. *Curr Gene Ther*. 16(3):156-67 (2016).

65. Baron U, Bujard H. Tet repressor-based system for regulated gene expression in eukaryotic cells: principles and advances. *Methods Enzymol.* 327:401-21 (2000).

66. Tumbar, T. *et al.* Defining the Epithelial Stem Cell Niche in Skin. *Science* 303(5656):359-63 (2004).

67. McLellan, M. A., Rosenthal, N. A. & Pinto, A. R. Cre-loxP-Mediated Recombination: General Principles and Experimental Considerations. *Curr Protoc Mouse Biol* 7(1):1–12 (2017).

68. Kim, H., Kim, M., Im, S.-K. & Fang, S. Mouse Cre-LoxP system: general principles to determine tissue-specific roles of target genes. *Lab Anim Res* 34(4):147-159 (2018).

69. Utomo A. R. H. et al., Temporal, spatial, and cell type–specific control of Cre-mediated DNA recombination in transgenic mice. *Nat Biotechnol.* 17(11):1091-6. (1999)

70. Sauer, B. Inducible Gene Targeting in Mice Using the Cre/Lox System. *Methods* 14(4):381-92 (1998).

71. Ranjbarvaziri, S. *et al.* Generation of Nkx2-5/CreER transgenic mice for inducible Cre expression in developing hearts. *Genesis* 55(8):10.1002/dvg.23041 (2017).

72. Bosenberg, M. *et al.* Characterization of melanocyte-specific inducible Cre recombinase transgenic mice. *Genesis* 44(5):262–7 (2006).

73. Chan, C. K. F. *et al.* Identification and specification of the mouse skeletal stem cell. *Cell* 160(1-2):285–98 (2015).

74. Liu, Y. *et al.* Osterix-Cre Labeled Progenitor Cells Contribute to the Formation and Maintenance of the Bone Marrow Stroma. *PLoS One* 8(8):e71318 (2013).

75. Ono, N., Ono, W., Nagasawa, T. & Kronenberg, H. M. A subset of chondrogenic cells provides early mesenchymal progenitors in growing bones. *Nat Cell Biol* 16(12):1157–67 (2014).

76. Worthley, D. L. *et al.* Gremlin 1 identifies a skeletal stem cell with bone, cartilage, and reticular stromal potential. *Cell* 160(1-2):269–84 (2015).

77. Novak, S. & Kalajzic, I. AcanCreER lacks specificity to chondrocytes and targets periosteal progenitors in the fractured callus. *Bone* 166:116599 (2023).

78. Mizuhashi, K. *et al.* Resting zone of the growth plate houses a unique class of skeletal stem cells. *Nature* 563(7730):254–58 (2018).

79. Südbeck, P. & Scherer, G. Two independent nuclear localization signals are present in the DNA- binding high-mobility group domains of SRY and SOX9. *Journal of Biological Chemistry* 272(44):27848–52 (1997).

80. Südbeck, P. *et al.* Sex Reversal by Loss of the C-Terminal Transactivation Domain of Human SOX9. *Nat Genet.* 13(2):230-2 (1996).

81. Kwok, C. *et al.* Mutations in SOX9, the Gene Responsible for Campomelic Dysplasia and Autosomal Sex Reversal. *Am. J. Hum. Genet* 57:1028-36 (1995).

82. Wagner, T. *et al.* Autosomal Sex Reversal and Campomelic Dysplasia Are Caused by Mutations q and around the SRY-Related Gene SOX9. *Cell* 79:1111-20 (1994).

83. Purba T. S. *et al.* Mapping the expression of epithelial hair follicle stem cell-related transcription factors LHX2 and SOX9 in the human hair follicle. *Experimental Dermatology* 24(6):462-7 (2015)

84. Fantauzzo, K. A., Kurban, M., Levy, B. & Christiano, A. M. Trps1 and Its Target Gene Sox9 Regulate Epithelial Proliferation in the Developing Hair Follicle and Are Associated with Hypertrichosis. *PLoS Genet* 8(11):1-12 (2012).

85. Stüfchen, I. *et al.* Sox9 regulates melanocytic fate decision of adult hair follicle stem cells. *iScience* 26(6):1-18 (2023).

86. Trogisch, F. A. *et al.* Endothelial Cells Drive Organ Fibrosis in Mice by Inducing Expression of the Transcription Factor SOX9. *Sci. Transl. Med* 16(736):eabq4581 (2024).

87. Antoniou, A. *et al.* Intrahepatic Bile Ducts Develop According to a New Mode of Tubulogenesis Regulated by the Transcription Factor SOX9. *Gastroenterology* 136(7):2325–33 (2009).

88. Han, X. *et al.* Lineage Tracing Reveals the Bipotency of SOX9+ Hepatocytes during Liver Regeneration. *Stem Cell Reports* 12(3):624–38 (2019).

89. Guo, W. *et al.* Slug and Sox9 cooperatively determine the mammary stem cell state. *Cell* 148(5):1015–28 (2012).

90. Suzuki, Y., Sasaki, T., Kakisaka, K., Abe, H. & Takikawa, Y. Evaluation of SOX9-positive hepatocytes in human liver specimens and mature mouse hepatocytes. *Methods in Molecular Biology* 2544:217–25 (2022).

91. Roche, K. C. *et al.* SOX9 maintains reserve stem cells and preserves radioresistance in mouse small intestine. *Gastroenterology* 149(6):1553-1563.e10 (2015).

92. Kopp, J. L. *et al.* Sox9+ ductal cells are multipotent progenitors throughout development but do not produce new endocrine cells in the normal or injured adult pancreas. *Development* 138(4):653–65 (2011).

93. McDonald, E., Krishnamurthy, M., Goodyer, C. G. & Wang, R. The emerging role of SOX transcription factors in pancreatic endocrine cell development and function. *Stem Cells and Development* 18(10):1379–87 (2009).

94. Belo, J., Krishnamurthy, M., Oakie, A. & Wang, R. The role of SOX9 transcription factor in pancreatic and duodenal development. *Stem Cells and Development* 22(22):2935–43 (2013).

95. Henry, S. P., Liang, S., Akdemir, K. C. & De Crombrugghe, B. The postnatal role of Sox9 in cartilage. *Journal of Bone and Mineral Research* 27(12):2511–25 (2012).

96. Farhat, S. *et al.* Title: Self-renewing Sox9+ osteochondral stem cells in the postnatal skeleton Authors. https://doi.org/10.1101/2023.12.07.570646 doi:10.1101/2023.12.07.570646.

97. Stöckl, S. *et al.* Sox9 modulates cell survival and adipogenic differentiation of multipotent adult rat mesenchymal stem cells. *J Cell Sci* 126(13):2890–902 (2013).

98. Hallett, S. A. *et al.* RUNX2 is essential for maintaining synchondrosis chondrocytes and cranial base growth. *Bone Res* 13(1):57 (2025).

99. Komori, T. Signaling networks in RUNX2-dependent bone development. *Journal of Cellular Biochemistry* 112(3):750–5 (2011).

100. Komori, T. Bone development by Hedgehog and Wnt signaling, Runx2, and Sp7. *Journal of Bone and Mineral Metabolism* 43:33–38 (2025).

101. Komori, T., Yagi, H. & Nomura, S. Targeted Disruption of Cbfa1 Results in a Complete Lack of Bone Formation Owing to Maturational Arrest of Osteoblasts. *Cell* 89:755-64 (1997).

102. Maeno, T. *et al.* Early onset of Runx2 expression caused craniosynostosis, ectopic bone formation, and limb defects. *Bone* 49(4):673–82 (2011).

103. Jiang, Q. *et al.* Roles of Sp7 in osteoblasts for the proliferation, differentiation, and osteocyte process formation. *J Orthop Translat.* 47:161–175 (2024).

104. Runt-related transcription factor-2 (Runx2) is required for bone matrix protein gene expression in committed osteoblasts in mice. *Journal of Bone Mineral Research* 36(10):2081-95 (2021).

105. Molofsky, A. V., He, S., Bydon, M., Morrison, S. J. & Pardal, R. Bmi-1 promotes neural stem cell self-renewal and neural development but not mouse growth and survival by repressing the p16Ink4a and p19 Arf senescence pathways. *Genes Dev.* 19(12):1432–37 (2005).

106. Yang, Y., Topol, L., Lee, H. & Wu, J. Wnt5a and Wnt5b exhibit distinct activities in coordinating chondrocyte proliferation and differentiation. *Development* 130(5):1003-15 (2003).

107. Regard, J. B., Zhong, Z., Williams, B. O. & Yang, Y. Wnt signaling in bone development and disease: Making stronger bone with Wnts. *Cold Spring Harb Perspect Biol* 4(12): a007997 (2012).

108. Day, T. F., Guo, X., Garrett-Beal, L. & Yang, Y. Wnt/β-catenin signaling in mesenchymal progenitors controls osteoblast and chondrocyte differentiation during vertebrate skeletogenesis. *Dev Cell* 8(5):739–50 (2005).

109. Matsushita, Y. *et al.* A Wnt-mediated transformation of the bone marrow stromal cell identity orchestrates skeletal regeneration. *Nat Commun* 11(1):332 (2020).

110. Hallett, S. A. *et al.* Chondrocytes in the resting zone of the growth plate are maintained in a wnt-inhibitory environment. *Elife* 10:e64513 (2021).

111. Friedenstein, A. J., Chailakhjan, R. K. & Lalykina, K. S. The development of fibroblast colonies in monolayer cultures of guinea-pig bone marrow and spleen cells. *Cell Prolif* 3(4):393–403 (1970).

112. Castro-Malaspina, H. *et al.* Characterization of Human Bone Marrow Fibroblast Colony-Forming Cells (CFU-F) and Their Progeny. *Blood* 56(2):289-301 (1980).

113. Moskalewski, S. & Malejczyk, J. Bone Formation Following Intrarenal Transplantation of Isolated Murine Chondrocytes: Chondrocyte-Bone Cell Transdifferentiation? *Development* vol. 107:473-80 (1989).

114. Morikawa, S. *et al.* Prospective identification, isolation, and systemic transplantation of multipotent mesenchymal stem cells in murine bone marrow. *Journal of Experimental Medicine* 206(11):2483–96 (2009).

115. Kuznetsov, S. A. *et al.* Single-Colony Derived Strains of Human Marrow Stromal Fibroblasts Form Bone After Transplantation In Vivo. *Journal of Bone and Mineral Research* 12(9):1335-47 (1997).

116. Caplan, A. I. Mesenchymal stem cells. *Journal of Orthopaedic Research* 9(5): 641-50 (1991).

117. Horwitz, E. M. *et al.* Clarification of the nomenclature for MSC: The International Society for Cellular Therapy position statement. *Cytotherapy* 7(5):393–395 (2005).

118. Caplan, A. I. & Sorrell, J. M. The MSC curtain that stops the immune system. *Immunol Lett* 168(2):136–9 (2015).

119. Pape, F. Le *et al.* Adhesion, proliferation and osteogenic differentiation of human MSCS cultured under perfusion with a marine oxygen carrier on an allogenic bone substitute. *Artif Cells Nanomed Biotechnol* 46(1):95–107 (2018).

120. Carrancio, S. *et al.* Optimization of mesenchymal stem cell expansion procedures by cell separation and culture conditions modification. *Exp Hematol* 36(8):1014–21 (2008).

121. Dusfour, G. *et al.* Mesenchymal stem cells-derived cartilage micropellets: A relevant in vitro model for biomechanical and mechanobiological studies of cartilage growth. *Materials Science and Engineering C* 112:110808 (2020).

122. Brady, K. *et al.* Human fetal and adult bone marrow-derived mesenchymal stem cells use different signaling pathways for the initiation of chondrogenesis. *Stem Cells Dev* 23(5):541–54 (2014).

123. Xu, J., Wang, W., Kapila, Y., Lotz, J. & Kapila, S. Multiple differentiation capacity of STRO-1 +/CD146 + PDL Mesenchymal Progenitor Cells. *Stem Cells Dev* 18(3):487-96 (2009).

124. Stewart, K. *et al.* Further Characterization of Cells Expressing STRO-1 in Cultures of Adult Human Bone Marrow Stromal Cells. *Journal of Bone and Mineral Research* 14(8):1345-56 (1999).

125. Williams, E. L., White, K. & Oreffo, R. O. C. Isolation and enrichment of stro-1 immunoselected mesenchymal stem cells from adult human bone marrow. *Methods in Molecular Biology* 1035:67–73 (2013).

126. Adesida, A. B., Mulet-Sierra, A. & Jomha, N. M. Hypoxia mediated isolation and expansion enhances the chondrogenic capacity of bone marrow mesenchymal stromal cells. *Stem Cell Res Ther.* 3(2):9 (2012).

127. Tsai, C. C., Huang, T. F., Ma, H. L., Chiang, E. R. & Hung, S. C. Isolation of mesenchymal stem cells from shoulder rotator cuff: A potential source for muscle and tendon repair. *Cell Transplant.* 22(3):413–22 (2013).

128. Ng, C. P. *et al.* Enhanced ex vivo expansion of adult mesenchymal stem cells by fetal mesenchymal stem cell ECM. *Biomaterials* 35(13):4046–57 (2014).

129. Munshi, A. *et al.* A comprehensive proteomics profiling identifies NRP1 as a novel identity marker of human bone marrow mesenchymal stromal cell-derived small extracellular vesicles. *Stem Cell Res Ther.* 10:401 (2019).

130. Pinho, S. *et al.* PDGFRα and CD51 mark human Nestin+ sphere-forming mesenchymal stem cells capable of hematopoietic progenitor cell expansion. *Journal of Experimental Medicine* 210(7):1351–67 (2013).

131. Baghaei, K. *et al.* Isolation, Differentiation, and Characterization of Mesenchymal Stem Cells from Human Bone Marrow. Gastroenterology and Hepatology From Bed to Bench. *Gastroenterol Hepatol Bed Bench* 10(3):208-213 (2017).

132. Herrmann, M. *et al.* Phenotypic characterization of bone marrow mononuclear cells and derived stromal cell populations from human iliac crest, vertebral body and femoral head. *Int J Mol Sci* 20:3454 (2019).

133. Houlihan, D. D. *et al.* Isolation of mouse mesenchymal stem cells on the basis of expression of Sca-1 and PDGFR-α. *Nat Protoc* 7(12):2103–11 (2012).

134. Matthews, B. G. *et al.* Analysis of αsMA-labeled progenitor cell commitment identifies notch signaling as an important pathway in fracture healing. *Journal of Bone and Mineral Research* 29(5):1283–94 (2014).

135. Greenbaum, A. *et al.* CXCL12 in early mesenchymal progenitors is required for haematopoietic stem-cell maintenance. *Nature* 495(7440):227–230 (2013).

136. Talele, N. P., Fradette, J., Davies, J. E., Kapus, A. & Hinz, B. Expression of α-Smooth Muscle Actin Determines the Fate of Mesenchymal Stromal Cells. *Stem Cell Reports* 4(6):1016–1030 (2015).

137. Ono, N., Balani, D. H. & Kronenberg, H. M. Stem and progenitor cells in skeletal development. in *Current Topics in Developmental Biology* 133:1–24 (Academic Press Inc., 2019).

138. Nilsson, O. *et al.* Evidence that estrogen hastens epiphyseal fusion and cessation of longitudinal bone growth by irreversibly depleting the number of resting zone progenitor cells in female rabbits. *Endocrinology* 155(8):2892–99 (2014).

139. Schoenau, E., Neu, C. M., Rauch, F. & Manz, F. The Development of Bone Strength at the Proximal Radius during Childhood and Adolescence. *J Clin Endocrinol Metab.* 86(2):613-8 (2001).

140. Seeman, E. Clinical review 137 Sexual Dimorphism in Skeletal Size, Density, and Strength. *Clin Endocrinol Metab.* 86(10):4576-84. (2001).

141. Callewaert, F. *et al.* Sexual dimorphism in cortical bone size and strength but not density is determined by independent and time-specific actions of sex steroids and

IGF-1: Evidence from pubertal mouse models. *Journal of Bone and Mineral Research* 25(3):617–26 (2010).

142. Brockstedt, H., Kassem, M., Eriksen, E. F., Mosekilde, L. & Melsen, F. Age-and Sex-Related and Remodeling Changes in Iliac Cortical Bone Mass. *Bone* 14:681-91 (1993).

143. Almeida, M. *et al.* Estrogens and Androgens in Skeletal Physiology and Pathophysiology. *Physiol Rev* 97:135–87 (2017).

144. Lupu, F., Terwilliger, J. D., Lee, K., Segre, G. V. & Efstratiadis, A. Roles of growth hormone and insulin-like growth factor 1 in mouse postnatal growth. *Dev Biol.* 229(1):141–62 (2001).

145. Vanderschueren, D. *et al*. An Aged Rat Model of Partial Androgen Deficiency: Prevention of Both Loss of Bone and Lean Body Mass by Low-Dose Androgen Replacement. *Endocrinology* 141(5):1642-47 (2000).

146. Sims, N. A., Brennan, K., Spaliviero, J., Handelsman, D. J. & Seibel, M. J. Perinatal testosterone surge is required for normal adult bone size but not for normal bone remodeling. *Am J Physiol Endocrinol Metab* 290(3):E456 (2006).

147. Zhang, X. Z., Kalu, D. N., Erbas, B., Hopper, J. L. & Seeman, E. The effects of gonadectomy on bone size, mass, and volumetric density in growing rats are gender-, site-, and growth hormone-specific. *Journal of Bone and Mineral Research* 14(5):802-9 (1999).

148. Govoni, K. E., Wergedal, J. E., Chadwick, R. B., Srivastava, A. K. & Mohan, S. Prepubertal OVX increases IGF-I expression and bone accretion in C57BL/6J mice. *Am J Physiol Endocrinol Metab* 295: E1172-80 (2008).

149. Callewaert, F., Sinnesael, M., Gielen, E., Boonen, S. & Vanderschueren, D. Skeletal sexual dimorphism: Relative contribution of sex steroids, GH-IGF1, and mechanical loading. *Journal of Endocrinology* 207(2):127–34 (2010).

150. Shen, V., Birchman, R., Wu, D. D. & Lindsay, R. Skeletal effects of parathyroid hormone infusion in ovariectomized rats with or without estrogen repletion. *Journal of Bone and Mineral Research* 15(4):740–6 (2000).

151. Liu, Z., Mohan, S. & Yakar, S. Does the GH/IGF-1 axis contribute to skeletal sexual dimorphism? Evidence from mouse studies. *Growth Hormone and IGF Research* 27:7–17 (2016).

152. Yakar, S. *et al.* Circulating levels of IGF-1 directly regulate bone growth and density. *Journal of Clinical Investigation* 110(6):771–81 (2002).

153. Michael, H., Härkönen, P. L., Väänänen, H. K. & Hentunen, T. A. Estrogen and testosterone use different cellular pathways to inhibit osteoclastogenesis and bone resorption. *Journal of Bone and Mineral Research* 20(12):2224–32 (2005).

154. Huber, D. M. *et al.* Androgens Suppress Osteoclast Formation Induced by RANKL and Macrophage-Colony Stimulating Factor. *Endocrinology* 142(9):3800-8 (2001).

155. Kameda, T. *et al.* Estrogen Inhibits Bone Resorption by Directly Inducing Apoptosis of the Bone-Resorbing Osteoclasts. *J. Exp. Med* 186(4):489-95 (1997).

156. Khosla, S., Atkinson, E. J., Dunstan, C. R. & O'fallon, W. M. Effect of Estrogen versus Testosterone on Circulating Osteoprotegerin and Other Cytokine Levels in Normal Elderly Men. *The Journal of Clinical Endocrinology & Metabolism* 87(4):1550-4 (2002).

157. Hughes D. E. *et al.* Estrogen promotes apoptosis of murine osteoclasts mediated by TGF-beta. *Nat Med.* 2(10):1132-6 (1996)

158. Abe, K. & Aoki, Y. Sex Differences in Bone Resorption in the Mouse Femur A Light-and Scanning Electron-Microscopic Study. *Cell Tissue Res* 255:15-21 (1989).

159. Mun, S. H. *et al.* Sexual Dimorphism in Differentiating Osteoclast Precursors Demonstrates Enhanced Inflammatory Pathway Activation in Female Cells. *Journal of Bone and Mineral Research* 36:1104–16 (2021).

160. Zhang, Y., Huang, S., Xie, B. & Zhong, Y. Aging, Cellular Senescence, and Glaucoma. *Aging and Disease* vol. 15(2):546–64 (2024).

161. Miura, N. *et al.* Progressive Telomere Shortening and Telomerase Reactivation During Hepatocellular Carcinogenesis. *Cancer Genet Cytogenet* 93:56-62 (1997).

162. Campisi, J. Aging, cellular senescence, and cancer. *Annual Review of Physiology* 75:685–705 (2013).

163. Seeman, E. Pathogenesis of bone fragility in women and men. *Lancet* 359(9320):1841-50 (2002).

164. Ermolaeva, M., Neri, F., Ori, A. & Rudolph, K. L. Cellular and epigenetic drivers of stem cell ageing. *Nature Reviews Molecular Cell Biology* 19(9):594–610 (2018).

165. Kaur, J. & Farr, J. N. Cellular senescence in age-related disorders. *Translational Research* 226:96–104 (2020).

166. Freund, A., Orjalo, A. V., Desprez, P. Y. & Campisi, J. Inflammatory networks during cellular senescence: causes and consequences. *Trends in Molecular Medicine* 16:238–246 (2010).

167. Coutu, D. L. & Galipeau, J. Molecular and Endocrine Mechanisms Underlying the Stem Cell Theory of Aging. In book: *Adult stem cells* pp.389–417 (Springer Inc., 2014).

168. Jeon, O. H., David, N., Campisi, J. & Elisseeff, J. H. Senescent cells and osteoarthritis: A painful connection. *Journal of Clinical Investigation* 128(4):1229-37 (2018).

169. Hayflick, L. The limited in vitro lifetime of human diploid cell strains. *Exp Cell Res* 37(3):614–636 (1965).

170. Hayflick, L. & Moorhead, P. S. The serial cultivation of human diploid cell strains. *Experimental Cell Research* 25:(1961).

171. Sharpless, N. E. & DePinho, R. A. How stem cells age and why this makes us grow old. *Nature Reviews Molecular Cell Biology* 8(9):703–13 (2007).

172. Van Zant, G. & Liang, Y. The Role of Stem Cells in Aging. *Experimental Hematology* 31:659-72(2003).

173. Serrano, M., Lin, A. W., McCurrach, M. E. & Beach, D. Oncogenic Ras Provokes Premature Cell Senescence Associated with Accumulation of P53 and P16INK4a. *Cell* 88:593-602 (1997).

174. Collins, C. J. & Sedivy, J. M. Involvement of the INK4a/Arf gene locus in senescence. *Aging cell* 2(3):145–50 (2003).

175. Farr, J. N. *et al.* Identification of Senescent Cells in the Bone Microenvironment. *Journal of Bone and Mineral Research* 31(11):1920–29 (2016).

176. Zhang, H. W. *et al.* Defects in mesenchymal stem cell self-renewal and cell fate determination lead to an osteopenic phenotype in Bmi-1 null mice. *Journal of Bone and Mineral Research* 25(3):640–52 (2010).

177. Xu, M. *et al.* Transplanted Senescent Cells Induce an Osteoarthritis-Like Condition in Mice. *J Gerontol A Biol Sci Med Sci* 72(6):780–85 (2017).

178. Madisen, L. *et al.* A robust and high-throughput Cre reporting and characterization system for the whole mouse brain. *Nat Neurosci* 13(1):133–40 (2010).

179. Kreher, N. C., Eugster, E. A. & Shankar, R. R. The use of tamoxifen to improve height potential in short pubertal boys. *Pediatrics* 116(6):1513–15 (2005).

180. Shi, Y. *et al.* Gli1+ progenitors mediate bone anabolic function of teriparatide via Hh and Igf signaling. *Cell Rep* 36(7):109542 (2021).

181. Wu, X., Walker, J., Zhang, J., Ding, S. & Schultz, P. G. Purmorphamine Induces Osteogenesis by Activation of the Hedgehog Signaling Pathway osteogenesis in mouse mesenchymal progenitor cells (C3H10T1/2). *Chem Biol* 11:1229–38 (2004).

182. Oliveira, F. S. *et al.* Hedgehog signaling and osteoblast gene expression are regulated by purmorphamine in human mesenchymal stem cells. *J Cell Biochem* 113(1): 204–8 (2012).

183. Beloti, M. M., Bellesini, L. S. & Rosa, A. L. Purmorphamine enhances osteogenic activity of human osteoblasts derived from bone marrow mesenchymal cells. *Cell Biol Int* 29(7):537–41 (2005).

184. Sinha, S. & Chen, J. K. Purmorphamine activates the Hedgehog pathway by targeting Smoothened. *Nat Chem Biol* 2(1):29–30 (2006).

185. Beloti, M. M., Bellesini, L. S. & Rosa, A. L. The effect of purmorphamine on osteoblast phenotype expression of human bone marrow mesenchymal cells cultured on titanium. *Biomaterials* 26(20):4245–48 (2005).

186. Adhikari, R., Chen, C. & Kim, W. K. Effect of 20(S)-hydroxycholesterol on multilineage differentiation of mesenchymal stem cells isolated from compact bones in chicken. *Genes* 11(11):1–26 (2020).

187. Kim, W. K., Meliton, V., Amantea, C. M., Hahn, T. J. & Parhami, F. 20(S)-hydroxycholesterol inhibits PPARγ expression and adipogenic differentiation of bone marrow stromal cells through a hedgehog-dependent mechanism. *Journal of Bone and Mineral Research* 22(11):1711–19 (2007).

188. Huang, Y. *et al.* 20(S)-hydroxycholesterol and simvastatin synergistically enhance osteogenic differentiation of marrow stromal cells and bone regeneration by initiation of Raf/MEK/ERK signaling. *J Mater Sci Mater Med* 30(8):87 (2019).

189. Lee, J. S., Kim, E., Han, S., Kang, K. L. & Heo, J. S. Evaluating the oxysterol combination of 22(S)-hydroxycholesterol and 20(S)-hydroxycholesterol in periodontal regeneration using periodontal ligament stem cells and alveolar bone healing models. *Stem Cell Res Ther* 8(1):276 (2017).

190. Bar, E. E. *et al.* Cyclopamine-Mediated Hedgehog Pathway Inhibition Depletes Stem-Like Cancer Cells in Glioblastoma. *Stem Cells* 25(10):2524–33 (2007).

191. Chen, J. K., Taipale, J., Cooper, M. K. & Beachy, P. A. Inhibition of Hedgehog signaling by direct binding of cyclopamine to Smoothened. *Genes Dev* 16(21):2743–48 (2002).

192. Spormann, L. *et al.* Cyclopamine and rapamycin synergistically inhibit mtor signalling in mouse hepatocytes, revealing an interaction of hedgehog and mtor signalling in the liver. *Cells* 9(8):1–22 (2020).

193. Coutu, D. L., Kokkaliaris, K. D., Kunz, L. & Schroeder, T. Multicolor quantitative confocal imaging cytometry. *Nat Methods* 15(1):39–46 (2018).

194. Balani, D. H., Ono, N. & Kronenberg, H. M. Parathyroid hormone regulates fates of murine osteoblast precursors in vivo. *Journal of Clinical Investigation* 127(9):3327–38 (2017).

195. Cohn-Schwartz, D. *et al.* PTH-Induced Bone Regeneration and Vascular Modulation Are Both Dependent on Endothelial Signaling. *Cells* 11(5):897 (2022).

196. Ma, C. *et al.* Exogenous PTH 1-34 Attenuates Impaired Fracture Healing in Endogenous PTH Deficiency Mice via Activating Indian Hedgehog Signaling

Pathway and Accelerating Endochondral Ossification. *Front Cell Dev Biol* 9:750878 (2022).

197. Samadfam, R., Xia, Q., Miao, D., Hendy, G. N. & Goltzman, D. Exogenous PTH and endogenous 1,25-dihydroxyvitamin D are complementary in inducing an anabolic effect on bone. *Journal of Bone and Mineral Research* 23(8):1257–66 (2008).

198. Faghihi, F., Baghaban Eslaminejad, M., Nekookar, A., Najar, M. & Salekdeh, G. H. The effect of purmorphamine and sirolimus on osteogenic differentiation of human bone marrow-derived mesenchymal stem cells. *Biomedicine and Pharmacotherapy* 67(1):31–8 (2013).

199. Wu, X., Walker, J., Zhang, J., Ding, S. & Schultz, P. G. Purmorphamine Induces Osteogenesis by Activation of the Hedgehog Signaling Pathway osteogenesis in mouse mesenchymal progenitor cells (C3H10T1/2). *Chem Biol* 11:1229–38 (2004).

200. Hadji, P. *et al.* The effect of exemestane and tamoxifen on bone health within the Tamoxifen Exemestane Adjuvant Multinational (TEAM) trial: A meta-analysis of the US, German, Netherlands, and Belgium sub-studies. *J Cancer Res Clin Oncol* 137(6):1015–25 (2011).

201. Grey, A. B. *et al.* The Effect of the Antiestrogen Tamoxifen on Bone Mineral Density in Normal Late Postmenopausal Women. *Am J Med*. 99(6):636-41 (1995).

202. Lee, S. J., Cha, C. D., Hong, H., Choi, Y. Y. & Chung, M. S. Adverse effects of tamoxifen treatment on bone mineral density in premenopausal patients with breast cancer: a systematic review and meta-analysis. *Breast Cancer* 31(4):717–25 (2024).

203. Felker, A. *et al.* In vivo performance and properties of Tamoxifen metabolites for CreERT2 control. *PLoS One* 11(4):1-17 (2016).

204. Hayashi, S. & McMahon, A. P. Efficient recombination in diverse tissues by a tamoxifen-inducible form of Cre: A tool for temporally regulated gene activation/inactivation in the mouse. *Dev Biol* 244(2):305–18 (2002).

205. Wang, S., Lai, X., Deng, Y. & Song, Y. Correlation between mouse age and human age in anti-tumor research: Significance and method establishment. *Life Sciences* 242:117242 (2020).

206. Xiao, Y. *et al.* Age and gender affect DNMT3a and DNMT3b expression in human liver. *Cell Biol Toxicol* 24(3):265–72 (2008).

207. Singh, L. *et al.* Aging alters bone-fat reciprocity by shifting in vivo mesenchymal precursor cell fate towards an adipogenic lineage. *Bone* 85:29–36 (2016).

208. Ponnapakkam, T., Katikaneni, R., Sakon, J., Stratford, R. & Gensure, R. C. Treating osteoporosis by targeting parathyroid hormone to bone. *Drug Discovery Today* 19(3):204–8 (2014).

209. Chen, J. K., Taipale, J., Cooper, M. K. & Beachy, P. A. Inhibition of Hedgehog signaling by direct binding of cyclopamine to Smoothened. *Genes Dev* 16(21):2743–48 (2002).

210. Dwyer, J. R. *et al.* Oxysterols are novel activators of the hedgehog signaling pathway in pluripotent mesenchymal cells. *Journal of Biological Chemistry* 282(12):8959–68 (2007).

211. Kim, K., Bansal, P. D. & Shukla, D. Cyclopamine modulates smoothened receptor activity in a binding position dependent manner. *Commun Biol* 7:1207(2024).

212. Jerome, C. P. *et al.* Effect of Treatment for 6 Months with Human Parathyroid Hormone (1-34) Peptide in Ovariectomized Cynomolgus Monkeys (Macaca Fascicularis). *Bone* 25(3):301-9 (1999).

213. Jerome, C. P., Johnson, C. S. & Lees, C. J. Effect of treatment for 3 months with human parathyroid hormone 1-34 peptide in ovariectomized cynomolgus monkeys (macacafascicularis). *Bone* 17(4 Suppl):415S-420S (1995).

214. Dobnig, H. & Turner, R. T. The Effects of Programmed Administration of Human Parathyroid Hormone Fragment (1-34) on Bone Histomorphometry and Serum Chemistry in Rats. *Endocrinology* 138(11):4607-12 (1997).

215. Hirano, T. *et al.* Anabolic Effects of Human Biosynthetic Parathyroid Hormone Fragment (1-34), LY333334, on Remodeling and Mechanical Properties of Cortical Bone in Rabbits. *Journal of Bone and Mineral Research* 14(4):536-45(1999).

216. Neer, R. M. *et al.* Effect of parathyroid hormone (1-34) on fractures and bone mineral density in postmenopausal women with osteoporosis. *N Engl J Med* 344(19):1434-41 (2001).

217. Misof, B. M. *et al.* Effects of intermittent parathyroid hormone administration on bone mineralization density in iliac crest biopsies from patients with osteoporosis: A paired study before and after treatment. *Journal of Clinical Endocrinology and Metabolism* 88(3):1150–56 (2003).

218. Dempster, D. W. *et al.* Effects of Daily Treatment with Parathyroid Hormone on Bone Microarchitecture and Turnover in Patients with Osteoporosis: A Paired Biopsy Study. *Journal of Bone and Mineral Research* 16(10):1846-53 (2001).

219. Shagufta & Ahmad, I. Tamoxifen a pioneering drug: An update on the therapeutic potential of tamoxifen derivatives. *European Journal of Medicinal Chemistry* 143:515–31 (2018).

220. Wang, A. S., Ong, P. F., Chojnowski, A., Clavel, C. & Dreesen, O. Loss of lamin B1 is a biomarker to quantify cellular senescence in photoaged skin. *Sci Rep* 7:15678 (2017).

221. Freund, A., Laberge, R. M., Demaria, M. & Campisi, J. Lamin B1 loss is a senescence-associated biomarker. *Mol Biol Cell* 23(11):2066–75 (2012).

222. Shimi, T. *et al.* The role of nuclear lamin B1 in cell proliferation and senescence. *Genes Dev* 25(24):2579–93 (2011).

223. Etourneaud, L. *et al.* Lamin B1 Sequesters 53BP1 to Control Its Recruitment to DNA Damage. *Sci. Adv* 7:eabb3799 (2021).

224. Coutu, D. L., François, M. & Galipeau, J. Inhibition of cellular senescence by developmentally regulated FGF receptors in mesenchymal stem cells. *Blood* 117(25):6801–12 (2011).

225. Ito, T., Sawada, R., Fujiwara, Y., Seyama, Y. & Tsuchiya, T. FGF-2 suppresses cellular senescence of human mesenchymal stem cells by down-regulation of TGF-β2. *Biochem Biophys Res Commun* 359:108–14 (2007).

226. Fu, X. *et al.* 27-Hydroxycholesterol Is an Endogenous Ligand for Liver X Receptor in Cholesterol-loaded Cells. *Journal of Biological Chemistry* 276(42):38378–87 (2001).

227. Nelson, E. R. *et al.* The oxysterol, 27-hydroxycholesterol, links cholesterol metabolism to bone homeostasis through its actions on the estrogen and liver X receptors. *Endocrinology* 152(12):4691–705 (2011).

228. Sun, M. M. G. & Beier, F. Liver X Receptor activation regulates genes involved in lipid homeostasis in developing chondrocytes. *Osteoarthr Cartil Open* 2:100030 (2020).

229. Janowski B. A. *et al.* An oxysterol signalling pathway mediated by the nuclear receptor LXR alpha. *Nature* 383(6602):728-31 (1996).

230. Reprinted from *Biochemical Pharmacology*, Vol. 174, Jana, S. *et al*, SOX9: The master regulator of cell fate in breast cancer. Page No. 113789, Copyright (2020), with permission from Elsevier.

231. Orikasa S. *et al.* Hedgehog activation promotes osteogenic fates of growth plate resting zone chondrocytes through transient clonal competency. *JCI Insight* 9(2):e165619 (2024).